INSIGHTS INTO MECHANISMS OF METAL HOMEOSTASIS IN STAPHYLOCOCCUS AUREUS

By

ZUELAY E. ROSARIO-CRUZ

A dissertation submitted to the

Graduate School – New Brunswick

Rutgers, The State University of New Jersey

In partial fulfillment of the requirements

For the degree of

Doctor of Philosophy

Graduate Program in Microbial Biology

Written under the direction of

Jeffrey M. Boyd

And approved by

_____

_____

_____

_____

New Brunswick, New Jersey

May 2016

ABSTRACT OF THE DISSERTATION

Insights into Mechanisms of Metal Homeostasis in *Staphylococcus aureus*

by ZUELAY E. ROSARIO-CRUZ

Dissertation Director:

Jeffrey M. Boyd, Ph.D.

Staphylococcus aureus is a major public health concern worldwide. The human immune system employs oxidative- and copper-dependent mechanisms that disrupt metal homeostasis within the invading microorganism. This thesis describes new factors involved in iron-sulfur cluster biogenesis and copper detoxification in *S. aureus*, representing additional mechanisms of metal homeostasis that might aid this pathogen during host infection. Strains lacking the low-molecular-weight thiol bacillithiol (*bshA* mutants) display growth defects that are alleviated by the addition of exogenous Fe or the amino acids leucine and isoleucine. The *bshA* strain has decreased activities of Fe-S proteins, such as LeuCD, IlvD, AcnA, and GltBD, suggesting that the absence of BSH leads to a general defect in Fe-S cluster biogenesis. The growth defects and decreased enzymatic activities of the *bshA* strain are exacerbated in strains lacking other factors involved in Fe-S cluster biogenesis, such as the Fe-S cluster carriers Nfu and SufA, and partially suppressed by their overexpression, suggesting a functional overlap between BSH and Fe-S cluster carriers in Fe-S cluster biogenesis. We also found a two-gene operon involved in preventing copper (Cu) intoxication. These genes encode an ATPase Cu transporter (*copB*) and a putative lipoprotein (*cbl*). Mutational inactivation of *copB* or *cbl* resulted in Cu sensitivity, and their phenotypes are exacerbated in strains also lacking the highly conserved Cu exporter CopA, suggesting that CopB and Cbl are additional mechanisms that prevent Cu intoxication in *S. aureus*.

Overexpression of either *copB* or *cbl* leads to increased Cu resistance in other *S. aureus* clinical isolates lacking these genes. We show that *copB* and *cbl* are co-transcribed, up-regulated under Cu stress, and repressed by CsoR. Genetic and biochemical evidence show that Cbl is a membrane-associated, surface-exposed lipoprotein that binds up to four Cu^{+} ions. Collectively, the research presented in this thesis describes new roles for BSH and Cbl in metal homeostasis in the human pathogen *S. aureus*.

ACKNOWLEDGEMENTS

I would like to extend my gratitude to the many people who helped me throughout these years. First and foremost, I would like to thank my advisor Jeff M. Boyd for his guidance and support, for always being available to provide feedback and discuss ideas, and for making this such a productive experience. I would also like to thank present and past members of the Boyd Lab, for their scientific contributions or for making life in lab more enjoyable. I would also like to thank my thesis committee, Dr. William J. Belden, Dr. Donald Y. Kobayashi, and Dr. Thomas Leustek, for their time and invaluable feedback.

Thanks to Dr. Max M. Häggblom and the Department of Biochemistry and Microbiology for providing me with the opportunity to join the Microbial Biology program and be part of the General Microbiology Laboratory during all these years. Being a Teaching Assistant has been one of the most rewarding experiences I have had as a graduate student. Special thanks to Dr. Diane F. Davis for being such an inspirational educator and teaching me how to teach. I would also like to thank Dr. Ines Rauschenbach for allowing us to be actively involved in the Teaching Lab and for always finding ways to make the teaching-learning experience more gratifying.

I would like to thank the Graduate School of New Brunswick, as well as, the many Alumni and friends of the Department that, through their generous donations, made fellowships, scholarships, and travel awards possible. I am deeply grateful for your financial support and, like you, I hope that someday I can give back some of what I have received.

Finally, I would like to thank my dad, my dear Mom Abby, and my partner Manuel for providing me with unfailing and continuous encouragement throughout these years. This accomplishment would have been impossible without their unconditional love and support.

TABLE OF CONTENTS

LIST OF TABLES

LIST OF FIGURES

PREFACE

Chapter 1 has been published as "Bacillithiol has a role in Fe-S cluster biogenesis in *Staphylococcus aureus*.", Rosario-Cruz Z, Chahal HK, Mike LA, Skaar EP, Boyd JM. 2015. *Mol Microbiol*. 98(2):218-42. PMID: 26135358.

Rosario-Cruz Z contribution: Figures 1, 2, 3A, 4, 5, 6, 7, 9 & 10; Supplementary Figures S1, S2, S3, S4, S6, S7, S8, S9; Table 1; Supplementary Table S1, S2.

Chapter 2 is in preparation for publication as "The *copBcbl* Operon Protects *S. aureus* From Copper Intoxication: Cbl is an Extracellular Membrane-Associated Copper-Binding Protein", by Rosario-Cruz Z and Boyd JM, to be submitted to the Journal of Biological Chemistry. Rosario-Cruz Z contribution: All data used to generate figures and tables included in this chapter.

INTRODUCTION

General Overview of *Staphylococcus aureus*. *Staphylococcus aureus* was discovered in the 1880s by Alexander Ogston, a surgeon who was trying to find the causative agent for the inflammation and suppuration of the surgical wounds of his patients. He used the Greek word "*staphyle*" to describe the grape-like clusters observed under the microscope. A few years later, Friedrich Julius Rosenbach suggested the species name "*aureus"* that means gold in Latin, due to the golden pigmentation of its colonies. *S. aureus* is a Gram-positive cocci, non-motile, non-spore forming bacterium that respires aerobically or, in the absence of oxygen, it can undergo fermentation or use nitrate as an alternate electron acceptor.

Staphylococcus aureus is a human commensal mostly found on the skin and nose of nearly one third of the population. It is normally asymptomatic, but it is considered an opportunistic pathogen because it can cause serious illnesses once it passes the skin barrier by abrasions, surgery, or injections, especially in individuals with a compromised immune system. *S. aureus* is known for causing mild skin and soft tissue infections, such as folliculitis, boils, and carbuncles, some of which can develop into more serious skin infections like cellulitis and necrotizing fasciitis. *S. aureus* can also cause more life-threatening infections such as meningitis, bacteremia, endocarditis, pneumonia, and osteomyelitis, as well as toxin-based illnesses like food poisoning and toxic shock syndrome (Klevens *et al*., 2007; Otto, 2010).

A major challenge of treating *S. aureus* infections derives from its ability to rapidly acquire resistance to antibiotics, a phenomenon documented as epidemic waves (Chambers and DeLeo, 2009). The first wave of antibiotic resistance occurred in the 1940s, when penicillin-resistant *S. aureus* arose as a result of treating staphylococcal infections with penicillin (Barber and Rozwadowska-Dowzenko, 1948). In 1959, methicillin was introduced

to treat penicillin-resistant *S. aureus*, but two years later the "birth" of methicillin-resistant *S. aureus* (MRSA) was reported (Barber, 1961), representing the onset of the second wave of antibiotic resistance. In the United States MRSA was first reported in a Boston hospital in 1968 (Barrett *et al*., 1968). After the 1970s, MRSA outbreaks were reported worldwide, representing the beginning of the third wave of antibiotic resistance. Until this moment, most MRSA infections were reported from intensive care units, hospital rooms, and nursing homes, as well as many cases among dialysis patients, diabetics, patients with intravenous lines, and other immunocompromised individuals. These infections were coined as healthcare-associated, or HA-MRSA infections. The fourth wave started in the 1990s when MRSA outbreaks started to become more prevalent outside healthcare facilities to individuals who had not been hospitalized or had undergone a medical procedure. These community-associated MRSA (CA-MRSA) infections continue to be commonly reported from childcare centers (McAdams *et al*., 2008), athletic teams (Benjamin *et al*., 2007), inmates (CDC, 2003), and soldiers (Morrison-Rodriguez *et al*., 2010). Their containment is difficult because the organism can easily spread from an infected wound through skin-to-skin contact, by touching a contaminated surface, or by using an item (equipment, clothes, towels, etc.) that an infected person has used before.

Methicillin-resistant *S. aureus* strains are resistant to all β-lactams (penicillins, cephalosporins, monobactams, and carbapenems), leaving a limited number of antibiotics to treat staphylococcal infections. Currently, invasive MRSA infections are treated with last resort drugs, such as vancomycin, daptomycin, and linezolid, but resistance to these antibiotics has already been reported (CDC, 2002; Marty *et al*. 2006; Sánchez *et al*., 2010).

Staphylococcus aureus outbreaks have been reported around the world (Skov *et al*., 2012), making this pathogen a major public health concern worldwide. According to the United States Centers for Disease and Control Prevention (CDC), more people died due to *S.*

aureus infections than AIDS in 2005. In 2011, reports on CA-MRSA infections surpassed HA-MRSA infections. In 2012, there were 74,693 cases of *S. aureus* infections and 9,937 deaths in the United States alone (CDC, 2013). Although this represents a significant decrease in incidence and mortality (Dantes *et al*., 2013), hospitalization and mortality rates continue to have a major financial burden. In the United States, CA-MRSA infections alone are estimated to cost at least $478 million every year (Lee *et al*, 2013). Direct medical costs (emergency room visit, hospitalization, and treatment) range between $2,277-$3,200 for a single CA-MRSA case (Lee *et al*., 2013), while there is a median charge of $6,916 per every HA-MRSA case due to prolonged hospitalizations and increased hospital (Cosgrove *et al*., 2005). This, combined with its high incidence, in both healthcare and community settings, and its ability to rapidly develop antibiotic resistance, underscore the importance of continuing to study staphylococcal biology in order to identify novel drug targets.

Oxidative Stress and Metal Imbalance at the Host-Pathogen Interface. In order to identify new drug targets, we first need to understand how our body kills invading microorganisms. One of the bacterial killing mechanisms employed by neutrophils and macrophages involves the generation of superoxide via an NADPH-dependent oxidase (NOX), a process known as the oxidative burst. The transfer of electrons from NADPH to molecular oxygen leads to the production of superoxide (O_2^-), that is then reduced to peroxide (H_2O_2). Peroxide can be further reduced to other secondary reactive oxygen species (ROS), including hydroxyl radicals ($OH^\bullet$) or hypochlorite (OCl-) and chloramines via the myeloperoxidase (MPO) complex. Overall, all of these ROS can accumulate within the phagocytosed microbe and cause oxidative stress. In addition to the oxidative burst process, macrophages also accumulate copper (Cu^+) via the ATP7A transporter. The accumulated Cu^+ can either react with H_2O_2, leading to an amplified effect of oxidative stress within the

phagolysosome, or it can diffuse into the phagocytosed microbe and cause toxicity by other mechanisms (discussed below).

The oxidative burst is critical in mounting an effective fight against pathogenic microorganisms. A defect in the NOX system results in an immunodeficiency disorder known as chronic granulomatous disease (CGD) (Song *et al*., 2011). CGD patients suffer frequent bacterial and fungal infections, mostly caused by *S. aureus*, *Pseudomonas* spp., *Nocardia* spp., *Aspergillus* spp., and *Candida albicans*. CGD affects about 1 in 200,000 people worldwide and is usually diagnosed during infancy or childhood with a life expectancy of 20 years old (Liese *et al*., 2000). A defect in the ATP7A transporter leads to a syndrome known as Menkes disease (Kaler, 2011). Menkes disease patients often suffer bacterial infections (Menkes *et al*., 1962; Gunn *et al*., 1984; Uno and Arya, 1987; Kreuder *et al*., 1993), highlighting the importance of Cu-mediated bacterial killing in the host immune system.

One of the bacterial targets of ROS are protein-bound cofactors composed of iron (Fe) and sulfur (S) called iron-sulfur (Fe-S) clusters (Hurst *et al*., 1991; Flint *et al*., 1993; Jang and Imlay, 2007). Oxidation of solvent-exposed Fe–S clusters results in protein inactivation and release of Fe^{2+}. This "free" iron can participate in Fenton chemistry, leading to the production of highly reactive $OH^{\bullet}$ that can oxidize DNA, lipids, and proteins. Like Fe^{2+}, Cu^{+} may also cause toxicity within the bacterium by performing Fenton-type chemistry. Alternatively, it can also compete with other metals and deplete cellular thiols, leading to an altered function of metalloproteins and changes in the redox state of the cell. Therefore, in order to cause infections, *S. aureus* must find ways to overcome the effects of the oxidative burst and copper toxicity at the host-pathogen interface.

Like other pathogens, *S. aureus* employs several strategies to prevent oxidative stress or overcome the effects of ROS toxicity (reviewed in Gaupp *et al*., 2012). Some of these

include the use of enzymes that can directly detoxify ROS, such as superoxide dismutase (*sodA* and *sodM*) (Clements *et al*., 1999; Wright Valderas and Hart, 2001), catalase (*katA*) (Horsburgh, Ingham, *et al*., 2001), and the alkyl hydroperoxide reductase system (*ahpCF*) (Cosgrove *et al*., 2007). Because "free", non-chelated Fe^{2+} can participate in Fenton chemistry, *S. aureus* uses transcriptional regulators that sense intracellular pools of Fe^{2+} and control Fe uptake (Horsburgh, Ingham, *et al*., 2001; Reniere and Skaar, 2008), as well as proteins that chelate or store intracellular Fe, such as ferritin and the DNA-binding homologue MrgA (Horsburgh, Clements, *et al*., 2001). The peroxide sensing regulator PerR derepresses *katA*, *ahpCF*, *ftn*, and *mrgA* expression, among other genes, when the PerR-bound Fe reacts with H_2O_2 (Horsburgh, Clements, *et al*., 2001). Several repair systems are employed when oxidation and damage of macromolecules occurs. In *E. coli* (Outten *et al*., 2004), oxidized Fe-S clusters are presumably repaired by the Suf scaffolding system. The thioredoxin system (TrxAB) not only facilitates H_2O_2 reduction, but it can also maintain cellular thiols in their reduced state (Uziel *et al*., 2004). When oxidized, protein bound-methionine residues are repaired by methionine sulfoxide reductases (Singh *et al*., 2015). *S. aureus* can also use non-protein thiol-containing molecules, like coenzyme A (CoA), cysteine (Cys), and bacillithiol (BSH) to help maintain a reduced cytoplasm.

To maintain copper homeostasis, *S. aureus* uses the copper-sensitive operon repressor (CsoR) that senses and binds intracellular copper leading to derepression of the *copAZ* operon (Baker *et al*., 2011). CopZ is a cytoplasmic chaperone that binds and delivers copper to target proteins, including CsoR and the copper exporter CopA. Like glutathione (GSH) in *Escherichia coli* (Helbig *et al*., 2008), other non-protein thiols, such as Cys and BSH, may also be involved in chelating intracellular Cu, preventing it from damaging other macromolecules.

Research Goal and Objectives. The overarching goal of this work was to identify and characterize additional factors involved in metal homeostasis in *S. aureus* that could provide insight into how this pathogen survives at the host-pathogen interface when facing oxidative burst and copper stress during infection. The work presented here led to updated models of iron-sulfur cluster biogenesis and copper homeostasis in *Staphylococcus aureus*.

- Chapter 1 examines the role of the low-molecular-weight thiol bacillithiol (BSH) in iron-sulfur cluster biogenesis.
- Chapter 2 describes the role of an additional copper exporter and a membrane-bound copper-binding protein in maintaining copper homeostasis.

CHAPTER 1

BACILLITHIOL HAS A ROLE IN IRON-SULFUR BIOGENESIS IN *STAPHYLOCOCCUS AUREUS*

Rosario-Cruz Z, *et al*. 2015. *Mol Microbiol*. PMID: 26135358.

Abstract

Staphylococcus aureus does not produce the low-molecular-weight (LMW) thiol glutathione, but it does produce the LMW thiol bacillithiol (BSH). To better understand the roles that BSH plays in staphylococcal metabolism, we constructed and examined strains lacking BSH. Phenotypic analysis found that the BSH-deficient strains cultured either aerobically or anaerobically had growth defects that were alleviated by the addition of exogenous iron (Fe) or the amino acids leucine and isoleucine. The activity of the iron-sulfur (Fe-S) cluster-dependent enzymes LeuCD and IlvD, required for the biosynthesis of leucine and isoleucine, were decreased in strains lacking BSH. The BSH-deficient cells also had decreased aconitase and glutamate synthase activities suggesting a general defect in Fe-S cluster biogenesis. The phenotypes of the BSH-deficient strains were exacerbated in strains lacking the Fe-S cluster carrier Nfu and partially suppressed by multicopy expression of either *sufA* or *nfu*, suggesting functional overlap between BSH and Fe-S carrier proteins. Biochemical analysis found that SufA bound and transferred Fe-S clusters to apo-aconitase, verifying that it serves as an Fe-S cluster carrier. The results presented are consistent with the hypothesis that BSH has roles in Fe homeostasis and the carriage of Fe-S clusters to apo-proteins in *S. aureus*.

Introduction

Staphylococcus aureus is the causative agent of a variety of diseases ranging from mild skin and soft tissue infections to life-threatening illnesses such as bacteremia, pneumonia, osteomyelitis and endocarditis (NCIRS, 2011). It is estimated that nearly half a million-staphylococcal infections occur every year in the United States alone, causing over 10,000 deaths (Klein *et al.*, 2007) and posing a large financial burden (Noskin *et al.*, 2007). The high prevalence of *S. aureus* infections and its ability to rapidly acquire resistance to antibiotics underscores the importance of studying the physiology of this human pathogen and identifying new antimicrobial targets.

In order to successfully cause infections, *S. aureus* must protect itself from a number of external stressors including reactive oxygen species (ROS). *S. aureus* is exposed to ROS during host colonization and infection when polymorphonuclear leukocytes and macrophages produce ROS as part of their antimicrobial killing mechanism (Quinn and Gauss, 2004). Humans that have a genetic predisposition rendering their phagocytic cells incapable of producing ROS often have chronic *S. aureus* infections, thereby highlighting the importance of ROS in preventing and combating infection (Song *et al.*, 2011).

One of the cellular targets of ROS are protein-bound cofactors composed of iron and inorganic sulfur called iron-sulfur (Fe-S) clusters (Hurst *et al.*, 1991; Flint *et al.*, 1993; Keyer and Imlay, 1997; Jang and Imlay, 2007). Proteins requiring Fe-S clusters have diverse cellular functions including: redox reactions (Orme-Johnson *et al.*, 1968; Pomposiello and Demple, 2001), DNA repair (Rudolf *et al.*, 2006), environmental sensing (Khoroshilova *et al.*, 1997; Kamps *et al.*, 2004; Sun *et al.*, 2012), cofactor biosynthesis (Martinez-Gomez and Downs, 2008), branched-chain amino acid (BCAA) biosynthesis (Flint and Emptage, 1988), and antibiotic resistance (Yan *et al.*, 2010). Oxidation of solvent-exposed Fe-S clusters by

ROS can result in cluster destruction and increased unincorporated iron (Fe), that can participate in Fenton chemistry (Imlay and Linn, 1988). Many bacteria are highly reliant on Fe-S cluster chemistry for metabolic processes, and therefore, cluster inactivation or disintegration may result in metabolic standstill (Imlay, 2006; Jang and Imlay, 2007).

Because of the toxic nature of Fe and S, organisms have evolved tightly regulated systems to metabolize Fe-S clusters (reviewed in Johnson *et al.*, 2005). *S. aureus* uses the SufCDSUB Fe-S cluster biosynthetic machinery (Diep *et al.*, 2006). In *S. aureus*, cysteine is used as a sulfur source to build Fe-S clusters, but the Fe and electron donors remain unknown (Selbach *et al.*, 2010). After synthesis, the pre-formed Fe-S clusters are transferred to carrier molecules that can then traffic the clusters to target apoproteins (reviewed in Py and Barras, 2010). Work by our group has shown that the *S. aureus nfu* gene (SAUSA300_0839) is an Fe-S cluster carrier (Mashruwala *et al.*, 2015). *S. aureus* also has a putative A-type Fe-S cluster carrier (Vinella *et al.*, 2009) that we name SufA (SAUSA300_0843). Additional *S. aureus* cellular components involved in Fe-S cluster biogenesis remain unidentified.

Among other functions, low-molecular-weight (LMW) thiols are involved in maintaining an intracellular reduced environment and repairing proteins damaged by ROS (Prinz *et al.*, 1997; Fahey, 2013). Like other *Firmicutes*, *S. aureus* does not synthesize the LMW thiol glutathione (GSH), but it does produce bacillithiol (BSH) (Newton *et al.*, 2009; Pöther *et al.*, 2013; Posada *et al.*, 2014). Although their chemical structures are not similar, BSH is a functional analog of GSH (Newton *et al.*, 2009; Sharma *et al.*, 2013). *S. aureus* strains lacking BSH are sensitive to thiol and oxidative stressors as well as to thiophilic metals (Rajkarnikar *et al.*, 2013; Posada *et al.*, 2014). Transcription of genes involved in BSH biosynthesis is induced by diamide in *S. aureus* and *B. subtilis* (Gaballa, Antelmann, *et al.*, 2013; Posada *et al.*, 2014), and the intracellular BSH concentration increases upon peroxide stress in *S. aureus* (Rajkarnikar *et al.*, 2013) and *Bacillus pumilus* (Handtke *et al.*,

2014). In *B. subtilis*, the BSH biosynthesis genes are under the transcriptional control of Spx that senses disulfide stress (Gaballa, Antelmann, *et al.*, 2013). These findings are consistent with the fact that LMW thiols have been associated with roles in metabolizing ROS or repairing proteins damaged by ROS (Carmel-Harel and Storz, 2000; Dickinson and Forman, 2002). BSH is also involved in toxin metabolism including the detoxification of the antibiotic fosfomycin in *S. aureus* and methylglyoxal in *B. subtilis* (Newton *et al.*, 2012; Roberts *et al.*, 2013; Chandrangsu *et al.*, 2014). In *B. subtilis*, BSH acts as a buffer to aid in controlling the size of the labile Zn pool to ensure proper metalation of apoproteins, but prevent Zn toxicity (Ma *et al.*, 2014). BSH binds Zn with high affinity *in vitro*.

To gain insight into the role(s) of BSH in staphylococcal metabolism, we constructed and examined BSH-deficient strains in diverse *S. aureus* isolates. The BSH-deficient strains have phenotypes resembling strains defective in Fe-S cluster biogenesis. Further analysis found that strains lacking BSH have decreased activity of Fe-S cluster-requiring enzymes. The phenotypes of the BSH-deficient strains were suppressed by multicopy expression of the Fe-S cluster carriers Nfu or SufA. Collectively, the results presented herein suggest that BSH has roles in Fe homeostasis and the carriage of Fe-S clusters in *S. aureus*.

Experimental Procedures

Reagents. Restriction enzymes, quick DNA ligase kit, deoxynucleoside triphosphates, and Phusion DNA polymerase were purchased from New England Biolabs. Oligonucleotides were obtained from Integrated DNA Technologies and are listed in Table S1. The plasmid mini-prep kit and gel extraction kit were purchased from Qiagen. Lysostaphin was purchased from Ambi Products. DL-Threo-3-isopropylmalic acid was purchased from Wako Chemicals. Tryptic Soy Broth (TSB) was purchased from MP Biomedicals. ELC chemiluminescent detection kit was purchased from Pierce. Primary and secondary antibiodies were purchased from Sigma-Aldrich and Bio-Rad, respectively. Unless specified, all other chemicals were purchased from Sigma-Aldrich and were of the highest purity available.

Bacterial Strains and Growth Conditions. Bacterial strains used in this work are listed in Table 1. Unless otherwise noted, the *S. aureus* strains used in this study are derived from the community-associated MRSA USA300 LAC strain was cured of the pUSA03 plasmid that confers erythromycin resistance (Voyich *et al.*, 2005; Pang *et al.*, 2010). *S. aureus* strains were cultured in TSB or a defined media and *Escherichia coli* strains were grown in Luria Broth (LB) medium. All bacteria were cultured at 37°C. The chemically defined media was modified from (Mah *et al.*, 1967) and contained: 1g $(NH_4)_2SO_4$, 4.5g KH_2PO_4, 10.5g K_2HPO_4, 110 mM NaCl, 30 mM KCl, 50 μg nicotinic acid, 50 μg pantothenic acid, 50 μg thiamine, 0.3 μg biotin and 2.5 mg of individual amino acids, per 100ml. The 11 amino acid media contained the following amino acids: Gly, Val, Leu, Thr, Phe, Tyr, Cys, Met, Pro, Arg, His. When supplemented to the media chemicals were added at the following concentrations: 50-200 μM $Fe_2(NH_4)_2(SO_4)_2$, 5-200 μM CoCl, 10-300 μM $CuSO_4$, 10-300 μM $MnSO_4$, 10-300 μM $ZnSO_4$. Iron was not added to growth media unless specified. For anaerobic growth on solid media, 20 mM nitrate was added to the plates as a terminal electron acceptor. Cultures were grown in one of four ways: (i) overnight cultures were

grown in 7 ml culture tubes containing 1 ml of TSB media with shaking at 200 rpm; (ii) 250 ml flask containing 50 ml of media with shaking at 200 rpm; (iii) 25 ml tubes containing 5 ml of media with shaking at 200 rpm; or (iv) in 96-well plates containing 200 µl of media per well and continuous shaking on high.

For phenotypic analysis, growth was monitored in 96-well plates using a BioTek 808E Visible absorption spectrophotometer and culture density as monitored at 595 nm. The chemically defined media contained either the 11 amino acids (AA) necessary for growth or the 20 canonical AA, unless otherwise specified. For inoculation, strains were cultured to either stationary (OD_{600} of ~10) or exponential (OD_{600} of 1) in TSB, 250 µL of cells were pelleted and resuspended in 1 mL of PBS before diluting 1:100 into fresh media.

When appropriate, antibiotics were added at the following concentrations: 150 µg ml^{-1} ampicillin (Amp), 6 or 30 µg ml^{-1} chloramphenicol (Cm) (defined or complex media, respectively), 10 µg ml^{-1} erythromycin (Erm), 3 µg ml^{-1} tetracycline (Tet), 50 µg ml^{-1} kanamycin (Kan), and 150 ng ml^{-1} anhydrotetracycline (A-Tet).

Construction of Plasmids and Mutant Strains. Unless otherwise specified, chromosomal DNA from JMB1100 was used as the template for PCR reactions used in the construction of plasmids. All plasmids were isolated from *E. coli* DH5α and transformed into electrocompetent *S. aureus* RN4220 using standard protocol (Kreiswirth *et al.*, 1983). Phage α80 was used for plasmid and chromosomal transductions (Novick, 1991). All bacterial strains were verified by PCR prior to analysis. DNA sequencing was conducted by Genewiz (South Plainfield, NJ).

Mutational inactivation of the *S. aureus bshA* and *bshC* genes was achieved by allelic replacement (*bshA*::*kanR*) or chromosomal deletion (*bshC*Δ). Approximately 500 base pairs upstream and downstream of the *bshA* gene (SAUSA300_1349) were PCR amplified using

chromosomal DNA as template and the following primers: 1349up5BamHIXmaI and 1349up3stopMluIKpnINheI; 1349down5NheKpnIMluI and1349down3SalI. PCR products were gel purified and fused by PCR using the 1349up5BamHIXmaI and 1349down3SalI primers. The PCR product was digested with EcoRI and SalI, and ligated into similarly digested pJB38 (Bose *et al.*, 2013). The recombinant vector was transformed into chemically competent *E. coli* DH5α. PCR was used to screen for colonies harboring the recombinant plasmid. The pJB38_*bshA*Δ plasmid was isolated and digested with MluI and NheI. A kanamycin cassette (*kanR*) was PCR amplified using pDG783 as a template (Fisher and Hanna, 2005). The PCR product was digested with MluI and NheI ligated to similarly digested pJB38_*bshA*Δ. After plasmids were mobilized into *S. aureus* (at 30°C), a single colony was used to inoculate 5 ml of TSB with Kan. Cultures were grown at 42°C for plasmid integration. Single colonies were inoculated in 5 ml of TSB at 30°C for plasmid resolution. To screen for the loss of plasmid, cultures were diluted 1:25,000 and plated (100 µl) on TSA containing A-Tet. Colonies were scored for Cm and Kan resistance. Colonies that were Cm sensitive and Kan resistant were screened for the double recombination event using the 1349comp5BamHI and 1349comp3SalI primers.

The *bshC* (SAUSA300_1071Δ) mutant was created using the same protocol mentioned above with the following changes. The 1071up5EcoRI and 1071upfuse primers and the 1071dwnfuse and 1071dwnSalI primers were used to amplify the upstream and downstream DNA, respectively. The 1071up5EcoRI and 1071dwnSalI primers were used for joining the two PCR products. The 1071vfyup and 1071vfyDwn primers were used to verify the *bshC*Δ strain.

For complementation and expression studies genes cloned into pEPSA5 (Forsyth *et al.*, 2002) contained an engineered *sodA* ribosomal binding site. Genes cloned into pCM28 (Pang *et al.*, 2010) contained the native promoters.

To construct the *bshA* complementing vector, the 1349comp5BamHI and 1349comp3SalI primers were used to PCR amplify the *bshA* gene; the PCR product was digested with BamHI and NheI and ligated into similarly digested pCM28 to yield pCM28_*bshA*. For the *nfu* overexpression vector, the nfu5BamRBS and nfu3SalI primers were used to PCR amplify the *nfu* gene; the PCR product was digested with BamHI and SalI and ligated into similarly digested pEPSA5 to yield pEPSA_*nfu*. For the *sufA* overexpression vector, the sufA5EcoRI and sufA3BamHI primers were used to PCR amplify the *sufA* gene; the PCR product was digested with EcoRI and BamHI and ligated into similarly digested pEPSA5 to yield pEPSA_*sufA*. To construct the pEPSA5_*ilvD* the ilvDBamHIRBS and ilvDmulIdwn primers were used to amplify *ilvD,* which was digested and ligated into similarly digested pEPSA5_*leuCD*_FLAG.

The pCM28_*sufCDSUB* plasmid was created by using yeast homologous recombination cloning (YRC) in *Saccharomyces cerevisiae* FY2 as previously described (Joska *et al.*, 2014). The pLL39_FLAG_*srrAB* plasmid was used as a template for the yeast cloning cassette (YCC) and the FLAG affinity tag (Joska *et al.*, 2014). The pCM28 vector was linearized with BamHI and SalI. The amplicons for the pCM28_*sufCDSUB* were created using the following primer pairs: pcm28YCCfor and sufYCC3; YccSuf and Sufinternal3; Sufinternal5 and SufpCM28rev.

For expression and purification of recombinant proteins from *E. coli* BL21 A1, the pET20b_*sufA* and pET24a_*acnA* were constructed to encode a C-terminal poly-histidine affinity tag. The sufA5ndeI and sufAXhoI or the AcnANheI and AcnAXhoI primers were used to PCR amplify the *sufA* and *acnA* genes, respectively. The PCR products were digested with either NdeI and XhoI or NheI and XhoI, and then ligated into similarly digested pET20b or pET24a.

Transcriptional Reporter Assays. *S. aureus* strains containing the pCM11-derived or pXEN-1 reporters were grown overnight in TSB with Erm or Cm, respectively. The overnight cultures (>16 hours) were subcultured into 5 ml of fresh media (1:100). Culture aliquots were periodically removed (200 µl) and culture optical density (A_{590}) and fluorescence or luminescence was monitored using a Perkin Elmer HTS 7000 Plus Bio Assay Reader. GFP was excited at 485 nm and emission was read at 510 nm. Relative fluorescence units or light intensities were normalized with respect to the culture optical density.

RNA isolation and quantification of mRNA transcripts. Cells were cultured in TSB overnight in biological triplicates. Cells were pelleted by centrifugation and resuspended in PBS before diluting 1:100 into defined media (20 AA, 11 AA or 11 AA + 100 µM Fe). Cells were cultured in one of two ways. Cultures used for assessing *rpsB, rpsL* and *tsf* transcript levels were grown in 250 ml flasks containing 50 ml media shaking at 200 rpm. Cells were harvested after 30 mins by centrifugation at 4000 rpm at 4°C. Cultures used for assessing transcript levels of *leuCD, acnA*, and *sufA* were cultured in 25 ml tubes containing 5 ml of chemically defined medium containing 20 AA and harvested at OD (A_{600}) of 1. All cells were harvested by centrifugation and treated with RNAProtect (Qiagen) for 10 minutes at room temperature. Cells were pelleted by centrifugation and stored at -80 °C. Pellets were thawed and washed twice with 0.5 ml of lysis buffer (50 mM RNAse-free Tris, pH 8). Cells were lysed with 20 µg DNAse and 20 µg Lysostaphin for 30 minutes at 37°C. RNAs were isolated as using TRIzol reagent (Ambion - Life Technologies) as per manufacturer protocol. DNA was digested with the TURBO DNA-*free* kit (Ambion - Life Technologies). cDNA libraries were constructed using isolated RNA as a template. An Applied Biosystems StepOnePlus thermocycler was used to quantify DNA abundance. Primers for quantitative real-time PCR (qPCR) are listed in Table S1 and were designed using the Primer Express 3.0 software from Applied Biosystems.

Determination of Intracellular Iron Concentration. Bacterial strains were cultured as biological triplicates for 18 hours in TSB. For culturing in chemically defined medium, cells were pelleted, washed with PBS and subcultured (1:100) in new 250 ml polycarbonate flasks (Corning) containing 50 ml of defined medium containing 20 AA. Cells were cultured with shaking at 200 rpm to OD (A_{600}) of 0.8 (approximately 3.5 hours after inoculation). For culturing in TSB strains were subcultured into 5 ml of TSB in a 15 ml metal-free conical tubes at a ratio of 1:100. Cultures were grown to mid-log at 37˚C, shaking at 200 rpm until an OD_{600} of 5.5 was achieved.

Cells were pelleted by centrifugation at 4°C and supernatants removed and pellets were flash frozen and stored at -80°C until use. Pellets thawed and washed with 10 ml of 0.5 M EDTA to remove extracellular metals. Cells were washed two more times with 1 ml of deionized water before suspending in 1 mL of deionized water. An aliquot of 0.5 ml was transferred into a metal-free tube and 1 ml of 50% nitric acid was added (Fischer Optima Ultra-pure). Samples were incubated at 50˚C overnight and then diluted with 9 ml of deionized water.

The quantitative analysis of ^{56}Fe in digested samples was performed on a Thermal Element II double-focusing sector field high-resolution inductively coupled plasma mass spectrometer (HR-ICPMS, Thermo Fisher Scientific, Bremen, Germany) equipped with ESI auto sampler (Elemental Scientific, Omaha, NE). The sample uptake was achieved through self-aspiration via a 0.50 mm ID sample probe and sample capillary. The Fe concentrations were determined using the following operation parameters: RF power, 1250W; Cool gas, 16.00 L min^{-1}; Auxiliary gas, 0.83 L min^{-1}; Sample gas 1.03 L min^{-1}; Resolution mode medium; 10 Runs with 1 pass; 20 samples per peak; samples time 0.01 sec.

Protein Concentration Determination. Protein concentration was determined using a bicinchoninic acid assay modified for a 96-well plate (Olson and Markwell, 2007). Bovine serum albumin (2 mg ml^{-1}) was used as a standard.

Enzyme Assays. To examine enzyme activity in the WT and *bshA* mutant strains, overnight cultures grown in TSB-Cm were pelleted and resuspended in PBS (1:4). Resuspended cells were used to inoculate (1:100) defined media containing 20 AA (50 ml culture) with and without 1% xylose. To examine enzyme activity in lysates harvested from the *sufA* and *nfu* mutant strains shown in Figure 8, strains were cultured in 5 ml of TSB in 25 ml shake tubes.

(i) Isopropylmalate Isomerase (LeuCD). Cultures were grown in defined media until they reached an OD (A_{600}) of 1, harvested by centrifugation and resuspended in 50 mM Tris (pH 8.0) containing 10 mM $MgCl_2$ (lysis buffer). Cells were lysed by the addition of 2 µg DNAse and 2 µg lysostaphin and incubated at 37°C until confluent lysis was noted (30 minutes). Cellular lysates were clarified by centrifugation and LeuCD was assayed by the addition of 25 µl of cell-free extract to 620 µl of lysis buffer and 10 mM DL -Threo-3-isopropylmalic acid (Wako Chemicals). LeuCD was assayed for the ability to convert 3-isopropylmalate to dimethylcitraconate acid spectrophotometrically at 240 nm (dimethylcitraconate ε240nm = 4.35 mM^{-1} cm^{-1}, (Gross *et al.*, 1963)) as previously described (Boyd *et al.*, 2008). Strains were cultured in 5 ml of TSB-Cm in 25 ml tubes for *sufA* and *nfu* mutant analysis.

(ii) Dihydroxy-acid Dehydratase (IlvD). Cultures were cultured, harvested and lysed as described above. IlvD activity was assayed by adding 25 µl of cell-free lysate to 620 µl of lysis buffer and 10 mM D,L-2,3-dihydroxy-isovalerate (Wako Chemicals). The ability of IlvD to produce keto-acids from D,L-2,3-dihydroxy-isovalerate was monitored spectrophotometrically at 240 nm (keto acids ε240nm = 0.19 mM^{-1} cm^{-1}, (Flint *et al.*, 1993)).

(iii) Aconitase (AcnA). Cells were cultured and harvested as described above. Cellular pellets were resuspended in 25 mM Tris-citrate, 25 mM NaCl, pH 8 buffer (AcnA buffer). Twenty-five µl of cellular lysates were added to 620 µl of AcnA buffer buffer containing 20 mM DL-isocitrate (Sigma-Aldrich). When indicated, crude extracts were anaerobically incubated with 50 µM $(NH_4)_2Fe(SO_4)_2$ for 1 hr and AcnA activity assayed. When indicated, 100 µM Fe or 500 µM DTT were added. AcnA activity was determined by monitoring the conversion of isocitrate to cis-aconitate spectrophotometrically at 240 nm (cis-aconitate ε240 nm = 3.6 mM^{-1} cm^{-1}, (Kennedy *et al.*, 1983)).

(iv) Glutamate synthase (GltBD or GOGAT). Cells were cultured and harvested as described above. Cells were harvested and resuspended in 50 mM Tris–HCl (pH 7.7). Cells were lysed as described above. Cellular lysates were clarified by centrifugation and GOGAT was assayed by the addition of 60 µl of 50 mM glutamine (pH 7.7), 60 µl of 5 mM α-ketoglutarate (pH 7.7), 60 µl of cell-free extract and 60 µl of NADPH (0.75 mM) to 600 µl of lysis buffer. GOGAT activity was determined by monitoring the rate of NADPH oxidation at 340 nm (ε340 nm = 6.22 mM^{-1} cm^{-1}, (Dougall, 1974)).

Immunoblot Analysis. A total of 20 or 45 µg of total protein (p*leuCD* or p*acnA* samples, respectively) were separated using an 8% SDS-PAGE gel. Proteins were then transferred to a PVDF membrane and incubated with mouse monoclonal anti-FLAG primary antibody (1:4000 dilution) and subsequently HRP conjugated secondary antibody (1:12000 dilution). The blots were developed using chemi-luminescent detection (Pierce). The blots were scanned as TIFF images.

Measurement of Endogenous Reactive Oxygen Species. Intracellular ROS was measured as previously described (Myhre *et al.*, 2003; Arenas *et al.*, 2011; Tavares *et al.*, 2011). Cultures were grown in TSB until they reached an OD_{600} of 6. Cells were harvested, washed

twice with PBS and resuspended in PBS. The 2',7'-dichlorofluorescein diacetate (DCFH-DA) probe was added to a final concentration of 10 μM. Fluorescence was monitored using a Perkin Elmer HTS 7000 Plus Bio Assay Reader by exciting at 485 nm and emission was read at 535 nm. Fluorescence units were normalized with respect to (i) the auto-fluorescence of DCFH-DA and then to (ii) the optical density (A_{590}) of each culture.

Recombinant Protein Overproduction and Purification. *E. coli* strain BL21 AI containing a protein expression vector was grown in 2x standard LB at 37°C in 3 L Fernbach flasks containing 1 L of media. Cultures were grown to an OD_{600} of 0.6 then cooled to 25°C. Arabinose (1 mM) and IPTG (0.1 mM) were added. Cultures were grown for an additional 12 hours before cells were harvested by centrifugation. Cell paste was flash frozen with liquid nitrogen and stored at -80°C.

Frozen cell paste was suspended in two volumes of buffer A (50 mM Tris-HCl, pH 8.0, 150 mM NaCl) containing DNase (0.03 mg ml^{-1}). Cell suspensions were passed three times through a chilled French pressure cell at 4°C. Cell lysates were clarified by centrifugation (39,000 X g for 40 min at 4°C). The clarified cell extract was loaded onto a 1.6 x 10 cm pre-equilibrated Ni^{2+}-loaded Chelating Sepharose Fast Flow (Qiagen) column and washed with 20 column volumes of 50 mM Tris, pH 8.0, 1 M NaCl. The column was equilibrated with buffer A and recombinant protein was eluted during a 30 column volume linear gradient from 0 to 100% elution buffer (50 mM Tris, pH 8.0, 250 mM imidazole). Fractions that contained the protein of interest at >95% purity by SDS-PAGE analysis were pooled and dialyzed overnight in 50 mM Tris-HCl, pH 8.0, 10% (v/v) glycerol, and 150 mM NaCl. The SufA protein was concentrated over a 3,000 Da molecular mass cutoff membranes (Amicon). Finally, the proteins were pelleted into liquid nitrogen and stored at -80°C until needed. All steps were performed at 4°C and buffers used for dialysis had the pH adjusted at 4°C. Iron and sulfur determination was conducted as previously described (Boyd

et al., 2009). The SufA Fe-S cluster was destroyed and iron was removed from the sample as previously described (Kennedy and Beinert, 1988). EDTA was removed from the SufA solution by dialysis against buffer A and three successive buffer exchanges.

Anaerobic Work. Anaerobic work was performed using a Coy anaerobic chamber (Grass Lake, MI) or vacuum manifold. Solutions, plasticware and liquid and solid growth media was allowed to equilibrate (> 6 hours) inside the chamber before use. Petri plates containing solid media were incubated in an air incubator within the anaerobic chamber.

Fe-S Cluster Reconstitution. All the steps were performed under strictly anaerobic conditions (<1 ppm dioxygen). Purified SufA was adjusted to 60 μM in reconstitution buffer (50 mM Tris, 150 mM NaCl, 5 mM DTT, pH 7.5). Protein was allowed to reduce for 1 hr. Cluster reconstitution was initiated by adding a five-fold excess of ferrous ammonium sulfate and lithium sulfide (300 μM final concentration) as previously described (Boyd *et al.*, 2009). The reaction mixture was allowed to proceed for 1 hr before excess Fe and S were removed by desalting using a PD-10 column (GE Healthcare) that had been pre-equilibrated with reconstitution buffer. Reconstituted protein was concentrated using YM-3 Centriplus Centrifugal Concentrators (Millipore), prior to use in activity assays. UV-Visible absorption spectra were recorded using a Beckman-Coulter DU800 spectrophotometer.

Fe-S Transfer Assay. All steps were performed under anaerobic conditions (<1 ppm dioxygen), in a Coy anaerobic chamber. Purified, recombinant AcnA was incubated in reconstitution buffer for 30 minutes. Cluster transfer mixtures were obtained by combining 4 μM AcnA and 4 μM SufA in a final volume of 20 μl in reconstitution buffer. As a control, SufA was left out of the reaction mixture and replaced with 8 μM Fe^{2+} and 8 μM S^{2-} (in reconstitution buffer). Mixtures were incubated at room temperature (23°C) for the indicated amounts of time, at which point 16 μl aliquots were removed and assayed for AcnA activity.

Activity assays were performed in final volume of 1 ml and contained reconstitution buffer with 20 mM DL-isocitrate. AcnA activity was assayed as described above.

Results

An *S. aureus* strain lacking BSH has a growth defect in a chemically defined medium that is corrected by exogenous iron supplementation. The *bshA* (SAUSA300_1349) and *bshC* (SAUSA300_1071) gene products catalyze the first and last steps of the BSH biosynthetic pathway, respectively (Gaballa *et al.*, 2010; Parsonage *et al.*, 2010; Upton *et al.*, 2012). Inactivation of either *bshA* or *bshC* results in an inability to synthesize BSH in *S. aureus* (Rajkarnikar *et al.*, 2013). In order to study the physiological role(s) of BSH, we created *bshA* and *bshC* mutant strains in the *S. aureus* community-acquired MRSA strain USA300 LAC (Burlak *et al.*, 2007). The mutant strains were verified using PCR (**Figure 1.S1**) and phenotypic analysis found that the generation times of the wild-type (WT; 0.8 ± 0.1 hr) and BSH-deficient (*bshA*; 0.8 ± 0.1 hr) strains were not significantly different when cultured in complex liquid media (TSB).

To further investigate the physiological roles of BSH in *S. aureus*, we utilized a chemically defined medium for growth containing 11 amino acids (AA) (11AA; PRMCLVYTFGH), as well as, sources of nitrogen, phosphorus, sulfur, and four vitamins. The absence of any of the 11 AA or glucose resulted in either no growth or a severe growth defect in the WT strain, suggesting that the supplied AA did not provide sufficient carbon for growth (data not shown).

The WT and *bshA* mutant were cultured to either stationary or exponential growth phase in TSB before washing the cells and subculturing into a defined medium containing 11 AA. The *bshA* mutant strain displayed an extended lag prior to outgrowth when compared to the WT strain. This phenotype was noted when strains were subcultured from cultures grown to either stationary (**Figure 1.1A)** or exponential growth phase (**Figure 1.S2A**). The generation times of the *bshA* strain subcultured from either stationary or exponential growth

phase cultures were ~3-fold greater than the generation times of the WT strain (**Table 1.S2**). Importantly, we were able to genetically complement these defects, verifying that the absence of the *bshA* gene was responsible for the observed phenotypes (**Figure 1.1A**).

We found that supplementation of the 11 AA growth medium with iron (>50 μM Fe^{2+}) decreased the time that it took for the *S. aureus* BSH-deficient strain to initiate outgrowth when subcultured from either stationary (**Figure 1.1B**) or exponential phase (**Figure 1.S2B**) cultures. In addition, supplementation of the growth medium with Fe significantly decreased the generation time of *bshA* mutant strain (**Table 1.S2**). Supplementing the medium with either Cu^{2+}, Zn^{2+}, Co^{2+}, or Mn^{2+} did not improve the extended lag phase or decrease the generation time of the *bshA* mutant, suggesting that the growth correction is specific to Fe (data not shown). For the remainder of this thesis, unless explicitly stated, the chemically defined or complex media was not supplemented with exogenously supplied Fe.

The *bshA* mutant strain displays poor growth in media lacking isoleucine or leucine. Results presented above show that a *bshA* mutant strain has a growth defect when cultured in an 11 AA medium, and such defect is alleviated by supplementing the medium with Fe. We examined whether any alternative factors could also correct the growth defect of the *bshA* mutant strain.

We found that the time taken for the *bshA* mutant strain to initiate outgrowth was also decreased when subcultured from either stationary or exponential growth phase cultures into defined medium containing the 20 canonical AA (**Figure 1.2A** and **Figure 1.S2C**). The generation time of the *bshA* mutant strain was ~1.5-fold greater than the WT when subcultured from either stationary or exponential phase cultures (**Table 1.S2**).

We individually removed amino acids from the growth medium and found that the *bshA* mutant strain did not grow during the course of the assays when subcultured from either stationary (**Figure 1.2B**) or exponential (**Figure 1.S2D**) growth phase cultures into defined liquid medium containing 19 AA lacking leucine (Leu). We also found that the BSH-deficient strain had an extended lag phase relative to the WT strain when subcultured from either stationary (**Figure 1.2C**) or exponential (**Figure 1.S2E**) growth phase cultures into defined liquid medium containing 19 AA lacking isoleucine (Ile). Moreover, the generation times of the BSH-deficient cultures were increased in absence of Ile (**Table 1.S2**). Supplementation of either the Leu- or Ile-deplete 19 AA liquid media with Fe (>50 μM) corrected the growth phenotypes of the *bshA* mutant strain (data not shown).

The *bshA* mutant strain also displayed growth defects when cultured on chemically defined solid media lacking either Leu or Ile. We cultured the WT and *bshA* mutant in complex media, serial diluted the cultures, and spot plated the strains atop solid defined media. As shown in **Figure 1.S3**, the colonies of the *bshA* mutant were smaller than the WT colonies when cultured on 19 AA media plates lacking either Ile or Leu. The growth defects of the *bshA* mutant on solid media containing 19 AA were alleviated by supplementing the medium with either of the missing AA or Fe (**Figure 1.S3**).

Iron or amino acid limitation leads to decreased expression of genes necessary for protein synthesis. When cultured on defined medium containing 11 AA, the WT strain displayed an extended lag prior to outgrowth and this lag was decreased when the medium was supplemented with the remaining 9 canonical AA (**Figures 1.2 and 1.S2**). In *S. aureus*, AA limitation results in accumulation of (p)ppGpp and the induction of the stringent response (Crosse *et al.*, 2000; Geiger *et al.*, 2010). The accumulation of (p)ppGpp can result in growth arrest and an extended lag before outgrowth (Gao *et al.*, 2010), that is, in part, the

result of decreased transcription of genes necessary for protein synthesis including *rpsB*, *rpsL*, and *tsf* (Geiger *et al.*, 2010; Reiss *et al.*, 2012).

We examined whether subculturing from complex medium (TSB) into chemically defined 11 AA medium was resulting in decreased transcription of *rpsB*, *rpsL*, and *tsf*, that were alleviated upon subculturing into media containing 20 AA. As shown in **Figure 1.S4A**, the abundances of the transcripts corresponding to *rpsB*, *rpsL*, and *tsf* were decreased in cells subcultured from TSB into chemically defined medium containing 11 AA relative to the abundances in cells subcultured into medium containing 20 AA.

Supplementation of the 11 AA growth medium with Fe also decreased the time taken for the WT strain to initiate outgrowth, suggesting that the *S. aureus* cells cultured in our chemically defined medium were starved for Fe (**Figures 1.1 and 1.S2**). Previous studies found that Fe starvation results in (p)ppGpp accumulation triggering the stringent response (Vinella *et al.*, 2005; Miethke *et al.*, 2006). We quantified the abundances of mRNA transcripts corresponding to the *rpsB*, *rpsL*, and *tsf* genes from WT cells subcultured from a complex medium (TSB) into chemically defined media containing 11 AA with and without Fe supplementation (100 μM). As shown in **Figure 1.S4B**, the abundances of mRNA transcripts corresponding to *rpsB* and *rpsL* were increased upon Fe supplementation, whereas transcription of *tsf* was not significantly altered. Collectively, these findings suggest that subculturing *S. aureus* cells from TSB medium into chemically defined medium containing 11 AA leads to the stringent response, that can be attenuated by supplementing the chemically defined growth medium with either AA or Fe.

An *S. aureus* strain lacking BSH is defective in intracellular iron metabolism. Iron is essential for a number of cellular processes, yet high intracellular Fe pools can result in toxicity (Imlay and Linn, 1988; Keyer and Imlay, 1996). Cells maintain a low concentration

pool of cytoplasmic Fe not ligated by macromolecules sometimes referred to as free or non-incorporated Fe, that is used to metalate Fe-dependent enzymes and synthesize Fe-containing cofactors (Woodmansee and Imlay, 2002).

The *S. aureus isdB* gene encodes a protein involved in iron acquisition that is under the transcriptional control of the ferric uptake regulator (Fur) (Reniere and Skaar, 2008). Fur acts as a transcriptional repressor when bound to Fe (Horsburgh, Ingham, *et al.*, 2001). We used an *isdB* transcriptional reporter to qualitatively monitor the Fur-accessible Fe pool in the WT and *bshA* mutant strains. Overnight cultures were diluted to an OD of 0.1 (A_{600}) in chemically defined media containing 20 AA and luciferase activity monitored over time. As illustrated in **Figure 1.3A**, *isdB* transcriptional activity was increased in the *bshA* mutant strain when compared to the WT. The largest difference in transcriptional activity was noted during late exponential growth phase (3.5 hours post subculturing; (OD of 0.8 (A_{600})). These data suggest that a BSH-deficient strain has less Fur-accessible Fe than the WT resulting in derepression of *isdB*.

Two scenarios can explain the decreased Fur-accessible Fe in the BSH-deficient strain. The absence of BSH either result in decreased in Fe uptake, thereby lessening the total Fe load of the cell, or it results in decreased Fur-accessible Fe, without affecting total cellular Fe load. To differentiate between these scenarios, we examined whether the amount of total cellular Fe was increased in cells lacking BSH. Cells were cultured to an OD of 0.8 (A_{600}) in chemically defined medium containing 20 AA without Fe supplementation prior to determining total ^{56}Fe load using inductively coupled plasma mass spectrometry (ICP-MS). As illustrated in **Figure 1.3B**, there was not a significant difference in cell associated Fe load between the WT and *bshA* mutant. There was also not a significant difference in Fe load between the WT and *bshA* cells cultured in complex medium (TSB) to late exponential growth phase (**Figure 1.S5**). Collectively, these data suggest that an *S. aureus bshA* mutant

strain has decreased pools of Fur-accessible Fe, but the same overall Fe load as the WT strain.

An *S. aureus* strain lacking BSH is defective in Fe-S cluster biogenesis. The growth defects of the *bshA* mutant strain grown in defined media without either Leu or Ile led us to hypothesize that the absence of BSH resulted in a defect in synthesizing these amino acids. The biosynthesis Leu and Ile requires the enzymes isopropylmalate isomerase (IPMI) and dihydroxy-acid dehydratase (IlvD), respectively. The IPMI and IlvD enzymes are dehydratases that require a [Fe_4-S_4] cluster for catalysis (Kennedy *et al.*, 1983; Kohlhaw, 1988; Flint and Emptage, 1988). In *S. aureus*, IPMI is encoded by the *leuCD* genes.

The *S. aureus bshA* mutant did not grow in defined media lacking Leu, and therefore, we were unable to measure the activity of the *leuCD* gene products expressed at chromosomal levels from cells cultured in a medium lacking Leu. We were unable to detect LeuCD activity in cell extracts from strains cultured in media containing Leu (data not shown). To circumvent these problems, we cloned the *leuCD* genes under the transcriptional control of XylRO (p*leuCD*), that allowed us to culture the *bshA* mutant in media containing Leu and induce *leuCD* expression by the addition of xylose. In addition, this construct contained an N-terminal FLAG affinity tag on LeuC allowing us to monitor LeuC protein abundance. We found that p*leuCD* genetically complemented the Leu auxotrophy of a *leuD* mutant strain, thus verifying the functionality of our construct (data not shown). To ensure that the detected LeuCD activity was originating from the plasmid-based *leuCD* alleles, assays were conducted in strains containing a null allele of the chromosomally encoded *leuD* gene. The p*leuCD* vector was mobilized into the *leuD* and *bshA leuD* mutant strains. Cultures were grown to an OD of 1 (A_{600}) in 20 AA media prior to assessing LeuCD activity in cell lysates. The strain lacking BSH displayed 57 ± 7% LeuCD activity when compared to the parent strain (**Figure 1.4A**). Western blot analyses revealed that FLAG_LeuC protein

accumulated in both strains, but accumulation was lower in the *bshA* mutant strain (**Figure 1.4A, inset**). We quantified the abundance of the mRNA transcript corresponding to *leuC* in cells cultured as described above and found that *leuC* was induced to statistically indistinguishable levels in the WT and *bshA* mutant strains (**Figure 1.S6**).

The *bshA* mutant displayed a long lag prior to outgrowth when cultured in the absence of Ile and we were unable to detect IlvD activity in cells cultured in media containing Ile. We used a similar strategy as outlined above to monitor IlvD activity in the WT and *bshA* mutant strains. We cloned the *ilvD* gene into a plasmid under the transcriptional control of XylRO (p*ilvD*). The p*ilvD* plasmid genetically complemented an *ilvD* mutant strain verifying, the functionality of the plasmid-encoded *ilvD* allele (data not shown). N- or C-terminal FLAG-tagged IlvD variants did not functional *in vivo*. The p*ilvD* was mobilized into the *ilvD* and *bshC ilvD* mutant strains. Strains containing p*ilvD* were cultured defined media containing 20 AA, *ilvD* expression induced and IlvD activity was assessed in cellular lysates. When compared to the parent the IlvD activity was 49 ± 8% in the strain lacking BSH (**Figure 1.4B**).

The data presented suggest that Fe-S cluster-dependent proteins have lower activity in the BSH-deficient strains. We wanted to determine if the lack of BSH resulted in a general defect in Fe-S cluster biogenesis or if the effect was specific to the enzymes required for BCAA biosynthesis. Like LeuCD and IlvD, aconitase (AcnA) is a [Fe_4-S_4]-requiring dehydratase enzyme. We cloned the *acnA* gene into a plasmid under the transcriptional control of XylRO (p*acnA*). The construct included a C-terminal FLAG affinity tag to aid in monitoring protein abundance. The FLAG-tagged *acnA* allele genetically complemented the glutamate (Glu) and glutamine (Gln) requirement of an *acnA* mutant strain, verifying the functionality of the FLAG-tagged AcnA allele (data not shown). Strains containing p*acnA* were cultured in defined media containing 20 AA to an OD of 1 (A_{600}) in the presence and

absence of xylose to induce *acnA* expression. As shown in **Figure 1.4C**, the BSH-deficient strain had 64 ± 1% AcnA activity in cell-free lysates when compared to the parent strain. Western blot analysis revealed that the AcnA protein accumulated in both strains (**Figure 1.4C, inset**), but accumulation was lower in the *bshA* mutant strain. We quantified the abundance of the mRNA transcript corresponding to *acnA* in the WT and *bshA* mutant strains cultured as described above and found that it was induced to similar levels in both strains (**Figure 1.S6**).

The Fe-S cofactor of AcnA can be damaged by univalent oxidants causing oxidation of the $[Fe_4\text{-}S_4]$ cluster and cofactor disintegration to the non-catalytically active $[Fe_3\text{-}S_4]^{1+}$ cluster and Fe^{3+} (Kent *et al.*, 1982). Anaerobic incubation of non-active $[Fe_3\text{-}S_4]^{1+}$ AcnA with Fe^{2+} and a reductant results in a repaired $[Fe_4\text{-}S_4]$ cluster and active AcnA (Kennedy *et al.*, 1983). To determine if cell lysates harvested from the BSH-deficient strains were enriched for the $[Fe_3\text{-}S_4]^{1+}$ form of AcnA, we incubated crude extracts generated from the *acnA* and *bshA acnA* strains containing the p*acnA* with Fe^{2+} and DTT prior to assessing AcnA activity. We found that the AcnA activity in lysates harvested from the *bshA* mutant was ~65% that of the WT, but anaerobic incubation with Fe^{2+} did not increase AcnA activity in cell lysates harvested from either the WT or BSH-deficient strain (data not shown). These data verify that that a strain lacking BSH has decreased AcnA activity and suggest that this is not the result of enrichment for the inactive, but repairable $[Fe_3\text{-}S_4]^{1+}$ form of AcnA.

An *S. aureus* BSH-deficient strain does not accumulate increased intracellular ROS. *S. aureus* strains lacking BSH are sensitive to thiol and oxidative stressors (Rajkarnikar *et al.*, 2013; Posada *et al.*, 2014). Fe-S clusters can be oxidized by ROS resulting in cluster destruction and decreased activity of enzymes that require Fe-S clusters for catalysis (Imlay, 2006). ROS are formed as byproducts of growth in an aerobic environment and strains lacking ROS scavenging mechanisms accumulate endogenous ROS resulting in damage to

Fe-S clusters and decreased enzymatic activity of proteins requiring these cofactors (Keyer and Imlay, 1996; Keyer and Imlay, 1997; Jang and Imlay, 2007; Mashruwala *et al.*, 2015). We conducted a series of experiments to determine if the decreased activity of Fe-S cluster-dependent enzymes in an *S. aureus* strain lacking BSH could be the result of increased intracellular ROS.

S. aureus uses an ortholog of the *B. subtilis* PerR transcriptional repressor to sense and respond to H_2O_2 (Lee and Helmann, 2006). The *dps* gene, that encodes an iron-binding protein that protects DNA from oxidative damage, is a member of the PerR regulon and expression of *dps* is upregulated upon PerR oxidation by H_2O_2 (Horsburgh, Clements, *et al.*, 2001). We examined the transcriptional activity of the *dps* promoter as a proxy for PerR-dependent alterations in transcription. As shown in **Figure 1.5A**, the transcriptional activity of the *dps* promoter was similar in the WT and *bshA* mutant when cultured in 20 AA defined medium, but the activity was increased in the *ahpC* and *perR* mutant strains. These data (i) confirm that PerR is a repressor of *dps* transcription, (ii) suggest that an *ahpC* mutant has elevated H_2O_2 stress resulting in PerR derepression, and (iii) verify that a strain lacking BSH does not result in PerR derepression.

S. aureus has two superoxide dismutases (SodA and SodM). A strain lacking SodA has a growth defect upon aerobic growth (increased generation time), whereas a strain lacking SodM does not (data not shown). These findings are consistent with previous work suggesting that SodA is the primary superoxide dismutase in *S. aureus* cells when cultured under standard laboratory conditions (Wright Valderas and Hart, 2001). Additional studies found that *sodA* was induced by incubation with the redox cycling molecule methyl viologen, suggesting that *sodA* is induced when intracellular ROS accumulates (Clements *et al.*, 1999; Karavolos *et al.*, 2003).

We used a *sodA* transcriptional reporter construct as a proxy for intracellular ROS accumulation in the WT and *bshA* mutant strain. Strains harboring this construct were grown aerobically in 20 AA medium and transcriptional activity was monitored. The transcriptional activity of the *sodA* gene was similar in the *bshA* mutant and WT strains (**Figure 1.5B**). Importantly, as previously noted, the promoter activity of *sodA* increased upon addition of methyl viologen and transcriptional activity increased to similar levels in the WT and *bshA* mutant strains. These data suggest that *bshA* mutant strain does not accumulate a higher titer of ROS than the WT strain.

We qualitatively measured intracellular ROS using the compound 2',7'-dichlorofluorescin diacetate (DCHF-DA) (Arenas *et al.*, 2011; Tavares *et al.*, 2011). DCHF-DA is membrane permeable and is converted to the fluorescent molecule 2',7'-dichlorofluorescein (DCF) upon oxidation (Wang and Joseph, 1999; Myhre *et al.*, 2003). We cultured the WT and *bshA* mutant strains aerobically to mid-exponential phase (OD of 6 (A_{600})) in TSB and monitored DCF formation in cell suspensions. The rate of DCF formation was also assessed in an *ahpC* mutant strain as a positive control. The WT and *bshA* mutant strains had similar rates of DCF formation, whereas the *ahpC* mutant had an increased rate of DCHF-DA oxidation indicative of increased ROS accumulation (**Figure 1.5C**).

Lastly, we examined whether the growth defects of the *bshA* mutant were dioxygen-dependent. To this end, we serial diluted cultures of the WT and *bshA* mutant and spot plated the strains on 19 AA solid media lacking either Leu or Ile and incubated the cultures either aerobically or anaerobically. We included 20 mM nitrate as a terminal electron acceptor for anaerobic incubations. When compared to the WT, the *bshA* mutant strain displayed a small colony phenotype on plates lacking either Leu or Ile when incubated in the presence or absence of dioxygen (data not shown). As previously noted, the growth defects of the *bshA* mutant were alleviated by supplementing the media with either the missing AA or Fe (data

not shown). These data suggest that the phenotypes exhibited by *S. aureus* strains lacking BSH are not oxygen-dependent or the result of increased intracellular ROS.

Genetic analyses provide insight into the function of BSH in Fe-S cluster biogenesis. The data presented led to the hypothesis that BSH has a role in Fe-S cluster biogenesis. We examined whether *bshA* had a genetic interaction with additional genes involved in Fe-S cluster biogenesis. Work in our group has found that the Nfu protein (SAUSA300_0839) can bind and transfer Fe-S clusters *in vitro* and that an *nfu* mutant strain has decreased activity of Fe-S cluster requiring proteins *in vivo* leading to the hypothesis that Nfu is an Fe-S cluster carrier (Mashruwala *et al.*, 2015). *S. aureus* also has a putative A-type Fe-S cluster carrier protein (SufA; SAUSA300_0843) (Krebs *et al.*, 2001; Vinella *et al.*, 2009). We have not been successful in constructing strains with null or deletion mutations in the SufCDSUB Fe-S cluster assembly system (Mashruwala *et al.*, 2015). Our findings, in conjunction with the findings of others, has led to a model wherein both the Nfu and SufA proteins can accept Fe-S clusters from the Suf Fe-S cluster biosynthetic machinery and traffic the cofactors to apoproteins (**Figure 1.10**).

We constructed the *bshA nfu* and *bshA sufA* double mutant strains and conducted auxanographic analysis. In addition to Ile and Leu auxotrophies, the *bshA nfu* double mutant strain did not grow in media lacking Glu and Gln (**Figure 1.6A**). The *bshA nfu* double mutant was proficient for growth in 20 AA defined medium (data not shown). Returning either the *nfu* or *bshA* genes to the *bshA nfu* double mutant abolished the need to supplement the media with Glu and Gln (data not shown). The growth of the *bshA sufA* double mutant in chemically defined media was indistinguishable from that of the *bshA* mutant strain (data not shown).

AcnA is necessary to produce α-ketoglutarate, the precursor for Glu and Gln biosynthesis and an *acnA* mutant cannot grow in media lacking Glu and Gln (**Figure 1.6A**). We assayed AcnA activity in cell-free lysates generated from the WT, *bshA*, *nfu,* and *sufA* strains, as well as, the *bshA sufA* and *bshA nfu* double mutant strains that had been cultured to an OD of 1 (A_{600}) in chemically defined medium containing 20 AA. As illustrated in **Figure 1.6B**, AcnA activity in the *bshA nfu* double mutant was lower than AcnA activity of the *bshA* and *nfu* single mutants. The *sufA* mutant strain did not display decreased AcnA activity and the AcnA activity in the *bshA sufA* double mutant was indistinguishable from that of the *bshA* mutant.

Glutamate synthase (GltBD or GOGAT) is an Fe-S cluster dependent enzyme that generates Glu from Gln and α-ketoglutarate (Vanoni and Curti, 1999). We hypothesized that the Glu and Gln requirment of the *bshA nfu* double mutant was, in part, due to a defect in GOGAT function. The WT, *bshA*, *sufA*, *nfu* strains, as well as, the *bshA sufA* and *bshA nfu* double mutant strains were cultured to an OD of 1 (A_{600}) in a defined medium containing 20 AA and GOGAT activity assessed in cell-free lysates. As a control, we included a *gltD* mutant strain. When compared to the GOGAT activity of the WT strain, the *bshA, nfu,* and *bshA nfu* strains showed 50 ± 2 %, 47 ± 2 %, and 23 ± 7 % GOGAT activity, respectively (**Figure 1.6C**). GOGAT activity was slightly decreased in the *sufA* mutant (79 ± 13 %), but the effects of the *bshA* and *sufA* mutations on GOGAT activity were not additive. The *gltD* mutant strain did not have detectable GOGAT activity (data not shown). These data suggest that the Nfu and BSH molecules are functionally redundant in Fe-S cluster biogenesis and their roles are not limited to Fe-S cluster-dependent dehydratase enzymes.

The defects of strains lacking BSH are suppressed by multicopy expression of genes encoding Fe-S cluster biogenesis factors. Functional overlap has previously been shown to exist between Fe-S cluster assembly and trafficking components. We examined whether the

growth defects of the BSH-deficient strain could be suppressed by multicopy expression of genes encoding alternate Fe-S cluster biogenesis factors. To this end, we placed additional copies of the *sufCDSUB* operon into the *bshA* mutant strain via multicopy plasmid (pCM28_*sufCDSUB*) and conducted phenotypic analysis. The presence of the *sufCDSUB* genes *in trans* did not correct the growth defects or the decreased AcnA activity of the *bshA* mutant strain (data not shown).

We individually introduced the *nfu* and *sufA* genes into the *bshA* mutant strain in multicopy via episome (p*nfu* and p*sufA*). As shown in **Figure 1.7A**, *sufA* overexpression partially rescued the Ile- and Leu-dependent growth defects of the *bshA* mutant strain on solid chemically defined media. The presence of *sufA* in multicopy also corrected the growth of the *bshA* mutant in defined liquid medium containing 19 AA, but lacking Ile (**Figure 1.S7**). We also found that multicopy expression of *sufA* increased the AcnA activity in cell-free lysates harvested from a BSH-deficient strain (**Figure 1.7B**), while it did not significantly affect the growth or AcnA activity of the WT strain.

Overexpression of *nfu* provided a slight correction of the Leu- and Ile-dependent growth defects of the *bshA* mutant on solid media (**Figure 1.7A**). The presence of *nfu* in multicopy also increased the AcnA activity in cell-free lysates harvested from the *bshA* mutant strain, but no significant difference was observed in the WT strain (**Figure 1.7B**).

We next examined whether *sufA* expression was altered in a *bshA* mutant. To this end, we cultured the WT, *bshA*, and *sufA* mutant strains to an OD of 1 (A_{600}) in chemically defined media containing 20 AA and quantified the abundance of the mRNA transcript corresponding to *sufA*. We found that the *sufA* transcript accumulated to similar levels in the WT and *bshA* strains, but was undetectable in the *sufA* mutant **(Figure 1.S8)**. These data suggest that *sufA* is transcribed in the *bshA* mutant, but not expressed at a level sufficient to

compensate for absence of BSH. Collectively, these data suggest that the role of BSH in Fe-S cluster biogenesis in *S. aureus* has functional overlap with the proposed Fe-S cluster biogenesis factors SufA and Nfu.

The *S. aureus* SufA protein can bind and transfer Fe-S clusters. Results shown above show that *sufA* overexpression suppressed the phenotypes of *bshA* mutant strain, but the function(s) of the *S. aureus* SufA had not been verified. The SufA protein from *S. aureus* USA300 LAC shares 33-37% identity with the previously described A-type trafficking proteins SufA, ErpA, and IscA from *E. coli*. In addition, the cysteine residues thought to act as ligands for the Fe-S cluster (Cys: 37, 101, and 103) are conserved in the *S. aureus* SufA proteins from diverse clinical isolates. Phenotypic studies found that the *sufA* mutant strain did not display any growth defects and has the same generation times as the WT strain when cultured in defined or complex media (data not shown).

The *sufA* mutant strain did not have decreased AcnA activity in cellular lysates when AcnA was expressed from the chromosome using the native promoter **(Figure 1.6B)**, but we had not controlled for possible differences in *acnA* expression between the WT and *sufA* mutant strain. We examined whether a *sufA* mutant had lower AcnA activity when *acnA* expression is decoupled from the native promoter. We disrupted the chromosomal *acnA* allele and mobilized the p*acnA* plasmid into the *acnA* and *sufA acnA* double mutant strains. Using p*acnA* allowed us to assay AcnA activity and monitor protein abundance in cell free lysates. We assessed AcnA activity in a *nfu acnA* double mutant as a control (Mashruwala *et al.*, 2015). As shown in **Figure 1.8A**, the AcnA activity in the cell-free lysates harvested from the *sufA* or *nfu* mutant strains was 66 ± 1% and 56 ± 3% of the AcnA activity of the parent strain, respectively. Western blot analysis revealed that AcnA protein accumulated in all strains (**Figure 1.8A, inset**).

To verify these findings, we constructed the *sufA leuD* and *nfu leuD* double mutant strains and mobilized the p*leuCD* plasmid into these strains. The LeuCD activity was assayed in the *nfu leuD* double mutant as a control. The LeuCD activity in cell-free lysates harvested from the *sufA* and *nfu* mutant strains was 64 ± 9% and 54 ± 1% of the LeuCD activity of the parent strain, respectively (**Figure 1.8B**).

We next tested the hypothesis that SufA could bind an Fe-S cluster *in vitro*. The *S. aureus* SufA was overproduced in and purified from *E. coli*. The purified SufA protein had a reddish brown color, similar to that of Fe-S cluster-containing proteins, but the color diminished upon aerobic dialysis consistent with SufA binding a labile, dissociable cofactor (data not shown). The protein was transferred to an anoxic atmosphere and the Fe-S cluster was chemically reconstituted. The holo-SufA had a UV-Visible absorption spectrum similar to previously examined holo-A-type carrier proteins (**Figure 1.8C**) (Krebs *et al.*, 2001; Gupta *et al.*, 2009). Metal analysis found that holo-SufA bound 2.4 ± 0.2 atoms of S and 2.3 ± 0.3 atoms of Fe (n = 4) per protein monomer. The stoichiometry of metal binding and spectral data are suggestive of Fe-S cluster binding by the *S. aureus* SufA protein.

We then examined whether holo-SufA could transfer an Fe-S cluster to an apoprotein. We overproduced and purified *S. aureus* AcnA from *E. coli*. We removed the Fe-S cluster from AcnA resulting in a protein that was enzymatically inactive. Upon chemical reconstitution, the *S. aureus* holo-AcnA had a maximal specific activity of 48 units mg^{-1} with isocitrate as a substrate. We then combined apo-AcnA (4 μM) with an equimolar concentration of reconstituted holo-SufA (4 μM) or a two-fold excess of Fe^{2+} and S^{2-} (8 μM each). Samples were periodically removed and AcnA activity assessed. As illustrated in **Figure 1.8D**, the holo-SufA was able to activate the AcnA enzyme whereas the combination of DTT, Fe and S did not significantly increase AcnA activity during the course of the assay. Our results show that the holo-SufA (4 μM) activated ~54% of the AcnA (4 μM; assuming

that maximal activity is 48 units mg^{-1}) during the course of the assays. Metal analysis found that holo-SufA bound 2.4 Fe per monomer implying that we added ~9.6 μM Fe to our assays via holo-SufA. It requires 16 Fe atoms to fully activate 4 μM AcnA, and therefore, we expected ~60% activation upon holo-SufA addition, which is slightly higher than the 54% activation witnessed upon incubation of apo-AcnA with holo-SufA. Collectively, the results presented are consistent with the hypothesis that the *S. aureus* SufA protein is an Fe-S cluster carrier protein.

BSH has a conserved role in staphylococcal metabolism. We aimed to determine if alternate *S. aureus* isolates lacking BSH are defective in Fe-S cluster biogenesis. We constructed and examined the phenotypes of BSH-deficient strains in the *S. aureus* isolates Newman, MW2, and COL. Strains lacking BSH displayed various phenotypes when grown in defined media. The Newman *bshA* mutant strain did not grow in the 18 AA medium lacking both Ile and Leu (**Figure 1.9A**) and it displayed an increased generation time in the 20 AA medium (**Table 1.S2**). The MW2 strain lacking BSH did not grow without Ile and Leu supplementation (data not shown), as well as, Glu and Gln (**Figure 1.9B**), and the *S. aureus* COL strain lacking BSH had an extended lag before outgrowth when cultured in the absence of Ile (**Figure 1.9C**). The generation times of the MW2 *bshA* and COL *bshA* mutant strains were not statistically different from their respective parent strains (**Table 1.S2**).

We examined AcnA activity (expressed from the chromosome) in cellular lysates of the BSH-deficient and BSH-proficient strains in the different *S. aureus* backgrounds. In all isolates examined, strains lacking BSH had lower AcnA activity than the respective parent strain (**Figure 1.9D**).

Results presented above found that the presence of *sufA* in multicopy partially corrected the phenotypic defects of an *S. aureus* USA300 LAC *bshA* mutant strain. We

examined whether the presence of *sufA* in multicopy also corrected the phenotypes of the *S. aureus* strains COL, MW2 or Newman lacking BSH. The presence of the *sufA* gene in multicopy corrected the growth defects of the COL *bshA* mutant strain (**Figure 1.S9A**) and the Glu and Gln auxotrophies of the MW2 *bshA* mutant strain (**Figure 1.S9B**). Surprisingly, the presence of the *sufA* gene in multicopy in the Newman background resulted in a severe growth defect in the parental strain (data not shown). Collectively, the data presented suggest that BSH has a conserved role in Fe-S cluster biogenesis in *S. aureus*.

Discussion

Staphylococcus aureus does not synthesize the well studied low-molecular-weight (LMW) thiol glutathione (GSH), but it does produce the LMW thiols bacillithiol (BSH), coenzyme A and cysteine (delCardayré *et al.*, 1998; Newton *et al.*, 2009; Gaballa *et al.*, 2010). Work by others found that BSH, like GSH, can function as an intracellular redox buffer and detoxification agent (Newton *et al.*, 2009; Chi *et al.*, 2011; Sharma *et al.*, 2013; Gaballa, Chi *et al.*, 2013; Chandrangsu *et al.*, 2014). The work presented herein suggests that BSH also functions in the biogenesis of Fe-S clusters.

There are various links between LMW thiols and Fe-S clusters. In many organisms, cysteine serves as the sulfur source to synthesize Fe-S clusters (Zheng *et al.*, 1993). In addition, a majority of Fe-S clusters are bound by proteins using cysteine thiolates as ligands (Beinert *et al.*, 1997). LMW thiols can directly ligate Fe-S clusters or act as ligands for Fe-S clusters in conjunction with a protein (Bandyopadhyay, Gama, *et al.*, 2008; Qi *et al.*, 2012). Lastly, LMW thiols can provide electrons for (i) the reduction of disulfide bonds freeing potential Fe-S ligating cysteine thiols (Schafer and Buettner, 2001), and (ii) the reduction of peroxides, thereby preventing damage to Fe-S clusters (Mills, 1957; Jang and Imlay, 2007).

Genetic and biochemical studies have defined roles for GSH in Fe-S cluster biogenesis in both eukaryotes and prokaryotes (Gardner and Fridovich, 1993; Rodríguez-Manzaneque *et al.*, 2002; Skovran and Downs, 2003; Gralnick and Downs, 2003; Thorgersen and Downs, 2009). In fact, it is possible that GSH has a role in all four modules of Fe-S cluster biogenesis: synthesis, trafficking, insertion and repair.

GSH has a role in trafficking and inserting Fe-S clusters. A number of monothiol glutaredoxin proteins are involved in sensing and trafficking intracellular iron. Strains lacking specific monothiol glutaredoxins display growth defects, have altered intracellular

iron pools and have decreased activity of enzymes that require Fe-S clusters for catalysis (Rodríguez-Manzaneque *et al.*, 2002; Mühlenhoff *et al.*, 2010; Yeung *et al.*, 2011). In conjunction with monothiol glutaredoxins, GSH can ligate an Fe-S cluster, that can subsequently be transferred to an apoenzyme (Feng *et al.*, 2006; Iwema *et al.*, 2009; Luo *et al.*, 2010; Zhang *et al.*, 2013). GSH can also directly bind and transfer an Fe-S cluster *in vitro*, but whether this occurs *in vivo* is currently unknown (Qi *et al.*, 2012). In addition, GSH has a role in inserting Fe-S clusters by maintaining reduced thiols in apoproteins that can act as ligands for Fe-S clusters. Evidence also exists suggesting that GSH plays a role in trafficking Fe-S clusters or a molecule necessary for Fe-S synthesis from the mitochondrion to the cytosol in eukaryotic cells (Srinivasan *et al.*, 2014).

GSH could function in *de novo* Fe-S cluster synthesis and repair. GSH acts as a cytosolic Fe buffer by ligating Fe, thus decreasing the concentration of non-incorporated Fe in the cytosol (Thorgersen and Downs, 2008; Hider and Kong, 2011), and therefore, it is possible that GSH has a role in providing Fe for *de novo* Fe-S cluster biogenesis. In *E. coli*, the activity of AcnA is inversely proportional to the concentration of headspace dioxygen, that is likely due to dioxygen or ROS damage to the Fe-S cluster. Reactivation of damaged AcnA was slowed in the absence of GSH although it was not determined whether this was the result of defective *de novo* Fe-S cluster biogenesis or defective Fe-S cluster repair (Gardner and Fridovich, 1993). After oxidation, $[Fe_4\text{-}S_4]^{3+}$ clusters can disintegrate into $[Fe_3\text{-}S_4]^{1+}$ and Fe^{3+} (Djaman *et al.*, 2004). Repair of the $[Fe_3\text{-}S_4]^{1+}$ cluster requires an electron and Fe^{2+} and it has been proposed that GSH can provide electrons to reduce Fe^{3+} to Fe^{2+} (Nappi and Vass, 1997). GSH could also act as the Fe^{2+} donor for Fe-S cluster repair. It should be noted that a GSH deficient *E. coli* repair $[Fe_3\text{-}S_4]^{1+}$ clusters at the same rate as GSH proficient strains (Djaman *et al.*, 2004).

The study herein demonstrates that BSH also has a role in Fe-S cluster biogenesis, but our findings raise the question as to what function BSH might perform in this process. We have placed BSH in the Fe-S cluster trafficking module of Figure 10 because of the following findings: (i) strains lacking BSH have phenotypic similarities to a strain lacking the Fe-S cluster trafficking molecule Nfu, (ii) strains lacking BSH have decreased activities of Fe-S cluster-requiring enzymes, (iii) the decreased activity of AcnA in a *bshA* mutant strain is not corrected by incubation with reductant and Fe^{2+}, suggesting that the lack of BSH does not result in an enrichment of the [Fe_3-S_4] form of AcnA, (iv) the phenotypes of a strain lacking BSH are exacerbated in a strain lacking an Fe-S cluster carrier (Nfu), and (v) the phenotypes of the BSH-deficient strains are partially suppressed by multicopy expression of either the SufA or Nfu Fe-S cluster carriers.

In *B. subtilis*, BSH acts as a cytosolic Zn buffer and BSH binds Zn *in vitro* with high affinity (Ma *et al.*, 2014). It is reasonable to hypothesize that BSH also serves as an Fe buffer in *S. aureus*. In such a capacity, BSH could aid in providing Fe for cellular processes such as Fe-S cluster biogenesis. In support of this hypothesis, we found that *S. aureus* strains lacking BSH (i) had growth defects that are corrected by supplementing the growth media with Fe, (ii) had decreased Fur accessible Fe, but the same overall Fe load as the WT, and (iii) had phenotypes that were corrected by overexpression of the A-type carrier SufA. In addition to their roles as Fe-S cluster carriers, A-type carriers bind Fe^{2+} and Fe^{3+} *in vitro* (Huangen Ding and Clark, 2004; Mapolelo *et al.*, 2012). The Fe^{3+} bound forms of A-type carriers can provide Fe for Fe-S cluster assembly on the U-type (NifU and IscU) Fe-S cluster scaffolds *in vitro* in the presence of cysteine (Baojin Ding *et al.*, 2005; Mapolelo *et al.*, 2012). Further genetic and biochemical studies support a role for Fe binding by A-type carriers in Fe-S cluster assembly *in vivo* (Huangen Ding *et al.*, 2004; Landry *et al.*, 2013). We should note that *nfu* overexpression also corrected the decreased AcnA activity of BSH-deficient cells

and Nfu has not been shown to bind mononuclear Fe. Our lab is actively testing the hypothesis that BSH acts as a cellular Fe buffer.

Similar to our findings, studies in *S. enterica* found that the addition of exogenous Fe corrects the growth defects and auxotrophies of strains deficient in Fe-S cluster biogenesis (Skovran and Downs, 2003; Skovran *et al.*, 2004). Moreover, *S. enterica* mutants lacking GSH have decreased Fur-accessible Fe (Thorgersen and Downs, 2008). Likewise, we found that the BSH-deficient strains have decreased Fur accessible Fe and the growth defects are corrected by supplementing the growth medium with Fe. *E. coli* strains missing the Isc Fe-S cluster biosynthetic system or the NfuA Fe-S cluster trafficking protein are sensitive to Fe starvation (Outten *et al.*, 2004; Angelini *et al.*, 2008). Work by Rolfe et al. found that during the lag phase of growth, *S. enterica* increased transcription of genes that function in Fe acquisition (Rolfe *et al.*, 2012). The mRNA transcript abundances corresponding to the *suf*ABCDE genes, that are induced under Fe starvation conditions (Outten *et al.*, 2004), also increased during the lag growth phase. These transcriptional changes resulted in increased Fe uptake and an overall increased cellular Fe load in preparation for exponential growth. Interestingly, transcriptional profiling in *S. aureus* found that mRNA abundance corresponding to genes encoding putative Fe acquisition proteins (*isdA*, *isdC*, *feoA*, *feoB*, *fhuA, fhuB* and *sirA*) were altered in a strain lacking BSH (Posada *et al.*, 2014). To our knowledge, strains lacking GSH do not have an extended lag prior to outgrowth or have increased generation times that are corrected by the addition of Fe to the growth media.

Our results show that the activities of the Fe-S cluster dependent enzymes AcnA, LeuCD, IlvD and GOGAT were decreased in the *bshA* mutant. We also found that AcnA and LeuC proteins accumulated in both the WT and *bshA* mutant, but accumulated to lower levels in the strains lacking BSH. Interestingly, the *acnA* and *leuC* genes were induced to similar levels in the WT and *bshA* strains. It is currently unknown why these proteins accumulate to

lower levels in the *bshA* mutant, but we have noted similar phenomena in alternate *S. aureus* strains missing Fe-S cluster biogenesis factors (Nfu or SufT; Figure 8A and A.A. Mashruwala and J.M. Boyd, unpublished results). As previously mentioned, damaged $[Fe_3\text{-}S_4]^{1+}$ clusters can be repaired by anaerobic incubation with Fe^{2+}. We found that the addition of Fe^{2+} and DTT did not increase the activity of AcnA in cell-free lysates of the *bshA* mutant suggesting that we were not enriching for the $[Fe_3\text{-}S_4]^{1+}$ form of AcnA in the *bshA* mutant under the conditions examined. One possible explanation for our findings is that the rate of Fe-S cluster incorporation into apo-AcnA and apo-LeuCD is decreased in a BSH-deficient strain and the cellular proteolytic machinery degrades the apo-forms of the enzymes at a faster rate than the holo-forms. This scenario is supported by the findings that particular Fe-S proteins are turned over by the cellular proteolysis machinery at a faster rate in the apo-form relative to the holo-form (Mettert and Kiley, 2005; Wang *et al.*, 2007; Crooks *et al.*, 2010; Pan *et al.*, 2012). We are currently examining the role(s) of the Clp proteasome in processing holo- and apo-forms of Fe-S proteins.

The growth phenotypes and decreased AcnA activity of the BSH-deficient strains was partially alleviated by multicopy expression of genes that encode Fe-S cluster carriers. Work by our group and others has found that the growth defects of strains lacking a particular Fe-S cluster biosynthesis scaffolding/trafficking protein can be suppressed by overexpression of a gene encoding alternative biosynthesis scaffolding/trafficking protein (Takahashi and Tokumoto, 2002; Tokumoto *et al.*, 2004; Santos *et al.*, 2007; Bandyopadhyay, Naik, *et al.*, 2008; Boyd *et al.*, 2008; Vinella *et al.*, 2009). It should be noted that while overexpression of *sufA* or *nfu* correct some or all of the phenotypes of a BSH-deficient strain, multicopy expression of the *sufCDSUB* operon does not correct these phenotypes. These findings suggest that the presence of BSH may not augment Fe-S cluster biosynthesis in a linear pathway consisting of SufCDSUB and Fe-S cluster carrier molecules.

Biochemical studies on the *S. aureus* SufA found that it bound equimolar quantities of Fe and S and had spectral properties similar to alternate characterized A-type proteins ligating an Fe-S cluster (Wollenberg *et al.*, 2003; Gupta *et al.*, 2009; Mapolelo *et al.*, 2012). A-type proteins have been found to ligate either [Fe_2-S_2] or [Fe_4-S_4] clusters *in vitro*, but native *E. coli* SufA purifies with a [Fe_2-S_2] cluster (Gupta *et al.*, 2009; Mapolelo *et al.*, 2012). The nature of the Fe-S cluster bound by *S. aureus* SufA is currently unknown and will require additional biophysical experimentation. The holo-SufA protein was also able to activate *S. aureus* AcnA protein, whereas apo-SufA or a combination of Fe, S, and DTT were not. The rate at which *S. aureus* holo-SufA activated apo-AcnA was similar to the reported rates for Fe-S cluster transfer from *E. coli* SufA to apo-ferredoxin, as well as, *Synechocystis* PCC6803 IscA to apo-adenosine 5'-phosphsulfate reductase (Wollenberg *et al.*, 2003). Higher rates of Fe-S cluster transfer from holo-A-type carriers (both [Fe_2-S_2] and [Fe_4S_4] forms) to apoproteins have been noted and it is currently unknown why there are discrepancies in the rates of Fe-S cluster transfer to apoproteins (Mapolelo *et al.*, 2013).

The growth of various *S. aureus* clinical and laboratory isolates lacking BSH displayed differences in the severity and complexity of phenotypes. Importantly, the growth phenotypes were suppressed by either providing amino acids that require Fe-S enzymes for synthesis or by the expression of *sufA* or *nfu* from a multicopy plasmid. In addition, the activity of AcnA was decreased in all BSH-deficient strains examined. The *S. aureus* BSH-deficient strain with the most amino acid auxotrophies (MW2; Leu, Ile, Glu an Gln) also had the lowest AcnA activity in extracts. Variations in the levels of BSH produced among different *S. aureus* isolates have been reported (Posada *et al.*, 2014), whereas some *S. aureus* laboratory strains (NCTC 8325 lineage) do not produce BSH as a result of an eight base pair duplication in the *bshC* gene (Newton *et al.*, 2012; Pöther *et al.*, 2013) and one strain produces twice as much Cys as BSH (Posada *et al.*, 2014). We do not provide evidence as to

why the growth phenotypes of these *S. aureus* strains differ, and therefore, we can only speculate that the necessity for the role(s) that BSH plays in Fe-S cluster biogenesis is more predominant in some isolates than in others.

In conclusion, the work herein highlights a previously undescribed function for BSH. Future studies will be necessary to determine the exact role(s) that BSH plays in the biogenesis of Fe-S clusters and whether this role is conserved in alternate species that synthesize BSH. Evidence suggests that the ability to synthesize Fe-S clusters is essential for *S. aureus* viability and, importantly, the mechanisms used by *S. aureus* to synthesize Fe-S clusters are different than the mechanisms utilized by mammals (Bae *et al.*, 2008; Chaudhuri *et al.*, 2009; Fey *et al.*, 2013). Moreover, due to its absence in humans, molecules like BSH are potential targets for antimicrobial therapy. The continued study of BSH and Fe-S cluster biogenesis could unveil attractive targets for therapeutic intervention against staphylococcal infections.

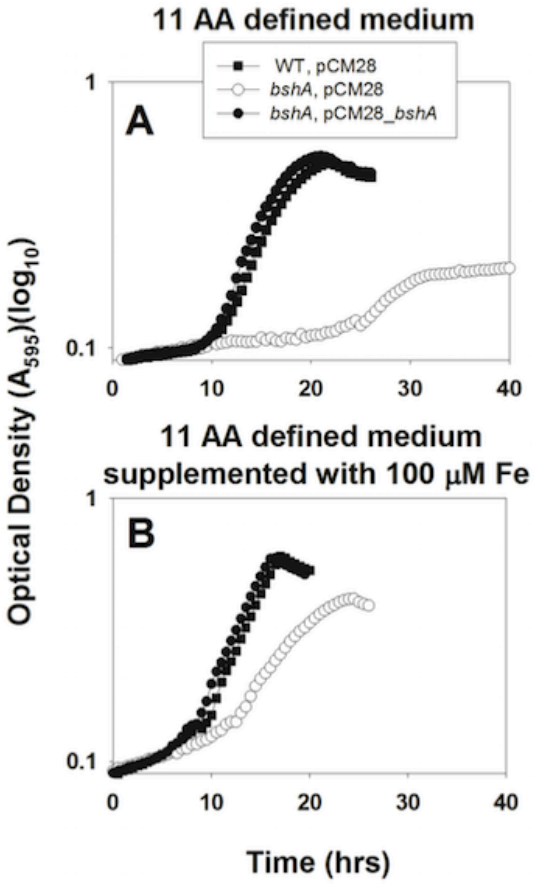

Figure 1.1. **An *S. aureus* strain lacking BSH has a growth defect in a chemically defined medium that is corrected by exogenous iron supplementation**. A representative experiment monitoring the growth of the wild-type (WT) strain with pCM28 (JMB1100; filled squares), *bshA* mutant with pCM28 (JMB1382; open circles) and *bshA* mutant with pCM28_*bshA* (JMB1382; filled circles) in chemically defined medium containing glucose and 11 amino acids (11 AA; PRMCLVYTPGH) without (Panel A) and with (Panel B) the addition of 100 μM Fe^{2+}. Strains were cultured to stationary phase in TSB prior to subculturing into defined media.

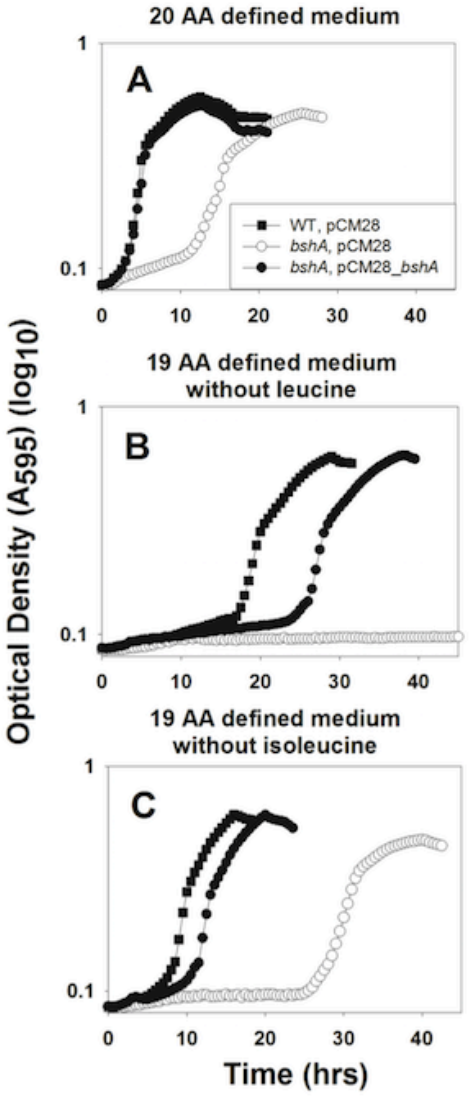

Figure 1.2. **A BSH-deficient strain has a growth defect in chemically defined media lacking either leucine or isoleucine**. Representative growth analyses of the wild-type (WT) strain with pCM28 (JMB1100; filled squares), *bshA* mutant with pCM28 (JMB1382; open circles) and *bshA* mutant with pCM28_*bshA* (JMB1382; filled circles) are shown. Strains were cultured in chemically defined media without Fe supplementation. The growth media contained either the canonical 20 amino acids (AA) (Panel A) or 19 AA lacking either leucine (Panel B) or isoleucine (Panel C). Strains were cultured to stationary phase prior to subculturing.

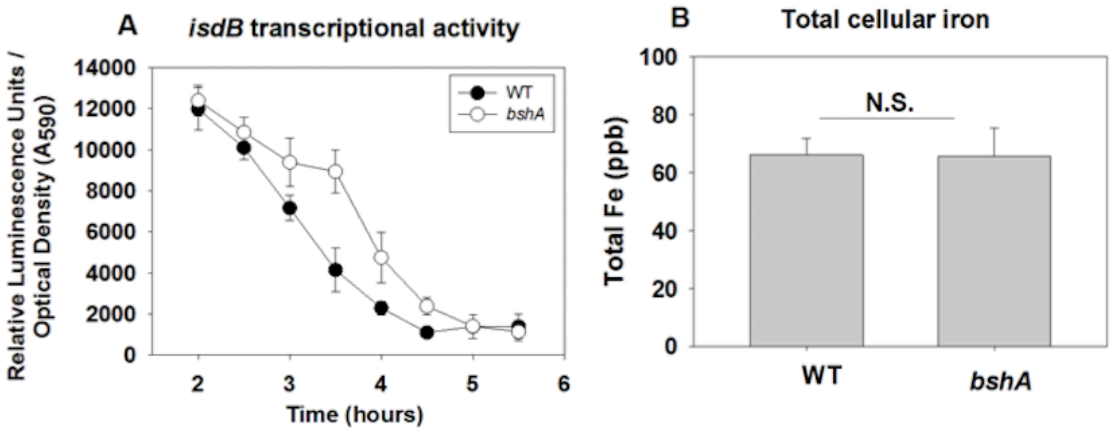

Figure 1.3. **An *S. aureus* strain lacking BSH has decreased Fur accessible iron when cultured in a chemically defined medium**. Panel A; The transcriptional activity of the *isdB* promoter is increased in a strain lacking BSH. The WT (filled circles; JMB1100) and *bshA* mutant (open circles; JMB1382) strains containing the *isdB* transcriptional reporter (pXEN-1_*isdB*) were cultured in defined medium containing the canonical 20 amino acids (AA) and luminescence was monitored over time. The luminescence data were standardized to culture optical density (A_{590}) before plotting. The data represent the average of three biological replicates with errors presented as standard deviations. Panel B; The WT and *bshA* mutant strains have the same amount of total cellular Fe when cultured in a defined medium. The WT (JMB1100) and *bshA* mutant (JMB1382) strains were cultured in 20 AA defined medium to an OD (A_{600}) of 0.8 prior to determining the total cell associated ^{56}Fe using ICP-MS. The data represent the mean of three independent experiments and each experiment was conducted in biological triplicate. Errors are presented as standard deviations. A paired t-test was performed on the samples in Panel B and N.S. denotes not significant ($p = 0.95$).

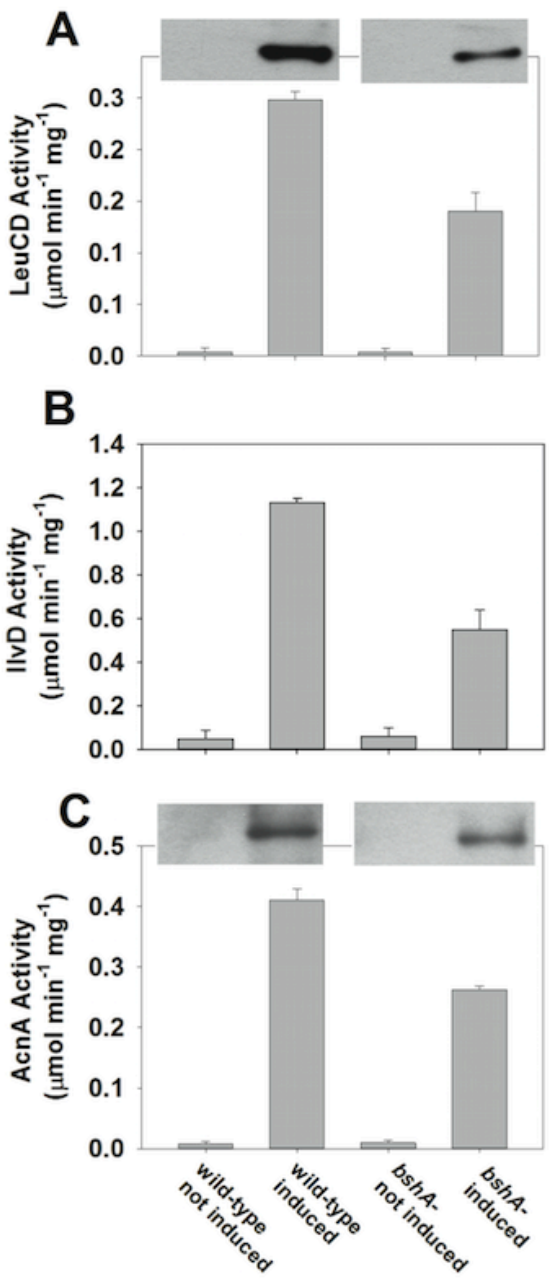

Figure 1.4. **The activities of Fe-S cluster-dependent enzymes are decreased in an *S. aureus* strain lacking BSH**. Panel A; Isopropylmalate isomerase (LeuCD) activity is decreased in cell-free lysates from strains lacking BSH, despite the accumulation of LeuCD protein. The *leuD* (JMB3707) mutant and *bshA leuD* (JMB5227) mutant strains containing p*leuCD* were cultured in the presence and absence of 1% xylose to induce *leuCD* expression prior to assessing LeuCD activity in cell-free lysates. Inset: Western blot analysis of the FLAG_LeuC protein showing that LeuC protein accumulates in both strains upon induction. Panel B; Dihydroxyacid dehydratase (IlvD) activity is decreased in cell-free lysates from strains lacking BSH. The *ilvD* (JMB3804) and *bshC ilvD* (JMB4417) mutant strains containing p*ilvD* were cultured in the presence and absence of 1% xylose to induce *ilvD* expression prior to assessing IlvD activity in cell-free lysates. Panel C; The activity of aconitase (AcnA) is decreased in cell-free lysates from strains lacking BSH, despite AcnA protein accumulating. The *acnA* (JMB3702) and *bshA acnA* (JMB5225) mutant strains containing p*acnA* were cultured in the presence and absence of 1% xylose to induce *acnA* expression prior to assessing AcnA activity in cell-free lysates. Inset: Western blot analysis of the AcnA_FLAG protein showing that AcnA protein

accumulates in both strains upon induction. Strains were cultured in a chemically defined medium containing the canonical 20 amino acids. The data shown represent the average of three experiments and errors are displayed as standard deviations.

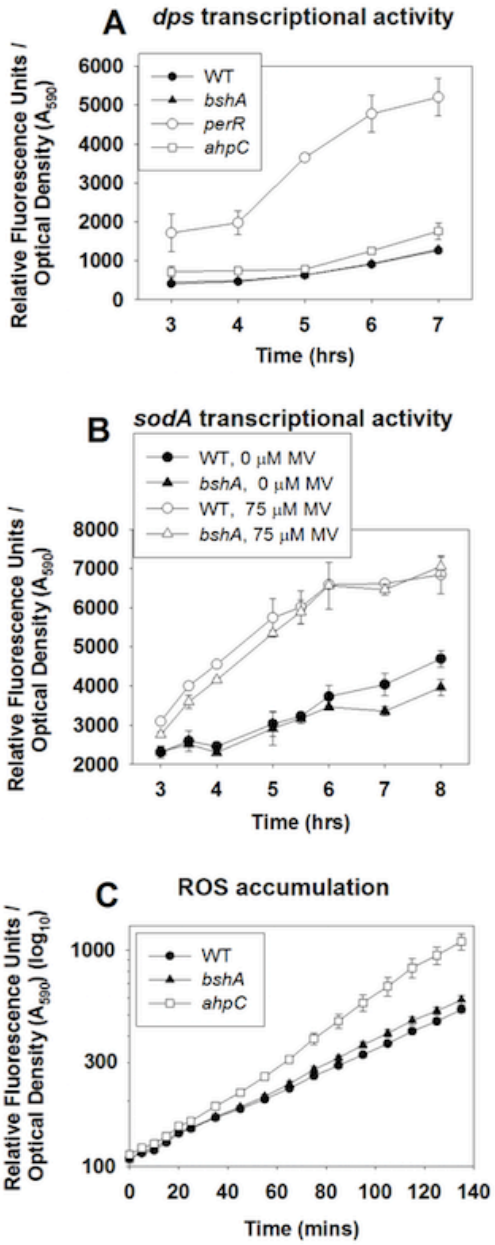

Figure 1.5. An *S. aureus* BSH-deficient strain does not have increased intracellular ROS accumulation. Panel A; PerR-dependent transcriptional activity is not altered in a strain lacking BSH. The transcriptional activity of the *dps* promoter was monitored in aerobically grown cultures of the wild-type (WT) (JMB1100), *bshA* mutant (JMB1382), *ahpC* mutant (JMB1163), and *perR* mutant (JMB2151) strains containing p*dps*. Panel B; The transcriptional activity of the *sodA* promoter is not increased in cells lacking BSH. The transcriptional activity of the *sodA* gene was monitored in aerobically grown cultures of the WT (JMB1100; circles) and *bshA* mutant (JMB1382; triangles) strains containing p*sodA* without (filled symbols) and with (open symbols) 75 μM methyl viologen. Panel C; Strains lacking BSH do not have an increased rate of 2',7'-dichlorofluorescein (DCF) formation. The WT strain (JMB1100; filled circles), *bshA* mutant (JMB1382; filled triangles) and *ahpC* mutant (JMB5511; open squares) strains were cultured aerobically in TSB to late-exponential growth phase before the addition of 2',7'-dichlorofluorescein diacetate to cell suspensions and the rate of DCF formation was monitored. The data shown represent the average of three biological replicates with errors presented as standard deviation.

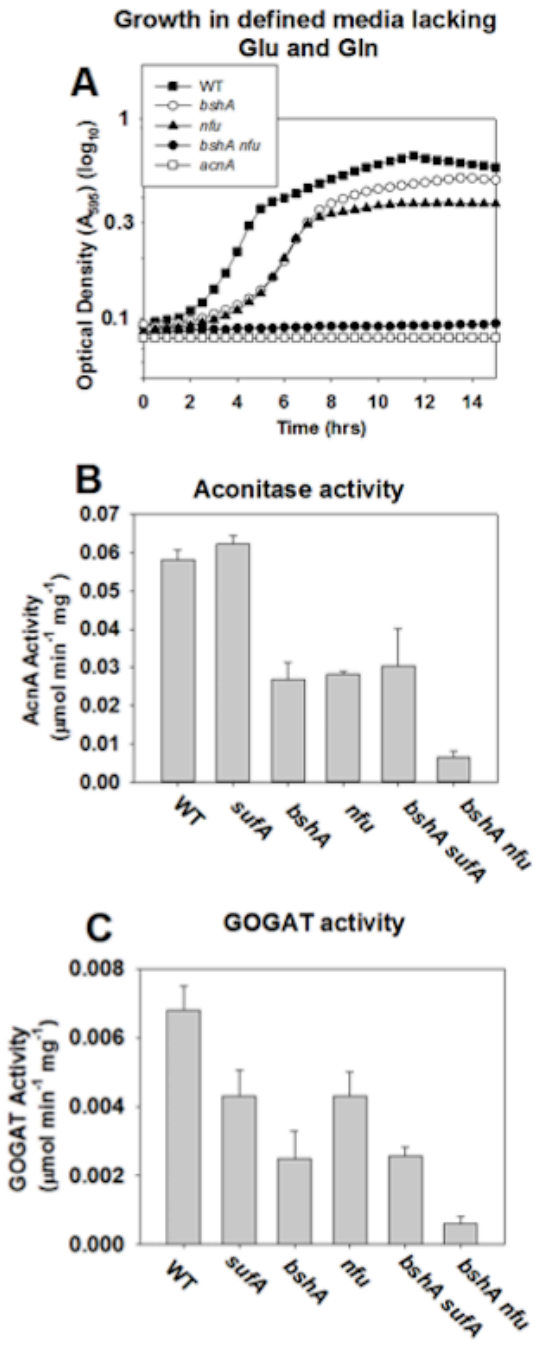

Figure 1.6. **Genetic analyses provide insight into the role of BSH in Fe-S cluster biogenesis**. Panel A; A *bshA nfu* double mutant strain is auxotrophic for glutamate and glutamine. Representative growth analysis of the wild-type (WT) (filled squares; JMB1100), *bshA* mutant (open circles; JMB1382), *nfu* mutant (filled triangles; JMB 2316), *bshA nfu* double mutant (filled circles; JMB2220) and *acnA* mutant (open squares; JMB1163) in defined medium containing 18 amino acids (AA) lacking Glu and Gln. Panel B; An *S. aureus* strain lacking BSH has decreased AcnA activity and the effect is exacerbated in an *nfu* mutant strain. AcnA activity was assessed in cell-free lysates harvested from the WT (JMB1100), *bshA* mutant (JMB1382), *nfu* mutant (JMB2316), and *sufA* mutant (JMB2223) strains, as well as, the *bshA sufA* (JMB5230) and *bshA nfu* (JMB2220) double mutant strains. Panel C; A strain lacking BSH has decreased glutamate synthase (GOGAT) activity and the effect is exacerbated in an *nfu* mutant strain. The activity of GOGAT was assessed in cell-free lysates of the WT (JMB1100), *bshA* mutant (JMB1382), *nfu* mutant (JMB2316) and *sufA* mutant (JMB2223) strains, as well as, the *bshA nfu* (JMB2220) and *bshA sufA* (JMB5230) double mutant strains. For Panels B and C, strains were cultured in a chemically defined medium

containing 20 AA prior to assaying AcnA or GOGAT. The data in Panels B and C represent the average of biological triplicates with errors presented as standard deviations.

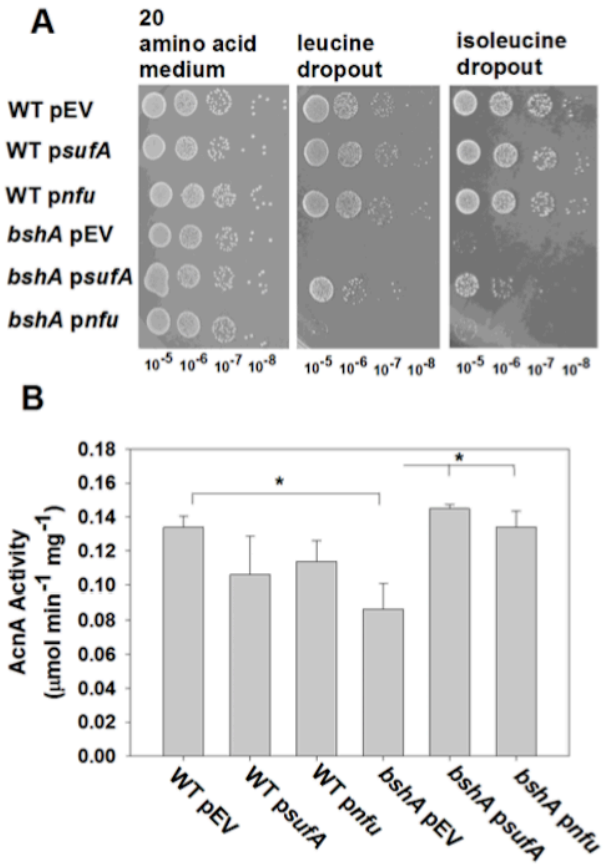

Figure 1.7. The phenotypes of a strain lacking BSH are partially suppressed by multicopy expression of genes encoding Fe-S cluster carrier proteins. Panel A; The isoleucine and leucine dependent growth defects of a strain lacking BSH are partially suppressed by multicopy expression of either *sufA* or *nfu*. Representative spot plate analysis of the wild-type (WT; JMB1100) or *bshA* mutant (1382) strains containing pEPSA, p*sufA* or p*nfu.* Strains were cultured overnight, serial diluted and spot plated on chemically defined solid media containing either 20 amino acids (AA) or 19 AA media, lacking either Ile or Leu. All media was supplemented with 0.1% xylose. Panel B; The decreased AcnA activity of the *bshA* mutant is suppressed by multicopy expression of either *sufA* or *nfu*. AcnA activity was assayed in cell-free lysates from strains cultured in chemically defined medium supplemented with 20 AA and 0.1% xylose. The strains were the same as those used to generate the data presented in Panel A. The data shown represent the average of biological quadruplicates with

errors presented as standard deviations. Paired t-tests were performed on the data illustrated in Panel B and * denotes $p < 0.05$.

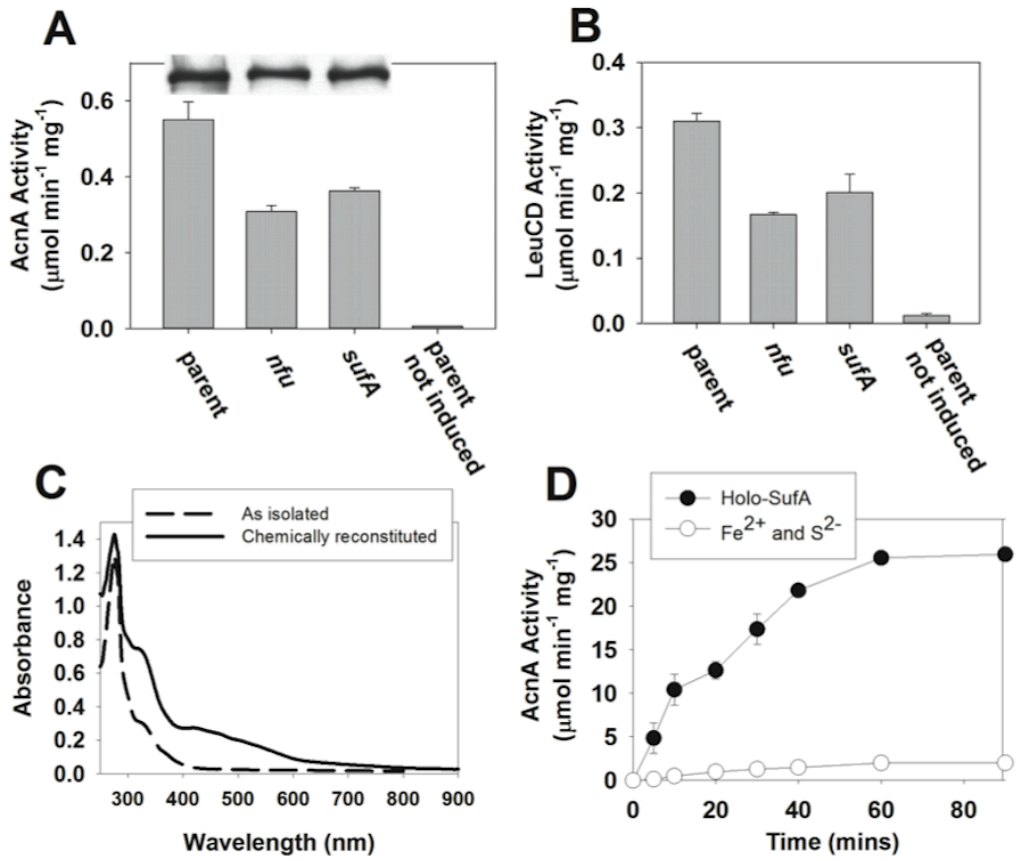

Figure 1.8. *S. aureus* SufA is an Fe-S cluster carrier. Panel A; AcnA activity is decreased in cell-free lysates from strains lacking either SufA or Nfu when *acnA* expression is decoupled from the native promoter. The activity of AcnA was determined in cell-free lysates from the *acnA* mutant (JMB3702), *sufA acnA* double mutant (JMB3632), and *nfu acnA* double mutant (JMB3538) strains containing p*acnA*. Strains were cultured aerobically in TSB with 1% xylose prior to assessing AcnA activity in cell lysates. The data represent is the average of biological triplicates with standard deviations shown. Inset: Western blot analysis of the AcnA_FLAG protein showing that AcnA protein accumulates in all strains. Panel B; LeuCD activity was decreased in cell-free lysates from strains lacking Nfu or SufA when *leuCD* expression was decoupled from the native promoter. The *leuD* mutant (JMB3707), *sufA leuD* double mutant (JMB3708), and *nfu leuD* double mutant (JMB3506)

strains containing p*leuCD* were cultured in TSB with 1% xylose before cells were harvested and LeuCD activity assessed in cell-free lysates. The data represent is the average of biological triplicates with standard deviations shown. Panel C; Chemically reconstituted *S. aureus* SufA has UV-Visible absorption spectra similar to known Fe-S cluster binding proteins. Representative UV-Visible absorption spectra of the SufA protein (230 μM) before (dashed line) and after chemical Fe-S cluster reconstitution (solid line). Panel D; Holo-SufA protein can transfer an Fe-S cluster to apo-AcnA protein. Apo-AcnA (4 μM) was incubated with either holo-SufA (4 μM) (closed circles) or 8 μM Fe^{2+} and 8 μM S^{2-} (open circles). At the indicated times, aliquots of the samples were removed and assayed for AcnA activity. The data presented represent the average of three experiments and errors presented as standard deviations.

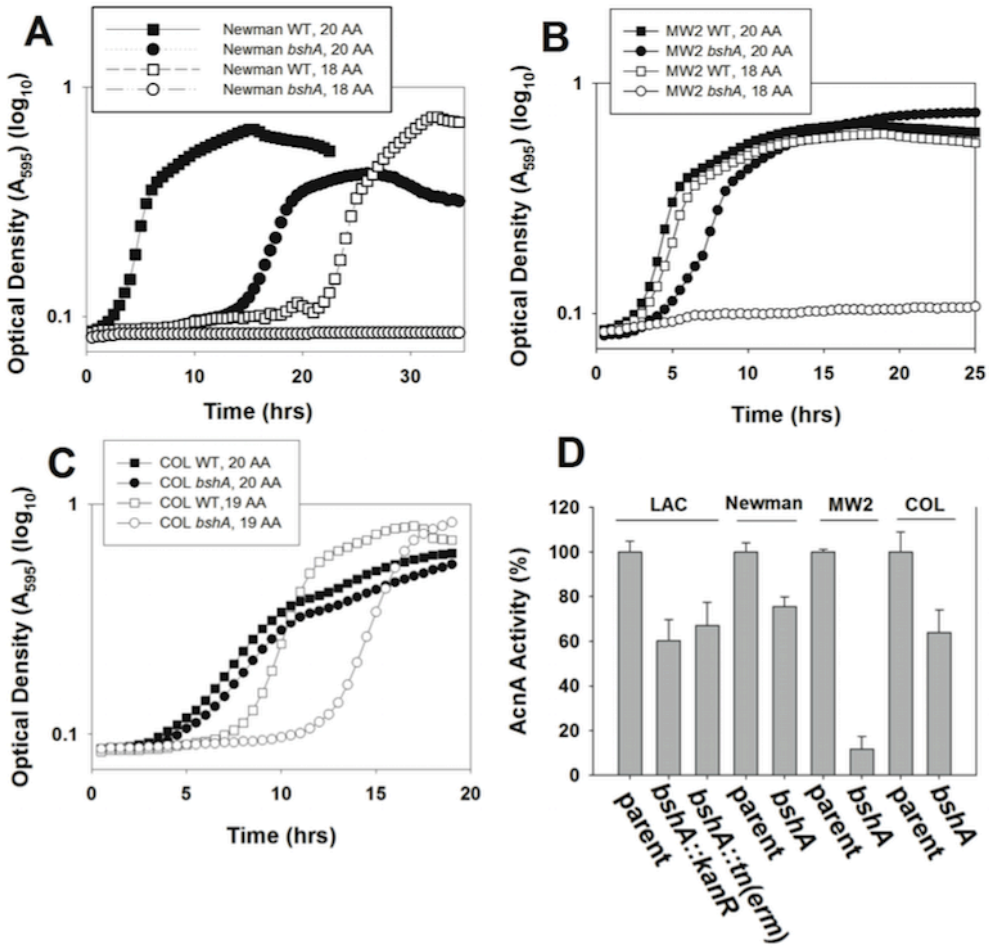

Figure 1.9. Diverse *S. aureus* isolates lacking BSH have defects in Fe-S cluster biogenesis. Panel A; An *S. aureus* Newman strain lacking BSH has a growth defect that is corrected by exogenously supplied Ile and Leu. The growth of strain Newman (squares; JMB1422) and the Newman *bshA* mutant (circles; JMB6253) was monitored in chemically defined media containing either 20 amino acids (AA) (filled symbols) or 18 AA lacking Ile and Leu (open symbols). Panel B; An *S. aureus* MW2 strain lacking BSH is auxotrophic for Glu and Gln. The growth of the strain MW2 (squares; JMB1324) and the MW2 *bshA* mutant (circles; JMB5197) was monitored in defined media containing either 20 AA (filled symbols) or 18 AA lacking Glu and Gln (open symbols). Panel C; An *S. aureus* COL strain lacking BSH has a growth defect that is corrected by exogenously supplied Ile. The growth of strain COL (squares; JMB1325) and COL *bshA* mutant (circles; JMB6167) were monitored in

defined media containing either 20 AA (filled symbols) or 19 AA lacking Ile (open symbols). All strains used in Panels A, B and C were cultured to stationary phase before subculturing. Panel D; AcnA activity is decreased in diverse *S. aureus* isolates lacking BSH. Strains with and without the ability to synthesize BSH were cultured in chemically defined media containing 20 AA. Cells were harvested and AcnA activity was monitored in cell-free lysates. AcnA enzymatic activity was standardized with respect to that of the parent strain and to the total protein concentration of the representative lysate. The data presented represent the average of three independent experiments and error is shown as standard deviation.

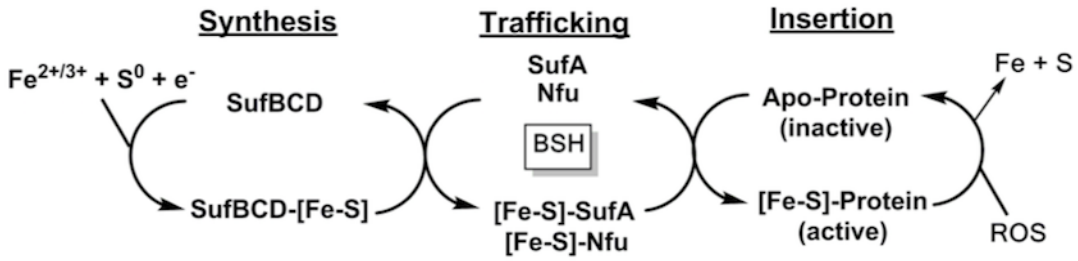

Figure 1.10. Working model for Fe-S cluster biogenesis in *S. aureus*. The activation of an apoprotein by the addition of an Fe-S cluster requires three steps: synthesis, trafficking and insertion. In our model the cysteine desulfurase SufS provides the S^0 to the scaffold complex SufBCD, where the Fe-S clusters are synthesized. The Nfu and SufA carrier molecules accept Fe-S clusters from SufBCD and traffic the Fe-S clusters to apoproteins. The Fe-S cluster is then inserted into the apoprotein thereby activating the protein. Data presented in this study suggest that BSH has roles in Fe homeostasis and Fe-S cluster trafficking.

Table 1.1. Strains and plasmids used in this study.

***Staphylococcus aureus* strains**

Strain	Genotype / Description	Background	Source / Reference
RN4220	Restriction-negative *S. aureus*	RN1	(Kreiswirth *et al.*, 1983)
JMB1100	Parent strain	LAC	A.R. Horswill
NE892	SAUSA300_2013(*leuD*)::Tn(*ermB*)	JE2	(Fey *et al.*, 2013)
NE718	SAUSA300_2006(*ilvD*)::Tn(*ermB*)	JE2	(Fey *et al.*, 2013)
NE861	SAUSA300_1246(*acnA*)::Tn(*ermB*)	JE2	(Fey *et al.*, 2013)
NE1728	SAUSA300_1349(*bshA*)::Tn(*ermB*)	JE2	(Fey *et al.*, 2013)
NE1100	SAUSA300_0446(*gltD*)::Tn(*ermB*)	JE2	(Fey *et al.*, 2013)
JMB1382	SAUSA300_1349(*bshA*)*::kanR*	LAC	
JMB1381	SAUSA300_1071(*bshC*)Δ	LAC	
JMB2151	SAUSA300_1842(*perR*)::*kan*	LAC	(Horsburgh *et al.*, 2002)
JMB1163	SAUSA300_0380(*ahpC*)::*tetM*	LAC	V. Torres
JMB1144	SAUSA300_0843(*sufA*)*Δ*	LAC	
JMB3707	SAUSA300_2013(*leuD*)::Tn (*ermB*)	LAC	
JMB5272	SAUSA300_1349*::kanR*, 2013(*leuD*)::Tn(*ermB*)	LAC	
JMB3804	SAUSA300_2006(*ilvD*)::Tn(*ermB*)	LAC	
JMB4417	SAUSA300_1071(*bshC*)Δ*,* 2006(*ilvD*)::Tn(*ermB*)	LAC	
JMB3702	SAUSA300_1246(*acnA*)::Tn(*ermB*)	LAC	
JMB5225	SAUSA300_1349(*bshA*)*::kanR*, 1246(*acnA*)::Tn(*ermB*)	LAC	
JMB3703	SAUSA300_1071(*bshC*)Δ, 1246(*acnA*)::Tn(*ermB*)	LAC	
JMB1165	SAUSA300_0839(*nfu*)Δ	LAC	(Mashruwala *et al.*, 2015)
JMB2316	SAUSA300_0839(*nfu)::tetM*	LAC	(Mashruwala *et al.*, 2015)
JMB2220	SAUSA300_1349(*bshA*)::*kan*, 0839(*nfu*)*::tetM*	LAC	
JMB1146	SAUSA300_0843(*sufA*)Δ	LAC	(Mashruwala *et al.*, 2015)
JMB2223	SAUSA300_0843(*sufA*)::*tetM*	LAC	
JMB5230	SAUSA300_1349(*bshA*)*::kanR,* 0843(*sufA*)*::tetM*	LAC	(Mashruwala *et al.*, 2015)
JMB3538	SAUSA300_ *nfuΔ*, 1246(*acnA*)::Tn(*ermB*)	LAC	(Mashruwala *et al.*, 2015)
JMB3632	SAUSA300*_sufA::tetM,* 1246(*acnA*)::Tn(*ermB*)	LAC	
JMB3506	SAUSA300_ *nfuΔ*, 2013(*leuD*)::Tn(*ermB*)	LAC	(Mashruwala *et al.*, 2015)

JMB3708	SAUSA300_*sufA::tetM*, 2013(*leuD*)::Tn(*ermB*)	LAC	
JMB6628	SAUSA300_0446(*gltD*)::Tn(*ermB*)	LAC	
JMB1422	parent strain	Newman	E. Skaar
JMB6253	*bshA*::Tn(*ermB*)	Newman	
JMB1324	parent strain	MW2	P. Schlievert
JMB5197	*bshA*::*kan*	MW2	
JMB1325	parent strain	COL	A. Horswill
JMB6167	*bshA*::Tn(*ermB*)	COL	

Other Strains

Name	**Relevant Genotype / Description**	**Source / Reference**
Escherichia coli PX5	Molecular cloning	Protein Express
E. coli BL21 AI	Protein production	Life Technologies
Saccharomyces cerevisiae FY2	*ura3-52* yeast recombination cloning	W. Belden

Plasmids

Plasmid Name	**Locus / Function**	**Source / Reference**
pJB38	Mutant construction	(Bose *et al.*, 2013)
pJB38_*bshA*Δ	SAUSA300_1349*Δ* for chromosomal deletion	
pJB38_*bshA::kanR*	SAUSA300_1349*::kanR* for allelic replacement	
pJB38_*bshC*Δ	SAUSA300_1071*Δ* for chromosomal deletion	
pCM11	Vector with promoterless *gfp* transcriptional reporter	(Malone *et al.*, 2009)
pCM11_*dps* (p*dps*)	SAUSA300_2092 (*dps*) transcriptional reporter	(Mashruwala *et al.*, 2015)
pCM11_*sodA* (p*sodA*)	SAUSA300_1513 (*sodA*) transcriptional reporter	(Mashruwala *et al.*, 2015)
pCM28	Genetic complementation vector	(Pang *et al.*, 2010)
pCM28_*bshA*	SAUSA300_1349 for complementation	
pCM28_*sufCDSUB*	SAUSA300_818-822	
pXEN-1_*isdB* (p*isdB*)	Transcriptional fusion of SAUSA300_1028 to *luxCDABE*	(Mashruwala *et al.*, 2015)
pEPSA5	Vector for genetic complementation with xylose-inducible promoter	(Forsyth *et al.*, 2002)
pEPSA5_*leuCD*_FLAG (p*leuCD*)	SAUSA300_2012-13 with N-terminal FLAG affinity tag	(Mashruwala *et al.*, 2015)

pEPSA5_*ilvD* (p*ilvD*)	SAUSA300_2006	(Mashruwala *et al.*, 2015)
pEPSA5_*acnA*_FLAG (p*acnA*)	SAUSA300_1246 with C-term FLAG affinity tag	(Mashruwala *et al.*, 2015)
pEPSA5_*nfu*	SAUSA300_0839 genetic complementation	(Mashruwala *et al.*, 2015)
pEPSA5_*sufA*	SAUSA300_0843 genetic complementation	
pET20b	Expression vector with C-terminal poly-histidine affinity tag	EMD Millipore
pET24a	Expression vector with C-terminal poly-histidine affinity tag	EMD Millipore
pET20b_*sufA*	Expression vector for expressing and purifying SufA	
pET24a_*acnA*	Expression vector for expressing and purifying AcnA	(Mashruwala *et al.*, 2015)

CHAPTER 2

THE *copBcbl* OPERON PROTECTS *STAPHYLOCOCCUS AUREUS* FROM COPPER INTOXICATION: CBL IS AN EXTRACELLULAR MEMBRANE-ASSOCIATED COPPER-BINDING PROTEIN

Abstract

Host macrophages accumulate copper during infection, forcing microbes to employ strategies to tightly control the intracellular concentration of copper. Among other mechanisms, bacteria utilize membrane proteins involved in the exportation of excess cytoplasmic copper. In addition to the copper exporter CopA, we found that the arginine catabolic mobile element (ACME) of the *Staphylococcus aureus* USA300 clone contains an additional copper exporter (CopB) and a putative lipoprotein (Cbl). Mutational inactivation of *copB* or *cbl* resulted in increased copper sensitivity and further inactivation of *copA* resulted in exacerbated phenotypes, suggesting that CopB and Cbl are additional mechanisms that prevent copper intoxication. We show that *copB* and *cbl* are co-transcribed and negatively regulated by CsoR in response to copper stress. We found that Cbl is a membrane-bound, surface-exposed lipoprotein that binds up to four Cu^{+} ions *in vitro*. These findings suggest that the *copBcbl* operon is an additional mechanism employed by the highly successful *S. aureus* USA300 clone to survive copper stress.

Introduction

Copper (Cu) is a trace element required by most organisms. Because of its ability to cycle between its reduced (Cu^{+}) and oxidized (Cu^{2+}) states, it can have catalytic and structural roles in metalloenzymes, such as dioxygen reductases (Sousa *et al.*, 2012), superoxide dismutases (Osman *et al.*, 2013), laccases (Claus, 2003), and several enzymes involved in denitrification (Tavares *et al.*, 2006). Although essential, high intracellular concentrations of Cu can be toxic. Cu toxicity may be, in part, due to its ability to compete with other transition metals and displace them from active centers of proteins. For example, Cu can displace iron from iron-sulfur cofactors leading to cluster destruction and protein inactivation (Macomber and Imlay, 2009; Chillappagari *et al.*, 2010; Fung *et al.*, 2013). Cu intoxication could also occur as a result of Fenton-type chemistry, in which Cu^{+} reacts with hydrogen peroxide leading to the formation of hydroxyl radicals (OH•) (Gunther *et al.*, 1995), that can, in turn, damage proteins, membrane lipids, and DNA. That said, in *Escherichia coli*, cells that accumulate Cu do not have heightened sensitivity to hydrogen peroxide or increased mutagenesis frequency, suggesting that the direct mechanism of copper toxicity is not due to oxidative damage in this organism (Macomber *et al.*, 2007).

One of the strategies our body uses to kill invading microorganisms is limiting the bioavailability of certain trace metals (Hood and Skaar, 2012). Recently, it was found that humans also use trace metals to intoxicate pathogens. In human macrophages, the ATP7A transporter facilitates Cu accumulation into the phagosome and impairment of ATP7A leads to a defect in bacterial killing (White *et al.*, 2009). The Cu-responsive fluorescent probe CS1 has been used to visualize changes in the distribution of Cu pools when mouse macrophages are challenged with *Salmonella enterica* sv. Typhimurium (Achard *et al.*, 2012). Together with superoxide generated via the phagosomal NADPH oxidase, Cu accumulated in

macrophages can amplify the toxicity effects and kill the invading pathogen (Hodgkinson and Petris, 2012).

A disrupted *ATP7A* gene also leads to poor dietary uptake of copper, affecting copper distribution in the body resulting in decreased activities of Cu-dependent enzymes, a syndrome known as Menkes disease (Kaler, 2011). As a complication, Menkes disease patients often suffer bacterial infections (Menkes *et al.*, 1962; Gunn *et al.*, 1984; Uno and Arya, 1987; Kreuder *et al.*, 1993), highlighting the importance of proper Cu homeostasis for proper function of the immune system.

The finding that copper has been used as an antimicrobial agent by our immune system is relatively recent, but the antimicrobial properties of this metal have been recognized for some time (Grass *et al.*, 2011), ranging from its uses to sterilize chest wounds and drinking water by ancient civilizations (Dollwet and Sorenson, 1985), to recent hospital trials showing its capacity to reduce microbial load on touch surfaces (Casey *et al.*, 2010; Marais *et al.*, 2010; Mikolay *et al.*, 2010; Schmidt *et al.*, 2012). The United States Environmental Protection Agency approved the use of nearly 300 copper alloys as a supplement for standard cleaning and disinfection practices for environmental surfaces, such as bed rails, door knobs, over-bed tables, sinks, faucets, among other surfaces.

Staphylococcus aureus is a public health concern worldwide that causes skin and soft tissue infections, as well as more severe and life-threatening diseases like pneumonia, osteomyelitis, and bacteremia (Klevens *et al.*, 2007; Otto, 2010). Like all pathogens, *S. aureus* must employ strategies to tightly control intracellular copper levels and avoid copper intoxication at the host-pathogen interface. Bacteria use copper-responsive transcriptional regulators, membrane transporters, intracellular copper chaperones and chelating molecules as mechanisms to prevent copper toxicity (Solioz and Stoyanov, 2003; Rensing and Grass, 2003; Osman *et al.*, 2013). In *S. aureus*, the copper-sensitive operon repressor (CsoR) binds

intracellular copper leading to derepression of the *copAZ* operon (Baker *et al.*, 2011). CopA is a membrane-bound protein that exports copper (Sitthisak *et al.*, 2007) and CopZ is a cytoplasmic chaperone that binds and delivers copper to target proteins, including CopA (Radford *et al.*, 2003). Some *S. aureus* strains have an additional copper transporter (*copB*), that is sometimes co-localized with a multicopper oxidase (*mco*) (Baker *et al.*, 2011). The *copBmco* operon is located on either a self-replicating plasmid or a chromosomally integrated plasmid (Baker *et al.*, 2011). The presence of the *copBmco* operon is associated with increased resistance to copper and, like the *copAZ* operon, *copBmco* expression is negatively regulated by CsoR (Baker *et al.*, 2011). In addition to its role in copper homeostasis, it has been suggested that Mco also has a role in preventing oxidative stress (Sitthisak *et al.*, 2005). How copper enters the cell in *S. aureus* remains unknown.

In the present work, we characterized the role of a two-gene operon consisting of a copper transporter protein (*copB*) and a putative lipoprotein (*cbl*). We tested the hypothesis that the *copB* and *cbl* gene products prevent Cu intoxication in *S. aureus*. Mutational inactivation of *copB* or *cbl* resulted in increased Cu sensitivity and the phenotype was exacerbated in strains unable to export Cu via CopA. We show that the *copB* and *cbl* genes are co-transcribed and negatively regulated by CsoR in response to Cu stress. Genetic and biochemical data suggest that the *cbl* gene product is a membrane-bound lipoprotein oriented to the extracellular environment and binds up to four Cu^{+} ions. This is the first study that shows roles for (i) the *copBcbl* operon in Cu homeostasis, and (ii) Cbl in preventing Cu intoxication in *S. aureus*.

Experimental Procedures

Reagents. Restriction enzymes, quick DNA ligase kit, deoxynucleoside triphosphates, and Phusion DNA polymerase were purchased from New England Biolabs. Primers listed in **Table 2.S1** were obtained from Integrated DNA Technologies. Plasmid mini-prep and gel extraction kits were purchased from Qiagen. Lysostaphin was purchased from Ambi Products. Tryptic Soy Broth (TSB) was purchased from MP Biomedicals. ELC chemiluminescent detection kit was purchased from Pierce. Primary and secondary antibiodies were purchased from Sigma-Aldrich and Bio-Rad, respectively. Pierce Protease and Phosphatase Inhibitor Mini Tablets were purchased from ThermoScientific. GSTrap 4B columns and PreScission Protease were purchased from GE Healthcare. Unless specified, all other chemicals were purchased from Sigma-Aldrich and were of the highest purity available.

Bacterial Strains and Growth Conditions. Bacterial strains used in this work are listed in **Table 2.1**. Unless otherwise noted, the *S. aureus* strains used in this study are derived from the community-associated MRSA USA300 LAC strain was cured of the pUSA03 plasmid that confers erythromycin resistance (Voyich *et al.*, 2005; Pang *et al.*, 2010). *S. aureus* strains were cultured in TSB or a defined media and *Escherichia coli* strains were grown in Luria Broth (LB) medium. Unless otherwise specified, all bacterial strains were cultured at 37 °C. The chemically defined media was modified from previous studies (Mah *et al.*, 1967): 1 g $(NH_4)_2SO_4$, 4.5 g KH_2PO_4, 10.5 g K_2HPO_4, 110 mM NaCl, 30 mM KCl, 50 μg nicotinic acid, 50 μg pantothenic acid, 50 μg thiamine, 0.3 μg biotin, and 2.5 mg of individual twenty amino acids, per 100 ml. When supplemented to the media, chemicals were added at the following concentrations: 10-300 μM $CuSO_4$; 50-200 μM $Fe_2(NH_4)_2(SO_4)_2$; 5-200 μM CoCl; 10-300 μM $MnSO_4$; 10-300 μM $ZnSO_4$. When appropriate, antibiotics were added at the following concentrations: 150 μg per ml ampicillin (Amp), 6 or 30 μg per ml chloramphenicol (Cm) (defined or complex media, respectively), 10 μg per ml erythromycin (Erm), 3 μg per ml

tetracycline (Tet), and 150 ng per ml anhydrotetracycline (A-Tet). Overnight cultures were grown in 7 ml culture tubes containing 2 ml of TSB, shaking at 200 rpm. When growing overnight cultures of strains containing pEPSA-derived plasmids, 2% xylose was added to the media. Cultures used for transcriptional studies were grown in 25 ml tubes containing 5 ml of media, shaking at 200 rpm.

Construction of Mutant Strains and Plasmids. Unless otherwise specified, chromosomal DNA from JMB1100 was used as the template for PCR reactions used in the construction of plasmids. All plasmids were isolated from *Escherichia coli* PH5α and transformed into electrocompetent *S. aureus* RN4220 using standard protocol (Kreiswirth *et al.*, 1983). Phage α80 was used for plasmid and chromosomal transductions (Novick, 1991). All bacterial strains were verified by PCR prior to analysis. DNA sequencing was conducted by Genewiz (South Plainfield, NJ).

Mutational inactivation of the *S. aureus copB* and *cbl* genes was achieved by chromosomal deletion to yield the *copB*Δ, *cbl*Δ, and *copB*Δ *cbl*Δ mutant strains. For the *copB*Δ mutant, upstream and downstream regions of the *copB* gene (SAUSA300_0078) were PCR amplified using the following primers: ZRC199 and ZRC200; ZRC164 and ZRC201. PCR products were gel purified and fused by PCR using the ZRC199 and ZRC201 primers. For the *cbl*Δ mutant, upstream and downstream regions of the *cbl* gene (SAUSA300_0079) were PCR amplified using the following primers: ZRC166 and ZRC167; ZRC168 and ZRC169. PCR products were gel purified and fused by PCR using the ZRC166 and ZRC169 primers. For the *copB*Δ *cbl*Δ double mutant, upstream and downstream regions of the *copBcbl* operon were PCR amplified using the following primers: ZRC185 and ZRC186; ZRC168 and ZRC169. PCR products were gel purified and fused by PCR using the ZRC185 and ZRC169 primers. The *copB*Δ, *cbl*Δ, and *copB*Δ-*cbl*Δ PCR products were digested with EcoRI and SalI, and ligated into similarly digested pJB38 (Bose *et al.*, 2013). The

recombinant vectors were transformed into chemically competent *E. coli* PH5α. PCR was used to screen for *E. coli* colonies harboring the recombinant plasmids using ZRC196 and ZRC201 primers for pJB38_*copB*Δ; ZRC196 and ZRC169 for pJB38_*cbl*Δ; and ZRC196 and ZRC169 for pJB38_*copB*Δ-*cbl*Δ. The plasmids were isolated and mobilized into RN4220 *S. aureus*. Single colonies were used to inoculate 5 ml of TSB with Cm. Cultures were grown at 42°C for plasmid integration. Single colonies were inoculated in 5 ml of TSB at 30°C for plasmid resolution. To screen for the loss of plasmid, cultures were serial diluted (1:50,000) and 50-100 µl were plated on TSA containing A-Tet. Colonies were scored for Cm sensitivity. Colonies that were Cm sensitive were screened using PCR for the double recombination event. The *copB*Δ mutant strain was verified using the ZRC139 and ZRC201 primers. The *cbl*Δ and *copB*Δ-*cbl*Δ mutants were verified using the ZRC139 and ZRC169 primers.

To construct the *copA*::Tn(*ermB*) and *csoR*::tn(*ermB*) mutants in the USA300 LAC background, lysates were generated from the respective NARSA (Fey *et al.*, 2013) strains and used to transduce the WT parent strain (JMB1100). These lysates were also used to make double mutant strains. The pTET plasmid was used to construct the *copA*::Tn(*tet*) and *csoR*::Tn(*tet*) in the USA300 LAC background by allelic exchange as previously described (Bose *et al.*, 2013).

Mutational inactivation of the following genes was confirmed using PCR with the following primers: *copA*::Tn*(ermB)*, *copA*::Tn*(tet)*, and *copZ*::Tn(*ermB*) with ZRC133 and ZRC134; *csoR*::Tn*(ermB)* and *csoR*::Tn*(tet)* with ZRC153 and ZRC155.

For complementation and expression studies genes cloned into pEPSA5 (Forsyth *et al.*, 2002) contained an engineered *sodA* ribosomal binding site. To construct the *copB* complementing vector, the ZRC146 and ZRC141 primers were used to PCR amplify the *copB* gene; the PCR product was digested with BamHI and SalI and ligated into similarly

digested pEPSA5 to yield pEPSA5_*copB*. To construct the *cbl* (full length) complementing vector, the ZRC149 and ZRC150 primers were used to PCR amplify the full length *cbl* gene; the PCR product was digested with BamHI and SalI and ligated into similarly digested pEPSA5 to yield pEPSA5_*cbl*(FL). For the truncated version of *cbl*, the ZRC184 and ZRC150 primers were used. The PCR product was digested with BamHI and SalI, and ligated into similarly digested pEPSA5 to yield pEPSA_*cbl*T. *E. coli*, RN4220, USA300, Newman, or MW2 strains containing plasmids were PCR verified, using the pEPSA5upveri and ZRC141 (pEPSA_*copB*), or pEPSA5upveri and ZRC150 [(pEPSA5_*cbl*(FL) or pEPSA_*cbl*(T)].

The pEPSA5_*cbl*-FLAG vector was constructed by using ZRC149 and ZRC181. The insert was digested with BamH1 and NheI, then ligated into similarly digested pEPSA5_CitB-FLAG (Mashruwala *et al.*, 2015). Strains containing the pEPSA5_*cbl*-FLAG plasmid were PCR verified using the pEPSA5upveri and ZRC181 primers.

The pEPSA5_*nuc2*(FL)-*cbl* and pEPSA5_*nuc2*(SS)-*cbl* vectors were created by using yeast homologous recombination cloning (YRC) in *Saccharomyces cerevisiae* FY2 as previously described (Joska *et al.*, 2014). The pEPSA5_CitB-FLAG vector was linearized with NheI. The amplicon for the pEPSA5_*nuc2*(FL)-*cbl* was created using the following primer pairs: ZRC188 and ZRC189; ZRC191 and ZRC193. The amplicon for the pEPSA5_*nuc2*(SS)-*cbl* was created using the following primer pairs: ZRC188 and ZRC190; ZRC192 and ZRC193. Strains containing the pEPSA5_*nuc2*(FL)-*cbl* and pEPSA5_*nuc2*(SS)-*cbl* plasmids were PCR verified using the ZRC188 and ZRC193 primers.

For expression and purification of recombinant proteins from *E. coli* BL21 DE3, the pGEX-6P-1 vector was used (GE Healthcare). The pGEX-6P-1_*cbl* was constructed using the ZRC198 and ZRC178 primers. The PCR product was digested with BamH1 and Xho, and then ligated into similarly digested pGEX-6P-1.

To construct the *copBcbl* transcriptional reporter, approximately 500-750 bp upstream of the *copB* RBS was amplified using the ZRC139 and ZRC140 primers. The PCR product was digested with HindIII and KpnI and ligated into similarly digested pCM11 (Malone *et al.*, 2009).

qRT-PCR. RNA isolation and quantitative real-time PCR were performed as previously described with a few modifications (Rosario-Cruz *et al.*, 2015). The WT (JMB1100) strain was cultured overnight in TSB in biological triplicates. Cells were pelleted by centrifugation and resuspended in PBS before diluting 1:100 into chemically defined media without and with 100 μM Cu. Cells were harvested 6 hr post-inoculation (OD ~1, A_{600}) by centrifugation, treated with RNAProtect (Qiagen) for 10 min at room temperature, and stored at -80 °C until their use. Pellets were thawed and washed twice with 0.5 ml of lysis buffer (50 mM RNAse-free Tris, pH 8). Cells were lysed with 20 μg DNAse and 20 μg Lysostaphin for 30 minutes at 37°C. RNAs were isolated as using TRIzol reagent (Ambion) as per manufacturer's protocol. DNA was digested with the TURBO DNA-free kit (Ambion - Life Technologies) and RNA quantified using a Nanodrop (ND-1000) Spectrophotometer. cDNA libraries were constructed using isolated RNA as a template with High Capacity RNA-to-cDNA Kit (Applied Biosystems). *Power* SYBR Green PCR Master Mix (Applied Biosystems) was used to perform qRT-PCR in an Applied Biosystems StepOnePlus thermocycler. Data was analyzed using the ΔΔCt method. CopARTfwd and CopARTrev primers were used to detect *copA* transcripts; CopBRTfwd and CopBRTrev primers were used to detect *copB* transcripts; CblRTfwd and CblRTrev primers were used to detect *cbl* transcripts. 16s transcripts detected with 16sfwdRT and 16srevRT primers were used as a reference. RT primers were designed using the Primer Express 3.0 software from Applied Biosystems.

Transcriptional Reporter Assays. Transcriptional or promoter reporter assays were performed as previously described with a few modifications (Rosario-Cruz *et al.*, 2015).

Strains containing the pCM11-derived reporters were grown overnight in TSB with Erm. The overnight cultures (>16 hours) were pelleted and resuspended in PBS. Washed cells were subcultured into 5 ml of fresh chemically defined media (1:100) with and without copper. Culture aliquots were periodically removed (200 µl) and culture optical density (A_{590}) and fluorescence was monitored using a Perkin Elmer HTS 7000 Plus Bio Assay Reader. GFP was excited at 485 nm and emission was read at 535 nm. Relative fluorescence units were normalized with respect to the culture optical density at each time point.

Cell Fractionation. Overnight cultures were diluted to 0.1 OD (Abs_{600}) in fresh TSB with Cm. Cultures were induced with 0 % or 0.2 % xylose at 1 OD (Abs_{600}), incubated for 2 hr, and harvested by centrifugation. Cultures were resuspended and washed with PBS. Cells were lysed (PBS with 10 µg DNAse, 10 µg Lysostaphin, Protease and Phosphatase Inhibitor Mini Tablets) at 37 °C for ~45 min. Cell fractionation protocol was followed as previously described with some modifications (Ranjit *et al.*, 2011). Cell lysates were spun for 10 min at 4 °C to remove unbroken cells. Supernatants (whole cell, crude lysates) were spun at 100,000 × g for 2 hr at 4 °C in Beckman Polyallomer Centrifuge Tubes using a Beckman Optima TLX Ultracentrifuge and TLA 120.2 rotor. The resulting supernatant was saved as the cytoplasmic fraction. The pellet (crude membrane fraction) was resuspended in membrane buffer (100 mM Tris-HCl [pH 7.5], 100 mM NaCl, 10 mM $MgCl_2$, 10 % glycerol, 0.1 % SDS) to solubilize membrane proteins and spun down as described above to to remove the detergent-insoluble material; supernatants were saved as the membrane soluble fractions. Protein concentrations from all fractions were determined as described above.

Western Blot Analysis. Protein concentration was determined using a bicinchoninic acid assay modified for a 96-well plate (Olson and Markwell, 2007) and bovine serum albumin (2.6 mg per ml) as a protein standard. A total of 40 µg of total protein per sample was separated using a 12 % SDS-PAGE gel. Proteins were then transferred to a PVDF membrane

and incubated with mouse monoclonal anti-FLAG primary antibody (1:4000 dilution) and subsequently HRP conjugated secondary antibody (1:12000 dilution). The blots were developed using chemi-luminescent detection (Pierce) and scanned as TIFF images.

Recombinant Protein Expression and Purification. *Escherichia coli* BL21 DE3 containing the pGEX-6P-1_*cbl* vector was grown overnight in LB Amp and used to inoculate 1L of 2x YT media (16 g tryptone, 10 g yeast extract, and 5 g NaCl, pH 7.0) with Amp to 0.1 OD (Abs_{600}). Cultures were grown shaking at 30°C, induced with 1 mM IPTG at 0.8 OD (Abs_{600}), and incubated for additional 4 hr. Cultures were harvested by centrifugation at 4°C, resuspended in cold PBS, and stored at -80°C. For lysis, thawed cell pastes were passed through a French press three times and cell lysates were clarified by centrifugation (15000 × g for 30 min at 4°C). Cell extracts were loaded onto GSTrap 4B columns (GE Healthcare) pre-equilibrated with binding buffer (PBS, pH 7.4) and then washed with 10 column volumes of binding buffer. Column was washed with PreScission cleavage buffer (50 mM Tris-HCl, 150 mM NaCl, 1 mM EDTA, 1 mM DTT, pH 7.5) and then incubated overnight at 4°C with the PreScission Protease Mix (PreScission cleavage buffer with PreScission Protease) before eluting the recombinant protein with PreScission cleavage buffer. All fractions were analyzed for purity by SDS-PAGE. Apo-Cbl concentrations were estimated using $\varepsilon = 19940\ M^{-1}\ cm^{-1}$ (based on amino acid content); Cu^{+}-Cbl were determined using the Bradford method and apo-Cbl as a standard.

Copper Binding and BCS Competition Assays. All biochemical assays were conducted under strict anaerobic conditions, either in a Coy anaerobic chamber (Grass Lake, MI) or using sealed cuvettes. After purification, apo-Cbl protein was transferred to the anaerobic chamber and the buffer exchanged (buffer R: 10 mM MOPS, 50 mM NaCl, pH 7.4) using a PD-10 column (GE Healthcare). When necessary, protein was concentrated using YM-3 Centriplus Centrifugal Concentrators (Millipore). CuCl stocks were prepared anaerobically.

For Cu^+-binding assays, 0-10 mol equivalents of CuCl were added to purified apo-Cbl (10-25 μM) using an airtight syringe in a final volume of 1 ml (buffer R). UV-Visible absorption spectra (200-800 nm) were recorded using a Beckman-Coulter DU800 spectrophotometer. The dilution of copper was considered negligible as the total added volume was less than 15 μl.

Competition assays with the Cu^+ specific chelator bathocuproine disulfonate (BCS) (Sigma) were conducted as previously described (Ma, Cowart, Scott, *et al.*, 2009; Grossoehme *et al.*, 2011). Varying concentrations of Cu^+ (0-50 μM) were added to apo-Cbl (10 μM) previously mixed with BCS (40 μM) in buffer R and the UV-visible absorption spectra recorded. BCS forms a complex with Cu^+ in a 2:1 ratio [Cu^+-$(BCS)_2$], that can be monitored by changes in absorbance at 483nm with an overall association constant of $\beta_2 = 10^{19.8}$ (Xiao *et al.*, 2004). To determine the Cu^+ binding constant of Cbl, apo-Cbl (5 μM) was incubated with 0, 80, 100, and 120 μM BCS in buffer R. Cu^+ (40 μM) was added to each sample, incubated anaerobically for 2 hr for equilibration, and absorption of spectra taken. The concentrations of apo-Cbl and metalated-Cbl were determined by the Bradford method using apo-Cbl as a standard. Assuming four binding sites *n*=4, the average association constant (K_{Cbl}), the dissociation constant (K_D), and the Hill coefficient (n_H) of Cbl were determined as follows:

$$K_{Cbl} = [Cu^+_4\text{-Cbl}] / ([\text{apo-Cbl}]\,[Cu^+]) = 1/K_D$$

$$n_H = (\log \{\theta / (1 - \theta)\} + \log K_D) / \log [Cu],$$

where the Cu^+ occupancy (θ) of Cbl is the ratio of Cu-bound Cbl to total Cbl:

$$\theta = [Cu^+_4\text{-Cbl}] / ([Cu^+_4\text{-Cbl}] + [\text{apo-Cbl}])$$

Results

Analyses of *S. aureus* genes involved in copper homeostasis. We analyzed the *S. aureus* USA300 FPR3757 genome (Diep *et al.*, 2006) for genes involved in copper (Cu) homeostasis. We found the copper-sensitive operon repressor (CsoR), that senses and binds intracellular Cu leading to derepression of the *copAZ* operon (Baker *et al.*, 2011). CopA is a membrane-bound Cu-exporting protein and CopZ is an intracellular Cu-binding chaperone (Sitthisak *et al.*, 2007).

Further analysis identified the SAUSA300_0078 locus as an additional copper transporter (CopB; **Figure 2.1A**). CopB shows 36% identity with CopA and contains most of the conserved structural elements of P_{1B}-ATPases (**Figure 2.S1**). These structural elements include the phosphatase domain (TGES), the conserved CPX metal-binding sequence, and the ATP-binding domain (MXGDGXNDXP). However, CopB lacks the metal-binding CXXC motifs in the N-terminal region present in CopA and instead has a His-rich N-terminus.

An additional 546-bp open reading frame encoding a putative lipoprotein (*cbl*) is located 17-bp downstream of *copB*. Cbl (copper-binding lipoprotein) contains a duplicated DUF1541 domain (Marchler-Bauer *et al.*, 2015) that has not been described previously. The *copB* and *cbl* genes are located within the arginine catabolic mobile element (ACME) (Diep *et al.*, 2006), a 31-kb transposable element located adjacent to the SCC*mec*IV cassette.

We conducted a search for *cbl* homologues in the genomes of other sequenced Prokaryotes. We identified ~200 Cbl-like proteins with the majority belonging to the *Actinobacteria* and *Firmicutes* phyla. Additional analysis revealed that these organisms also have at least one additional Cu detoxification protein (CopA, CopZ, or CopB) (**Table 2.S2**). The *cbl* gene is often co-localized near genes or within apparent operons encoding alternate

genes involved in Cu homeostasis (**Figure 2.S2**). The Cbl homologues contain the lipobox motif typical of lipoproteins, that is characterized by the presence of a L-[A/S/T]-[G/A]-C sequence (Hutchings *et al.*, 2009). Other staphylococci also have *cbl* located in an apparent operon with or nearby the *copB* gene (**Figure 2.S2**). Taken together, these findings led to the hypothesis that CopB and Cbl have roles in Cu homeostasis.

***S. aureus* strains lacking CopB or Cbl are sensitive to Cu**. We began testing the hypothesis that the *copB* and *cbl* genes have roles in Cu homeostasis by constructing mutant strains containing individual deletions of *copB* or *cbl* in the *S. aureus* USA300 strain LAC (**Figure 2.S3**), that differs from the *S. aureus* USA300 strain FPR3757 by a few SNPs (Li *et al.*, 2009). The wild-type (WT), *copB*, and *cbl* strains were spot plated on chemically defined media containing varying concentrations of Cu, zinc (Zn), iron (Fe), cobalt (Co), or manganese (Mn). The *copB* and *cbl* mutant strains only showed increased sensitivity to Cu as displayed by decreased number of colony forming units (CFUs) when cultured in the presence of Cu and these phenotypes were genetically complemented (**Figure 2.1B**).

We conducted genomic analysis and found that the *S. aureus* USA400 strain MW2 lacks the *copBcbl* operon. We mobilized the *copB* or *cbl* genes to the MW2 strain via plasmid and examined Cu sensitivity. As shown in **Figure 2.1C**, *copB* and *cbl* over-expression in the MW2 strain led to increased resistance to Cu. We also found that *cbl* over-expression in the *S. aureus* strains Newman, COL, and RN4220 strains led to increased Cu resistance (**Figure 2.S4**). These data suggest that CopB and Cbl have roles in Cu homeostasis.

Strains lacking CopB or Cbl display exacerbated phenotypes in cells unable to export cytoplasmic Cu. We next investigated whether CopB and Cbl had a functional redundancy with other factors involved in preventing Cu intoxication. Inactivation of genes involved in similar functions in the cell often lead to synergistic phenotypes (Pérez-Pérez *et al.*, 2009).

S. aureus strains lacking CopA accumulate cytoplasmic Cu and are sensitive to Cu intoxication (Sitthisak *et al.*, 2007). We constructed a *copA copB* double mutant strain and examined Cu sensitivity. We found that strains lacking either *copA* or *copB* had decreased growth on solid media containing >50 μM Cu, but the *copA copB* double mutant displayed an exacerbated sensitivity to Cu and at a much lower Cu concentration. (**Figure 2.2A**). These findings suggest that both CopA and CopB are involved in preventing Cu toxicity.

The *copA cbl* double mutant strain also displayed an increased sensitivity to Cu when compared to the *copA* and *cbl* single mutants (**Figure 2.2B**). Moreover, the *copA copB cbl* triple mutant was more sensitive to Cu intoxication than the *copA copB* double mutant strain (**Figure 2.2C**).

CopZ is a Cu chaperone involved in binding and trafficking intracellular Cu (Radford *et al.*, 2003). The *S. aureus copZ* mutant does not display a Cu sensitivity phenotype (data not shown). Moreover, the *copZ copB* and *copZ cbl* strains displayed Cu sensitivity phenotypes that were indistinguishable from the *copB* and *cbl* single mutants (data not shown).

Collectively, the results presented in **Figure 2.2** suggest that (a) strains lacking CopB or Cbl have increased sensitivity to Cu, (b) CopA and CopB have a functional overlap in Cu homeostasis and function as Cu exporters, (c) Cbl has an independent mechanism from CopB and CopA, and (d) CopZ is not required to prevent Cu intoxication under the conditions examined.

The *copBcbl* operon is upregulated under Cu stress. As mentioned above, the *copB* and *cbl* genes are separated by 17-bp and appear to be located in an apparent operon. To determine whether the *copB* and *cbl* genes are co-transcribed, RNA was isolated from WT cultures grown in chemically defined media with Cu and cDNA libraries were generated. Using cDNA as a template and primers nested within *copB* and *cbl*, we were able to obtain an

amplicon corresponding to the intergenic region between *copB* and *cbl* (**Figure 2.3A**). A PCR product was only obtained when RT was used in the generation of the cDNA libraries, confirming that the amplicon was not a result of contaminating genomic DNA.

We next investigated the transcriptional changes of the *copBcbl* operon in response to Cu. To this end, we cultured the WT strain without and with 100 μM Cu before isolating RNA and generating cDNA libraries. We monitored the expression of *copB* and *cbl* transcripts by quantitative RT-PCR. The *S. aureus copAZ* operon is induced during Cu stress (Sitthisak *et al.*, 2007; Baker *et al.*, 2010; Baker *et al.*, 2011), and therefore, we quantified abundance of the *copA* transcript as a control. As shown in **Figure 2.3B**, *copB* and *cbl* transcripts are upregulated ~4-fold upon Cu stress, whereas *copA* is upregulated by ~8-fold.

We used a *copBcbl* transcriptional reporter to further analyze the regulation of the *copBcbl* operon. To verify the functionality of the reporter, we monitored its activity in the WT strain grown in chemically defined media with varying Cu concentrations. As shown in **Figure 2.3C**, transcriptional activity of *copBcbl* increased in a dose-dependent manner.

P_{1B}-ATPases are a subgroup of membrane-bound proteins that participate in the transport of heavy metals (Cu, Zn, and Co) across membranes (Argüello *et al.*, 2007). We examined the transcriptional activity of *copBcbl* when the WT strain was challenged with excess Mn^{2+}, Fe^{2+}, Zn^{2+}, and Co^{2+}. As shown in **Figure 2.3D**, transcriptional activity of *copBcbl* is not altered upon challenge with the metals examined. Likewise, the *copB* and *cbl* mutant strains did not display increased sensitivity to Mn, Fe, Zn, or Co at concentrations that decreased the survival of the WT (data not shown). These results suggest that the *copBcbl* operon specifically responds to Cu stress.

Expression of the *copBcbl* operon is CsoR-dependent. CsoR is the copper-sensitive operon repressor that, upon binding intracellular Cu, derepresses the transcription of the *copAZ*

operon (Baker *et al.*, 2011). We were interested in knowing whether the expression of the *copBcbl* operon, like the *copAZ* operon, was also regulated by CsoR. The CsoR binding site was identified in the promoter region of *copZA* in *Bacillus subtilis* (Smaldone and Helmann, 2007) and is characterized by a G/C pseudo-inverted repeat region (TACCNNNNGGG-GGTA). We analyzed the promoter region of the *copBcbl* operon and, as depicted in **Figure 2.4A**, it contains a hypothetical CsoR binding site ~100-bp from the translational start site. Therefore, we hypothesized that *copBcbl* expression was regulated by CsoR.

We cultured the WT and the *csoR* strains containing the *copBcbl* reporter in chemically defined media and monitored transcriptional activity. As shown in **Figure 2.4B**, the transcriptional activity of *copBcbl* is higher in the *csoR* mutant strain, suggesting that the *copBcbl* operon is negatively regulated by CsoR. The addition of Cu led to increased transcription of *copBcbl* in the WT strain, but to a much less extent in the *csoR* mutant strain (**Figure 2.4B**), suggesting that transcription of the *copBcbl* operon is primarily controlled by CsoR. The *S. aureus* strain Newman lacks the *copBcbl* operon, but we found that *copBcbl* transcriptional activity was also increased in an *S. aureus* Newman *csoR* mutant strain (**Figure 2.S5**).

Cbl is membrane-associated and surface-exposed. Our results support the hypothesis that the *copBcbl* operon is involved in providing Cu resistance, but functions have not been assigned to Cbl or the DUF1541 domain. We conducted a series of experiments to determine the physiological function of the *cbl* gene product.

Cbl is a putative lipoprotein. We conducted cell fractionation experiments to verify the cellular location of the Cbl protein. We cloned the *cbl* gene under the transcriptional control of a xylose inducible promoter (*xylRO*) and included a C-terminal FLAG affinity tag (pEPSA5_*cbl*-FLAG). The FLAG-tagged *cbl* allele genetically complemented the Cu

sensitivity of the *cbl* mutant strain, verifying the functionality of Cbl-FLAG (data not shown). Cultures of the *cbl* mutant strain harboring the pEPSA_5_*cbl*-FLAG vector were grown in the presence and absence of xylose to induce *cbl* expression, cells were harvested, and components were separated into cytoplasmic and membrane fractions. Western blot using anti-FLAG antibodies was used to monitor Cbl_FLAG in whole cell extracts, cytoplasmic fractions, and membrane fractions. As shown in **Figure 2.5A**, the Cbl-FLAG protein (~21 kDa) was detected in whole cell extracts and membrane fractions, but not in cytosolic fractions, confirming that Cbl is a membrane-associated protein. Cbl-FLAG bands were also detected in non-induced samples, albeit at a much lower intensity, a result that is likely due to leaky expression of the *xylRO* promoter.

The TOPCONS algorithm (Bernsel *et al.*, 2009) predicted that Cbl contains an N-terminal signal-sequence (**Figure 2.S1A**) that is characteristic of proteins that are directed to secretory pathways for translocation across the cytoplasmic membrane (Hutchings *et al.*, 2009). We examined whether the functionality of the Cbl protein depends on its cellular localization. To do this, we cloned the *cbl* gene lacking the signal-sequence, referred to as the truncated Cbl or Cbl(T). As shown in **Figure 2.5B**, the Cbl(T) did not complement the Cu sensitivity phenotype of the *cbl* mutant strain, whereas the full-length Cbl did, suggesting that membrane localization is required for Cbl to prevent Cu intoxication.

While lipoproteins in Gram-negative bacteria may be anchored to the cytoplasmic membrane or the outer membrane, and facing either the periplasmic space or the extracellular surface, lipoproteins in Gram-positive bacteria are anchored to the cytoplasmic membrane with the C-terminal facing the extracellular surface (Navarre *et al.*, 1996; Kovacs-Simon *et al.*, 2011). We constructed chimeric proteins consisting of Cbl(T) and either Nuc2 or the Nuc2 signal sequence. Nuc2 is a membrane-bound, surface-exposed protein (Kiedrowski *et al.*, 2014). The chimeric proteins consisted of (a) Cbl(T) fused to the C-terminus of the full

length Nuc2 (pEPSA5_*nuc2*(FL)-*cbl*), or (b) Cbl(T) fused to the Nuc2 signal-sequence (pEPSA5_*nuc2*(SS)-*cbl*) (**Figure 2.5C**). Both chimeric constructs genetically complemented the Cu sensitivity phenotype of the *cbl* mutant strain (**Figure 2.5C**). Altogether, data presented in **Figure 2.5** suggest that Cbl is a membrane-associated protein that requires membrane localization and surface exposure to prevent Cu intoxication.

Cbl binds copper *in vitro*. The phenotypic and genetic analyses presented thus far show that Cbl is necessary for preventing Cu intoxication in *S. aureus*. We next tested the hypothesis that Cbl prevents Cu intoxication by binding Cu.

The soluble Cbl(T) protein was expressed and purified from *Escherichia coli* (**Figure 2.S8**). Cu^+ binding was examined using UV-visible absorption spectroscopy. Upon titrating Cu^+ into apo-Cbl, increases in the absorption spectrum in the UV region (A_{260nm}) were observed (**Figure 2.6A**). We found that Cu^+ binding reaches saturation after the addition of ~4 molar equivalents (**Figure 2.6B**). Moreover, the formation of Cu^+-Cbl follows a sigmoidal trend and, upon fitting the data to a Hill plot, the theoretical Hill coefficient (n_H) was determined to be ~4.3 with a dissociation constant (K_D) in the ~10^{-19} M range.

We conducted competition experiments to verify the Cu^+ binding affinity of Cbl. Bathocuprione disulfonate (BCS) is a Cu^+ specific chelator that forms a complex with Cu^+ in a 2:1 ratio [Cu^+-$(BCS)_2$], that can be monitored by the change in absorbance at 483 nm with an overall association constant of $\beta_2 = 10^{19.8}$ (Xiao *et al.*, 2004). Titration of Cu^+ (0-140 μM) into a solution containing a mixture of 5 μM apo-Cbl and 40 μM BCS leads to immediate formation of the Cu^+-$(BCS)_2$ complex (**Figure 2.S9**), indicating that BCS has a higher affinity for Cu^+ than Cbl. BCS becomes saturated after the addition of 80 μM Cu^+, corresponding to a Cu^+:BCS ratio of 2. Titration of more Cu^+ does not lead to additional

formation of the Cu^{+}-$(BCS)_2$ complex, suggesting that the additional Cu^{+} titrated into the mixture might be associating to Cbl.

To determine the Cu^{+} binding affinity of Cbl, mixtures containing apo-Cbl (5 μM) and Cu^{+} (40 μM) were prepared anaerobically. Different amounts of BCS (0, 80, 100, and 120 μM) were added to each sample and the UV-visible absorption spectra taken. In each sample, the formation of Cu^{+}-Cbl was detected at A_{260nm} and the formation of Cu^{+}-$(BCS)_2$ at A_{483nm} (**Figure 2.6C**). From these data, the Cu^{+} binding affinity of Cbl (log K_{Cbl}) was estimated to be 17.3 ± 0.1. We obtained an n_H of 3.8 ± 0.1, indicating positive cooperativity of Cu^{+} binding. The K_D was in the 10^{-18} M range and, like the n_H, these values were in close agreement with the theoretical values determined in using the Hill fit shown in **Figure 2.6B**.

Discussion

This study was initiated to further investigate the mechanisms of copper (Cu) homeostasis in *Staphylococcus aureus*. The work presented herein have re-affirmed the roles of CopA and CsoR in Cu efflux and intracellular Cu sensing, respectively. We have also assigned roles for the *copB* and *cbl* gene products in protecting against Cu intoxication. These data, as well as published work on CopA (Sitthisak *et al.*, 2007), CopZ, and CsoR (Baker *et al.*, 2011), resulted in a working model for Cu detoxification in the *S. aureus* USA300 strain LAC (**Figure 2.7**).

Upon sensing Cu in the cytosol, CsoR derepresses transcription of the *copAZ* and *copBcbl* operons. CopZ binds intracellular Cu and delivers it to its target proteins, such as CsoR, CopA, or CopB. The CopA and CopB proteins function to efflux Cu from the cytosol. Cbl is a membrane-associated, surface-exposed protein that binds Cu on the outside of the cell preventing it from entering the cytosol and/or binds Cu after efflux by CopA or CopB.

Our work shows that Cbl is a copper-binding lipoprotein with a Cu^+ binding affinity (log K_{Cbl}) of 17.3 ± 0.1. The reported Cu^+ binding affinity of the *S. aureus* (Grossoehme *et al.*, 2011) *B. subtilis* (Ma, Cowart, Scott, *et al.*, 2009) and *Mycobacterium tuberculosis* (Ma, Cowart, Ward, *et al.*, 2009) copper-sensing CsoR proteins have Cu^+ binding affinities of >18. The intracellular Cu^+ trafficking chaperone CopZ from *B. subtilis* shows a similar binding affinity for Cu^+ to that of Cbl (~17.0) (Singleton *et al.*, 2009), that is similar to the reported binding affinity of the metallochaperone HAH1 involved in Cu^+ trafficking to ATP7A (Badarau and Dennison, 2011). The CusCFBA system is involved in the detoxification of Cu^+ from the periplasm of *Escherichia coli* (Delmar *et al.*, 2013). The metallochaperone of this system, CusF, has a lower Cu^+ affinity (~14) than what we report here for Cbl (Bagchi *et al.*, 2013).

Methicillin-resistant *S. aureus* (MRSA) infections are highly prevalent in community settings and this epidemic is widely attributed to the spread of the USA300 clone (Tenover *et al.*, 2006; Talan *et al.*, 2011). The majority of the genetic differences between USA300 and other staphylococcal strains of clinical importance is the presence of mobile genetic elements including the arginine catabolic mobile element (ACME) (Diep *et al.*, 2006). Deletion of the ACME region does not alter global gene expression, but it does decrease the fitness of the USA300 clone in a rabbit bacteremia model (Diep *et al.*, 2008), and therefore, it is believed that genes encoded within the ACME region provide a fitness advantage to the pathogen. For instance, the constitutive expression of the ACME-arginine-deiminase system (*arc*) allows survival in acidic conditions (Thurlow *et al.*, 2013) and the ACME-encoded *speG* gene provides resistance to high levels of host-derived polyamines (Joshi *et al.*, 2011; Thurlow *et al.*, 2013), thereby contributing to the colonization and persistence of *S. aureus* on human skin.

The use of copper-mediated killing by the host macrophages, together with its increasing use in healthcare settings (Noyce *et al.*, 2006; Salgado *et al.*, 2013), may be factors that could be selecting for copper-resistant microorganisms by promoting the dissemination of mobile genetic elements that confer copper resistance. The highly successful USA300 clone (Diep *et al.*, 2006) lacks the *copBmco* present in alternate *S. aureus* strains (Baker *et al.*, 2011); however, we found a two-gene operon located within the ACME region consisting of CopB, a copper transporter, and Cbl, a copper-binding lipoprotein. The USA300 *copB* and *cbl* genes are also present in *S. epidermidis* (Zhang *et al.*, 2003). However, in *S. epidermidis*, a gene encoding a multicopper oxidase (SE0127, *mco*) is located between *copB* and *cbl,* but *mco* is absent in the USA300 clone (Diep *et al.*, 2006; Resch *et al.*, 2013). Although with some genetic variances, other genes of the USA300 ACME region are also present in the human commensal *S. epidermidis* (Diep *et al.*, 2006; Miragaia *et al.*, 2009), and phylogenetic

analysis suggests the horizontal transfer event occurred prior to the epidemic expansion of the USA300 strain (Planet *et al.*, 2013). It is worth noting that *S. epidermidis* has three copper-exporting proteins, perhaps providing the organism an increased fitness advantage for growth and survival on human skin. Both *S. aureus* and *S. epidermidis* are skin commensals, so it is tempting to speculate that the horizontal gene transfer events may have been promoted by copper stress conditions exerted by the host immune system. Our bioinformatics analysis revealed that, in addition to *S. epidermidis*, other staphylococcal species also have the *cbl* gene, including *S. xylosus*, *S. capitis*, and *S. haemolyticus*, all of which are skin commensals. Other studies show that the acquisition of genetic elements from other species that share the same niche is a strategy employed by *S. aureus* to adapt to new hosts (Lowder *et al.*, 2009; Resch *et al.*, 2013).

A USA300 Latin American variant (USA300-LV) has become one of the most prevalent clones associated to MRSA infections in community settings in South America. Phylogenetic analysis revealed that most of the genomic differences between USA300-LV and USA300 were associated to mobile genetic elements, specifically the absence of the ACME region in the USA300-LV clones (Planet *et al.*, 2015). Despite this finding, the *copB* and *cbl* genes were found in more than 50% of the examined USA300 and USA300-LV genomes. In the USA300-LV strains, the *copB* and *cbl* genes are located adjacent to their SCC*mec* variant, and the locus has been designated as the Copper and Mercury Resistance (COMER) mobile element (Planet *et al.*, 2015). The acquisition of mobile genetic elements containing copper pathogenicity islands has also been discovered in other organisms (Hao *et al.*, 2015). Overall, these studies provide additional evidence that constant copper exposure (immune system, healthcare settings, and/or diet) may not only promote the dissemination of genetic elements that result in the development of metal-resistant microorganisms, but also strains that are hyper-virulent and have antimicrobial resistance.

Copper resistance mechanisms acquired via transposable elements include copper transporters, multicopper oxidases or, as reported in this study, membrane-bound lipoproteins. Another lipoproteins involved in copper metabolism has been identified in the intracellular pathogen *Mycobacterium tuberculosis* (Festa *et al.*, 2011), but this lipoprotein does not have any structural similarities to Cbl. Comparable to the *S. aureus cbl* gene, the *M. tuberculosis lpqS* gene is co-localized with other copper homeostatic genes and is derepressed by one of the copper-sensing regulators under copper stress. Moreover, a strain lacking LpqS is sensitive to copper and has an attenuated growth phenotype in THP1-derived macrophages (Sakthi and Narayanan, 2013), suggesting a role in combating copper toxicity within macrophages.

Bacterial surface proteins are often attractive targets for the development of vaccines because of their potential roles in nutrient uptake and host adhesion. Proteome analysis revealed that the majority of the surface-associated proteins expressed by USA300 in a murine systemic infection are lipoproteins (Diep *et al.*, 2014). Interestingly, Cbl was detected from murine kidneys and livers 6 days post-infection (Diep *et al.*, 2014), however, it is unknown whether Cbl is also highly abundant during a natural human systemic infection or contributes to the virulence of *S. aureus*. Cbl is not conserved throughout all *S. aureus* clinical isolates, potentially excluding it as a suitable vaccine antigen.

In summary, this work describes an additional strategy by which the *S. aureus* USA300 clone prevents copper intoxication. The ACME-encoded *copBcbl* operon may also be contributing to the high success of this clone in surviving the copper-dependent killing mechanism employed by the host immune system. Having a better understanding on how pathogens prevent copper toxicity can be used to design compounds that can override the bacterial copper homeostatic mechanisms and, at the same time, enhance the effects of copper accumulation within the host macrophages.

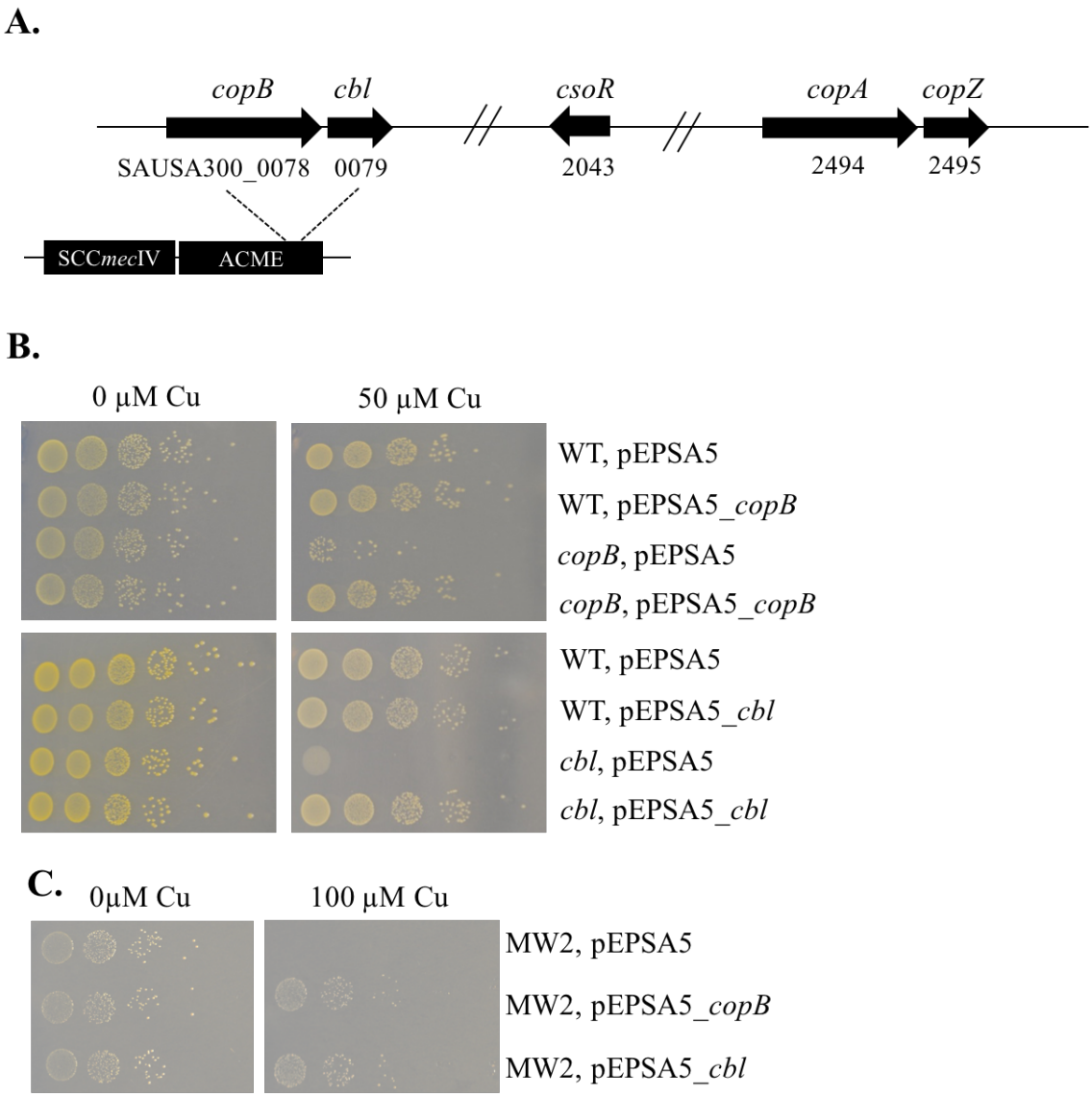

Figure 2.1. The *cbl* and *copB* gene products protect against copper intoxication. (A) Chromosomal location of genes involved in copper homeostasis in the *S. aureus* USA300 strain FPR3757. The *copB* (SAUSA300_0078) and *cbl* (SAUSA300_0079) genes are located in the Arginine Catabolic Mobile Element (ACME) region, adjacent to the SCC*mec*IV genetic element. (B) The *copA*, *copB*, and *cbl* gene products are necessary to prevent Cu intoxication. Top: The WT (JMB1100) and *copB* (JMB7900) strains containing the pEPSA5 and pEPSA5_*copB* are shown. Bottom: The WT (JMB1100) and

cbl (JMB7711) strains containing the pEPSA5 and pEPSA5_*cbl* are shown. Strains were serial diluted and spot plated on chemically defined media without or with 50 μM Cu. (C) *copB* or *cbl* overexpression leads to increased copper resistance in the *S. aureus* USA400 strain MW2. The *S. aureus* MW2 wild-type (JMB1325) containing the pEPSA5, pEPSA5_*copB*, or pEPSA_*cbl* vectors is shown. Strains were serial diluted and spot plated on chemically defined media without or with 100 μM Cu.

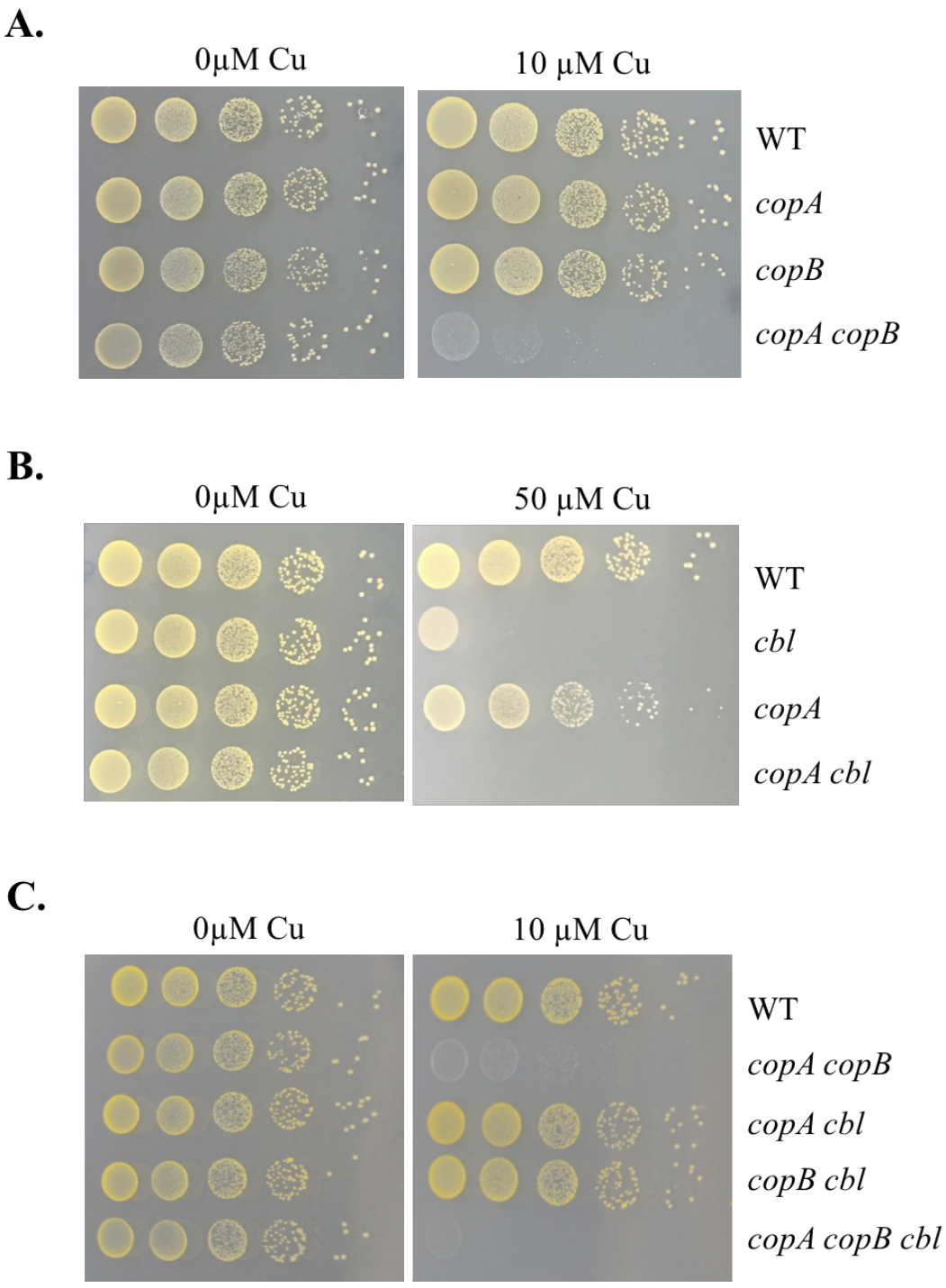

Figure 2.2. Cbl functions independently of CopA and CopB and intracellular Cu accumulation exacerbates the phenotypes of the *copB* and *cbl* mutants. (A) The phenotypes associated with *copB* and *copA* mutations are synergistic. The WT

(JMB1100), *copA* (JMB4084), *copB* (JMB7900), and *copA copB* (JMB8009) strains were serial diluted and spot plated on chemically defined media without or with 10 μM Cu. (B) A strain lacking CopA and Cbl shows increased sensitivity to Cu. The WT (JMB1100), *cbl* (JMB7711), *copA* (JMB4084), and *copA cbl* (JMB7803) strains were serial diluted and spot plated on chemically defined media without or with 50 μM Cu. (C) Cbl functions independently of CopB and CopA. The WT (JMB1100), *copA copB* (JMB8009), *copA cbl* (JMB7803), *copB cbl* (JMB7901), and *copA copB cbl* (JMB7972) strains were serial diluted and spot plated on chemically defined media without or with 10 μM Cu.

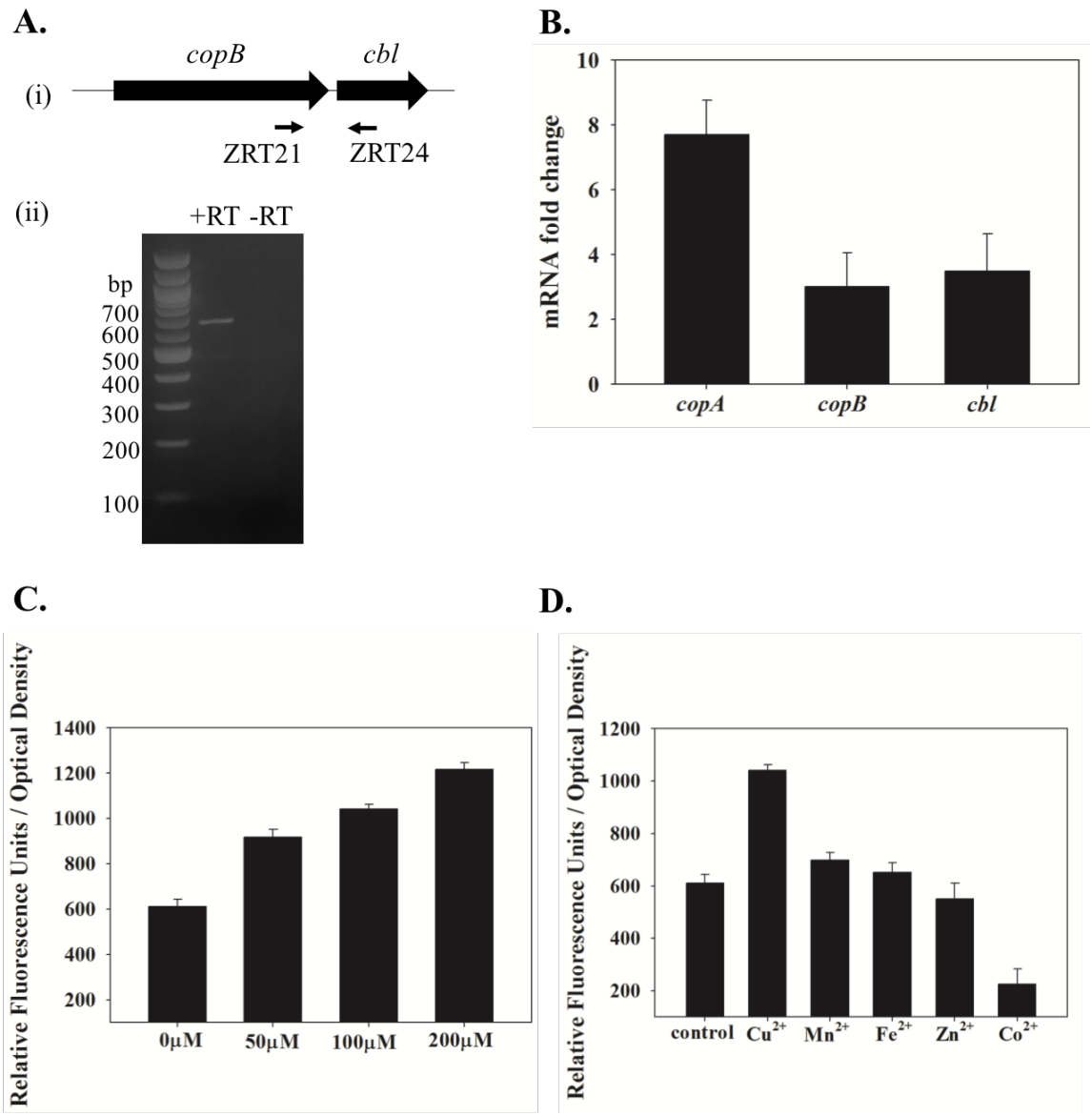

Figure 2.3. The *copBcbl* operon is upregulated under copper stress. (A) The *copB* and *cbl* genes are co-transcribed. RNA was isolated from the WT (JMB1100) strain grown in chemically defined medium with 100 μM Cu and cDNA libraries generated. (i) Schematic showing the primer pair (ZRT21 and ZRT24) used to detect the *copBcbl* transcript; expected size: 643-bp. (ii) Agarose gel electrophoresis was used to detect the *copBcbl* amplicon generated using cDNA libraries as template DNA. A reaction without reverse transcriptase (-RT) was included as a control for genomic DNA contamination.

(B) The *copA*, *copB*, and *cbl* genes are induced upon copper stress. The *S. aureus* WT (JMB1100) was cultured in chemically defined media containing 0 μM or 100 μM Cu. RNA was isolated, cDNA generated, and the abundance of the *copA*, *copB*, and *cbl* transcripts were quantified. Data show fold induction of genes of interest upon addition of Cu. Data represent the average of biological triplicates with errors presented as standard deviations. (C) Transcriptional activity of the *copBcbl* operon increases in synergy with Cu addition. Activity of the *copBcbl* transcriptional reporter was monitored in the *S. aureus* USA300 WT strain (JMB1100) grown in chemically defined media containing 0, 50, 100, or 200 μM Cu. (D) Transcriptional activity of the *copBcbl* operon is specific to copper stress. Activity of the *copBcbl* transcriptional reporter was monitored in the *S. aureus* USA300 WT strain (JMB1100) grown in chemically defined media containing 100 μM Cu^{2+}, 100 μM Mn^{2+}, 100 μM Fe^{2+}, 100 μM Zn^{2+}, or 50 μM Co^{2+}. For Panels (C) and (D), fluorescence data was standardized to culture optical density (A_{590}) and data represent the average of biological triplicates with errors presented as standard deviations.

A.

Bsu CsoO *copZA*	5' – A**TACC**CTAC**GGGGGTA**T –3'
SaNwmn CsoO *copAZ*	5' – A**TACC**TATA**GGGGGTA**C –3'
*Sa*FPR3757 *copAZ*	5' – A**TACC**TATA**GGGGGTA**C –3'
*Sa*FPR3757 *copBcbl*	5' – A**TACC**CTGG**GTGGGTA**T –3'

B.

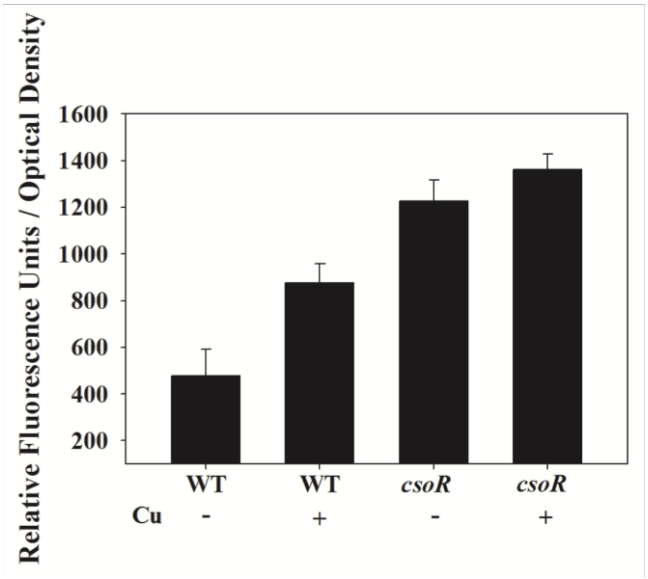

Figure 2.4. The *copBcbl* operon is regulated by CsoR. (A) Comparison of the *S. aureus* USA300_FPR3757 *copAZ* and *copBcbl* promoter regions to the *B. subtilis copZA* and *S. aureus* Newman *copAZ* promoter region. The proposed CsoR binding site is shown in bold. (B) Transcriptional activity of the *copBcbl* operon is higher in a *csoR* mutant. Activity of the *copBcbl* transcriptional reporter was monitored in the *S. aureus* USA300 WT strain (JMB1100) and *csoR* mutant (JMB6807) grown in chemically defined media containing 0 μM or 100 μM Cu 100 μM Cu. Fluorescence data was standardized to culture optical density (A_{590}). Data shown represent the average of biological triplicates with errors presented as standard deviations.

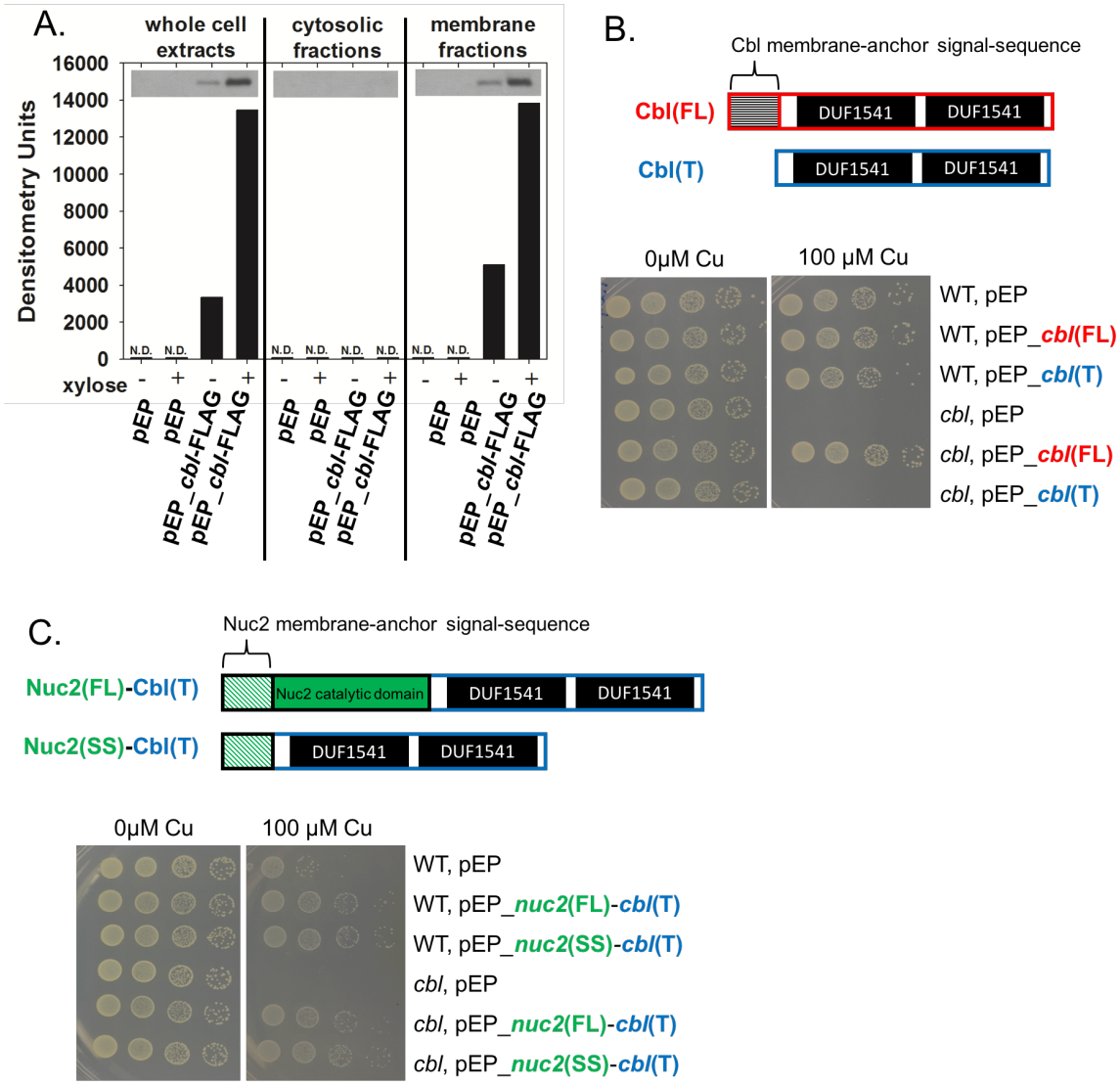

Figure 2.5. Cbl is a membrane-associated and surface-exposed protein. (A) Monitoring Cbl abundance in whole cell extracts, cytoplasmic fractions, and membrane fractions. The *cbl* mutant containing the pEPSA5_*cbl*(FL)-FLAG was cultured in the absence (0% xyl) and presence (0.1% xyl) of xylose prior to fractionation and analysis. ND; not detected. Representative densitometry and Western blot (inset) analysis shown. (B) The membrane-anchor and signal-sequence are necessary for Cbl function. (i)

Schematic showing the Cbl variants. The full length *cbl* gene or truncated *cbl* gene, lacking the N-terminus membrane-anchor signal-sequence, were cloned into the pEPSA5 plasmid to yield the pEPSA_*cbl*(FL) and pEPSA_*cbl*(T) vectors, respectively. (ii) The WT (JMB1100) and *cbl* (JMB7711) strains harboring the pEPSA5, pEPSA5_*cbl*(FL), or pEPSA5_*cbl*(T) vectors were serial diluted and spot plated on chemically defined media without and with 100 μM copper. (C) Cell surface exposure is necessary for Cbl function. (i) Schematic showing the Cbl chimeric variants. The truncated *cbl* gene, lacking the N-terminal membrane-anchor signal-sequence, was fused to either the full length *nuc2* or the *nuc2* membrane-anchor signal-sequence and cloned into the pEPSA5 plasmid to yield the pEPSA5_*nuc2*(FL)-*cbl* and pEPSA5_*nuc2*(SS)-*cbl* vectors, respectively. (ii) The WT (JMB1100) and *cbl* (JMB7711) strains harboring pEPSA5, pEPSA5_*nuc2*(FL)-*cbl*, or pEPSA5_*nuc2*(SS)-*cbl* vectors were serial diluted and spot plated on chemically defined media containing 0 μM or 100 μM Cu.

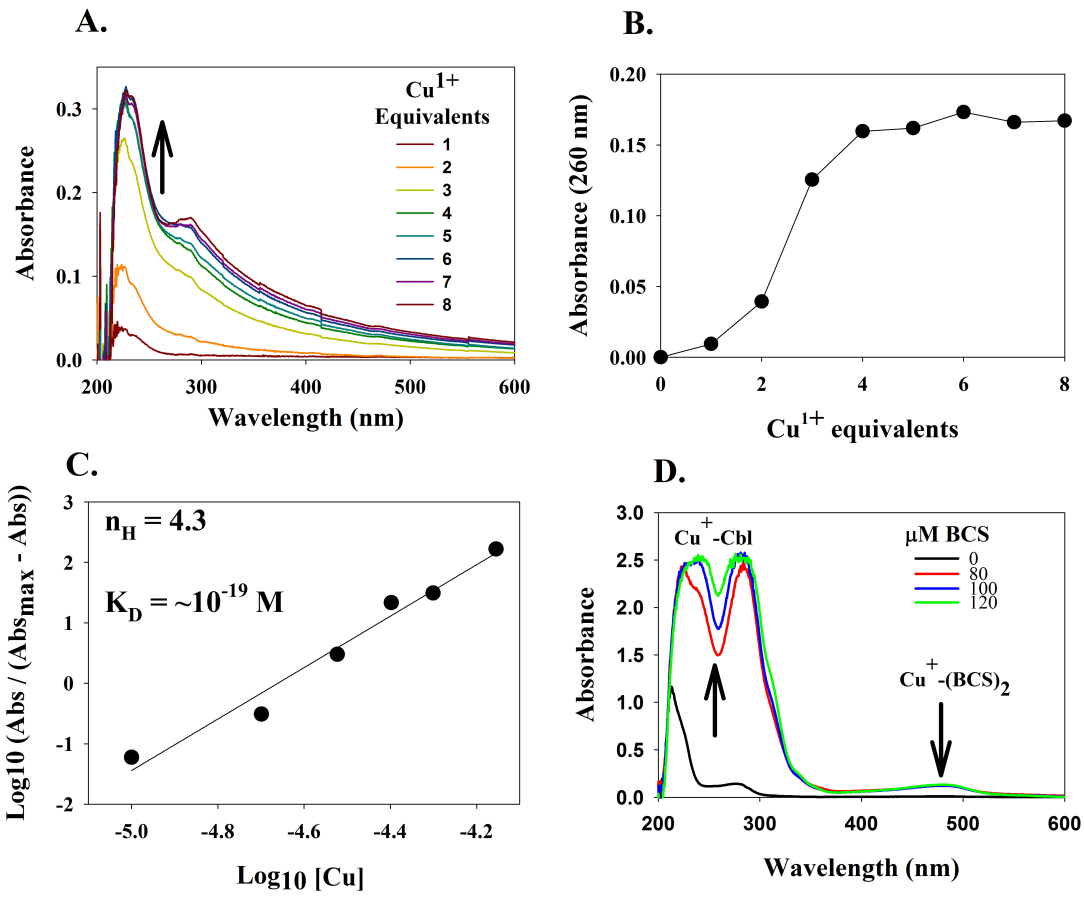

Figure 2.6. The *S. aureus* Cbl protein binds Cu^{+} *in vitro*. (A) UV-Visible absorption spectra of apo-Cbl (10 µM) anaerobically titrated with 1-8 Cu^{+} molar equivalents. (B) Cbl binds approximately 4 molar equivalents of Cu^{+}. Data are plotted as absorbance at 260 nm vs Cu^{+} molar equivalents (circles). (C) Hill plot of data from Panel B. (D) Determination of Cu^{+} binding affinity of Cbl. UV-visible absorption spectra after BCS (0, 80, 100, and 120 µM) was titrated into mixtures containing apo-Cbl (5 µM) and CuCl (40 µM). The graph shows spectral changes representing the formation of Cu^{+}-Cbl and Cu^{+}-BCS at 260nm and 483nm, respectively.

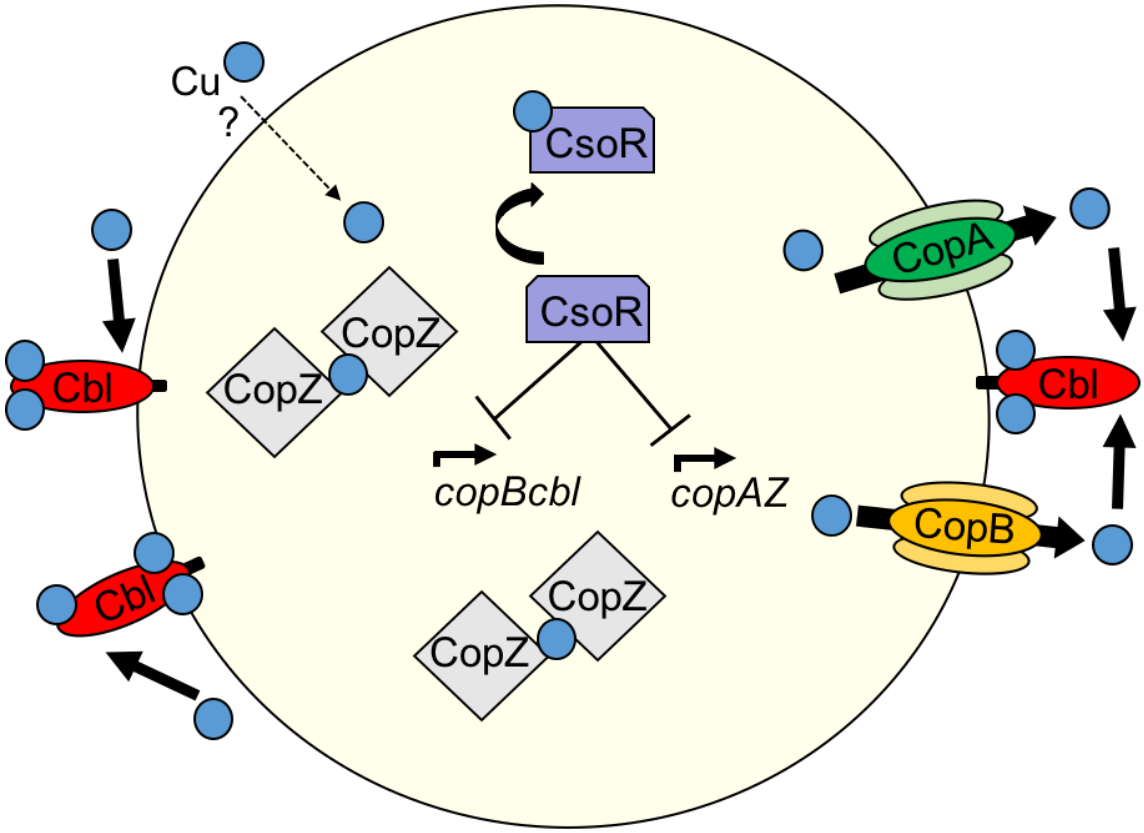

Figure 2.7. Working model for copper homeostasis in *S. aureus*. The CsoR transcriptional regulator senses and binds intracellular copper, leading to derepression of the *copAZ* and *copBcbl* operons. CopA is a copper-exporting transmembrane protein, while CopZ is a chaperone protein that binds and transfers copper to targets proteins. CopB is an additional copper-exporting protein, whereas Cbl is a membrane-bound, surface-exposed copper-binding lipoprotein. Cbl likely functions in (a) preventing copper uptake by tightly binding Cu in the extracellular environment, and (b) binding Cu exported via CopA or CopB to prevent it from re-entering the cell.

Table 2.1. Strains and plasmids used in this study.

***Staphylococcus aureus* strains**

Strain name	Genotype/Description	Background	Source / Reference
RN4220 (JMB1103)	Restriction-negative *S. aureus*	RN1	(Kreiswirth *et al.*, 1983)
JMB2790	SAUSA300_2494(*copA*)::Tn(*ermB*)	JE2	(Fey *et al.*, 2013)
JMB3488	SAUSA300_2043(*csoR*)::Tn(*ermB*)	JE2	(Fey *et al.*, 2013)
JMB1100	*S. aureus* USA300 wild-type strain	LAC	A.R. Horswill
JMB4084	SAUSA300_*copA*::Tn(*ermB*)	LAC	This study
JMB6807	SAUSA300_*csoR*::Tn(*tet*)	LAC	This study
JMB7900	SAUSA300_*copB*Δ	LAC	This study
JMB7711	SAUSA300_*cbl*Δ	LAC	This study
JMB7901	SAUSA300_*copB*Δ-*cbl*Δ	LAC	This study
JMB8009	SAUSA300_*copB*Δ, *copA*::Tn(*ermB*)	LAC	This study
JMB7803	SAUSA300_*cbl*Δ, *copA*::Tn(*ermB*)	LAC	This study
JMB7972	SAUSA300_*copB*Δ-*cbl*Δ, *copA*::Tn(*ermB*)	LAC	This study
JMB1324	parent strain	MW2	P. Schlievert
JMB1325	parent strain	COL	A. Horswill
JMB1422	parent strain	Newman	E. Skaar
JMB6338	NWMN_1991(*csoR*Δ)	Newman	E. Skaar

Other Strains

Name	Relevant genotype/Description	Source / Reference
Escherichia coli PH5α	Molecular cloning	Protein Express
E. coli BL21 DE3	Protein expression and purification	
Bacillus subtilis 168	Wild-type *Bsu* trpC2 (JMB7761)	V. Carabetta
Bacillus subtilis 168 *ydhK*::ery	*Bsu* strain lacking Cbl (BSU05790) (JMB7762)	V. Carabetta
Saccharomyces cerevisiae FY2	*ura3-52* yeast recombination cloning	W. Belden

Plasmids

Plasmid name	Locus/Function	Source / Reference
pJB38	Mutant construction	(Bose *et al.*, 2013)
pTET	pJB38 with *tet*(M)	(Bose *et al.*, 2013)
pJB38_*copB*Δ	*copB*Δ for chromosomal deletion	This study
pJB38_*cbl*Δ	*cbl*Δ for chromosomal deletion	This study

pJB38_*copB*Δ-*cbl*Δ	*copB*Δ-*cbl*Δ for chromosomal deletion	This study
pEPSA5	Vector for genetic complementation with XylRO promoter	(Forsyth *et al.*, 2002)
pCM11	Vector with promoterless *gfp* for transcriptional studies	(Malone *et al.*, 2009)
pCM11_*copB*	*copB* transcriptional reporter	This study
pEPSA5_*copB*	*copB* complementation vector	This study
pEPSA5_*cbl*(FL)	*cbl* (full length) complementation vector	This study
pEPSA5_*cbl*(T)	*cbl* (truncated version) complementation vector	This study
pEPSA5_*cbl*(FL)-FLAG	*cbl* (full length) containing a C-terminal FLAG tag	This study
pEPSA5_*nuc2*(FL)-*cbl*	*nuc2* (full length) fused to *cbl* (full length)	This study
pEPSA5_*nuc2*(SS)-*cbl*	*nuc2* (signal sequence) fused to *cbl* (full length)	This study
pGEX-6P-1	Expression and purification vector	GE Healthcare
pGEX-6P-1_*cbl*	*cbl* expression and purification vector	This study

CONCLUDING REMARKS

The goal of this work was to investigate additional metal homeostasis mechanisms employed by *Staphylococcus aureus* that could aid in surviving the oxidative and copper insults that the organism faces at the host-pathogen interface. The results from this work led to revised models of Fe-S cluster biogenesis and copper homeostasis in *S. aureus*, summarized in **Figure 3.1**.

S. aureus does not produce the nearly ubiquitous thiol glutathione (GSH), instead it produces bacillithiol (BSH). The work presented in Chapter 1 suggests that BSH has a role in Fe-S cluster biogenesis, but the exact role of BSH remains unknown. Genetic evidence suggests that BSH may participate as an Fe-S cluster carrier; the *bshA* mutant displays growth phenotypes that resemble strains lacking other Fe-S cluster carriers and their overexpression rescue the growth defects and lower enzymatic activities of Fe-S cluster-dependent proteins of the *bshA* mutant strain. Whether BSH can bind Fe-S clusters and transfer clusters to apo-proteins *in vitro*, without or with other proteins, requires further investigation. These roles have been shown for GSH, in which it can bind Fe-S clusters either by itself or in conjunction with glutaredoxins *in vitro* (Qi *et al*., 2012, Zhang *et al*., 2013). It would be interesting to know whether GSH can compensate for the loss of function of BSH in Fe-S cluster biogenesis and rescue the phenotypes shown by the *bshA* mutant, by either addition to the growth medium or by engineering strains to express GSH biosynthetic genes.

The findings that the *bshA* mutant has higher levels of "free" Fe and Fe supplementation to the growth medium corrects the growth defects of the *bshA* strain suggest that BSH could also be acting as an Fe buffer, analogous the the role it plays as a

Zn buffer (Ma *et al*., 2014). In this capacity, BSH may be participating as an Fe donor for Fe-S biogenesis. This hypothesis, however, has not been tested and requires further investigation.

The work presented in Chapter 2 elucidates the role of the *copBcbl* operon in copper homeostasis. CopB is a copper exporter and Cbl is a copper-binding lipoprotein. This work provides genetic and biochemical evidence showing that Cbl is a membrane-bound, surface-exposed protein that prevents copper toxicity by binding up to four Cu^{+} ions. Phenotypic and transcriptional analysis suggest that the *copBcbl* operon is upregulated only under copper stress, but it does not rule out the possibility that Cbl could bind other metals *in vitro*. We predict that the conserved histidine residues located within the DUF1541 regions are involved in binding copper. Structural studies are currently being performed to better understand which residues might be involved in binding copper. Once we gain insight into what residues are involved in ligand binding, site-directed mutagenesis of the proposed metal-binding residues can be used to determine the effect on Cu-binding affinity of Cbl. Because the human immune system uses copper to kill invading bacteria, ongoing experiments are examining whether CopB or Cbl, or both, are necessary to promote survival in human macrophages, a finding that could establish a direct link between the *copBcbl* operon and pathogenesis.

The presence of the *copBcbl* operon within a genetic mobile element raised the question about the possibility of these genes being present in other microorganisms. Bioinformatic analysis led to the discovery that Cbl is also present in several other *S. aureus* pathogens, specifically in a livestock-associated methicillin-resistant strain. We speculate that the use of copper-fed diets as an alternative to antibiotics for growth

promotion might have exerted a selective pressure for the *copBcbl* operon in this clone, albeit with a truncated *copB*. Collaborators are currently screening for *cbl* in a library of *S. aureus* strains isolated from various animals. Results from this study could provide additional evidence that support the hypothesis that copper resistance genes are spread via mobile genetic elements among staphylococcal strains.

The oxidative burst and copper toxicity killing mechanisms employed by phagocytes disrupts metal homeostasis within the pathogen. Having a better understanding on how *S. aureus* maintains metal homeostasis can help us identify potential drug targets to treat staphylococcal infections. This research identifies two potential biochemical pathways that could be as drug targets; Fe-S cluster biogenesis and Cu homeostasis. *S. aureus* has numerous Fe-S-cluster-dependent proteins, of which several are required for essential processes, making Fe-S cluster biogenesis an indispensable pathway in *S. aureus* (Roberts *et al*., in preparation). Strains lacking factors involved in Fe-S clusters biogenesis, such as Nfu or SufS, have decreased survival upon challenging with neutrophils (Mashruwala *et al*., 2015; Roberts *et al*., in preparation). Strains that do not produce BSH show decreased survival in murine macrophages (Pöther *et al*., 2013) and whole blood assays (Posada *et al*., 2014). These results suggest that disruption of Fe-S cluster biogenesis affects bacterial fitness during infection. Some of these molecules, including BSH, are not produced by humans and they could be used to design drugs that can affect the ability of the pathogen to synthesize Fe-S clusters. Targeting this essential process can thus lead to a metabolic standstill and eventual bacterial killing.

Strains lacking Cu defense mechanisms, such as the copper exporter CopA (White *et al*., 2009) and Cbl (data not shown), have decreased survival in macrophages. Inability of cells to export excess cytoplasmic Cu (*copA* mutants) also results in decreased survival on solid copper-coated surfaces (Groβe *et al*., 2014), providing additional evidence that Cu defense mechanisms are important for surviving the antimicrobial properties of Cu. Drugs targeting proteins that prevent Cu intoxication (CopA, CopB, and Cbl in *S. aureus*) could be used to override bacterial defense mechanisms and thus amplify the Cu-dependent killing mechanism of the host.

Recent studies identify Cbl as one of ~fifty cell-surface proteins expressed by *S. aureus* in a mouse model of infection (Diep *et al*., 2014). Bacterial surface proteins are often used as vaccine targets because of their roles in nutrient uptake, host adhesion, and bacterial pathogenesis (Grandi, 2010), making Cbl an attractive antigen that could be used as part of a multicomponent vaccine. Current clinical trials are evaluating the use of a vaccine against *S. aureus* that uses the lipoprotein MntC, required for Mn uptake, as one of the antigens of their multicomponent vaccine candidate (Anderson *et al*., 2014). Because *S. aureus* uses lipoproteins to acquire metals like Fe and Mn, that are depleted during infection, as well as other lipoproteins to prevent Cu intoxication, inactivation of the lipoprotein biogenesis pathway may be used an additional drug target. In Gram positive and Gram negative organisms, a diacylglyceryl transferase (Lgt) modifies exported lipoproteins for their anchoring to the cytoplasmic membrane (Hutchings *et al*., 2009). Drugs targeting this enzyme could be used to disrupt the proper localization of secreted proteins, thereby affecting numerous lipoproteins that are used by the organism to maintain metal homeostasis during infection.

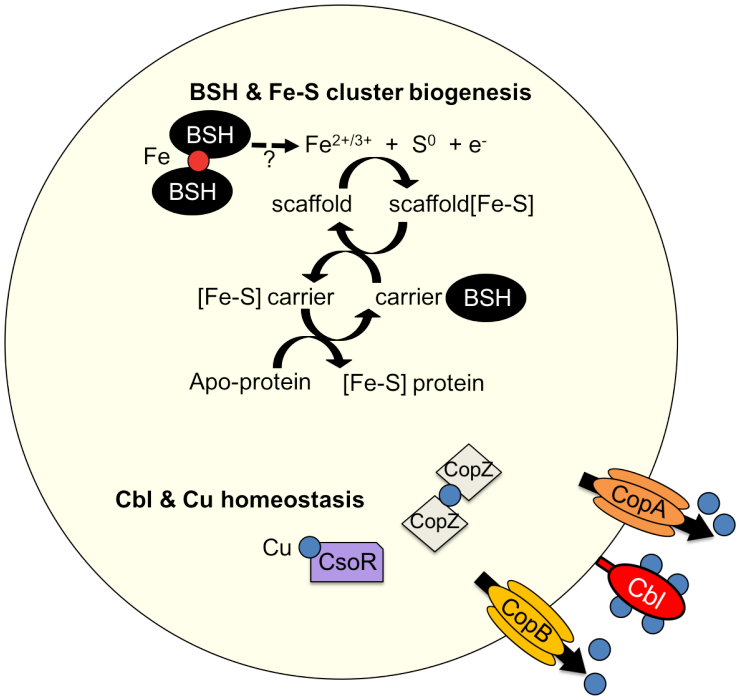

Figure 3.1. Summary of findings including revised models for Fe-S cluster biogenesis and copper homeostasis in *S. aureus*. This work describes a role for the low-molecular-weight thiol bacillitiol in Fe-S cluster biogenesis in *S. aureus* (Chapter 1). It also identifies the *copBcbl* operon, consisting of a copper exporter protein (CopB) and copper-binding lipoprotein (Cbl), and their role in copper detoxification in *S. aureus* (Chapter 2).

APPENDIX A

Supplementary Material for Chapter 1

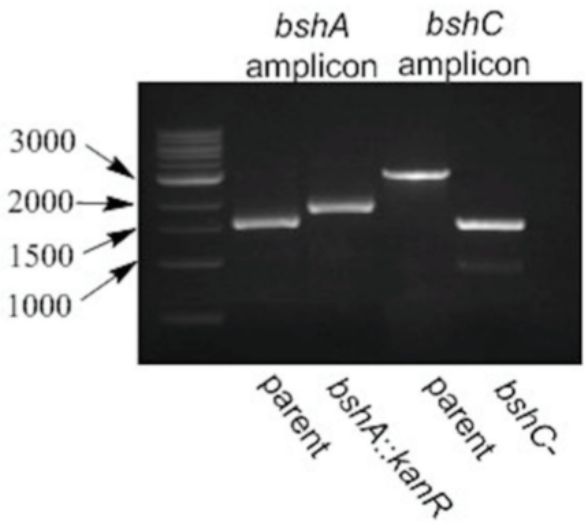

Figure 1.S1. **Verification of the *bshA* and *bshC* mutant strains.** Amplicons corresponding to the *bshA* locus amplified from the wild-type (WT) (JMB1100; lane 2) and *bshA::kanR* (JMB1382; lane 3) strains were separated using agarose gel electrophoresis. Amplicons corresponding to the *bshC* locus amplified from the WT (JMB1100; lane 4) and *bshC*Δ mutant (JMB1381; lane 5) strains were separated using agarose gel electrophoresis. The oligonucleotides used to verify the *bshA::kanR* mutant were 1349compBamHI and 1349compSalI. The oligonucleotides used to verify the *bshC*Δ mutant were 1071vfyup and 1071vfyDwn.

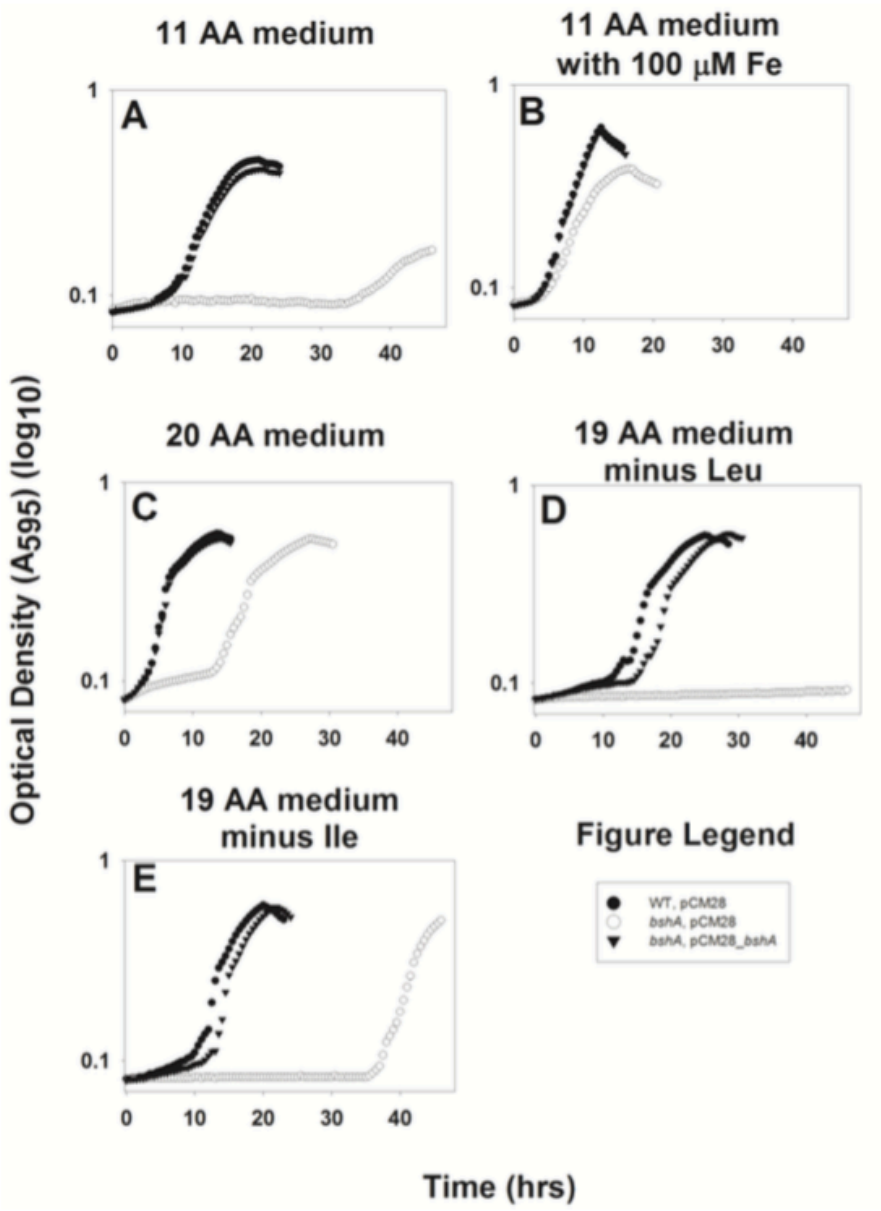

Figure 1.S2. An *S. aureus bshA* mutant strain displays growth defects in defined media when subcultured from an exponential growth phase culture. Representative growth traces of the wild-type (WT) with pCM28 (JMB1100; filled circles), *bshA* with pCM28 (JMB1382; open circles), and *bshA* with pCM28_*bshA* (JMB1382; filled triangles) are shown. Strains were cultured to an optical density of 1 (A_{600}) in TSB before cells were harvested, washed with PBS and subcultured into defined media. Panel A; An

S. aureus bshA mutant strain has a growth defect in a defined medium containing 11 amino acids (AA) (PRMCLVYTPGH). Panel B; Supplementing the 11 AA defined medium with 100 μM Fe^{2+} decreases the generation time and decreases the extended lag time before outgrowth of the *bshA* mutant strain. Panel C; An *S. aureus bshA* mutant strain displays a growth defect in defined medium containing 20 AA without Fe supplementation that manifests as a lag before outgrowth and an increased generation time. Panel D; An *S. aureus bshA* mutant strain does not grow in a liquid defined medium containing 19 AA, but lacking Leu. Panel E; An *S. aureus bshA* mutant strain has an increased lag before outgrowth when cultured in a liquid defined medium containing 19 AA, but lacking Ile.

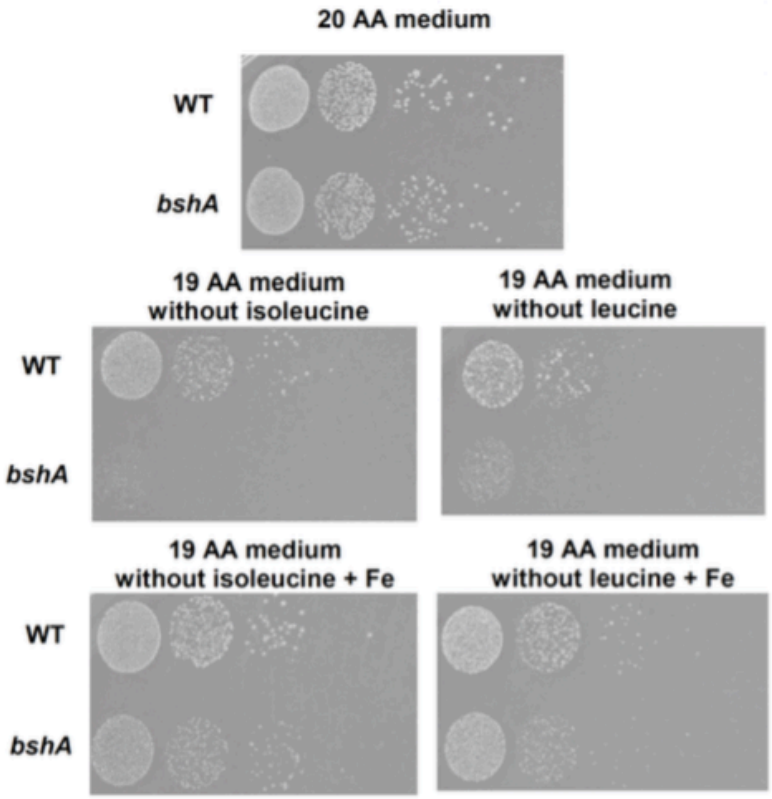

Figure 1.S3. A *bshA* mutant strain displays poor growth on solid chemically defined media lacking either Leu or Ile that is alleviated by either amino acid or Fe supplementation. The WT (JMB1100) and *bshA* mutant (JMB1382) strains were cultured overnight in TSB prior to serial diluting with PBS and spot plating on chemically defined media containing either 20 amino acids (AA) or 19 AA, lacking either Leu or Ile with and without supplementation with 100 μM Fe.

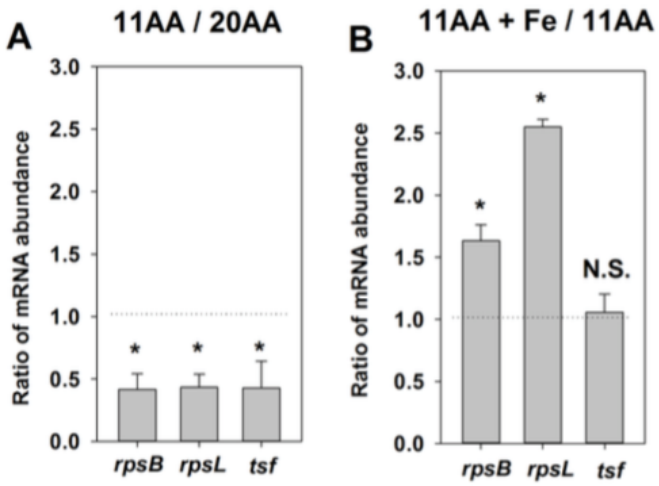

Figure 1.S4. Transcription of genes required for protein synthesis is decreased in *S. aureus* cells cultured in chemically defined media limited for either amino acids or Fe. Wild-type *S. aureus* cells (JMB1100) were subcultured from a complex medium (TSB) into chemically defined media containing either 11 amino acids (AA), 20 AA, or 11 AA + 100 μM Fe. After 30 minutes of incubation, RNA was isolated and the abundances of mRNAs corresponding to the *rpsB*, *tsf* and *rpsL* genes were quantified. Panel A; Ratios of mRNA abundances from cells cultured in a 11 AA medium to cells cultured in a 20 AA medium. Panel B; Ratios of mRNA abundances from cells cultured in a 11 AA + 100 μM Fe medium to cells cultured in a 11 AA medium. All cDNA libraries were prepared from biological triplicates and analyzed at least two times. All data represent averages with standard deviations shown. Paired t-tests were performed and * denotes $p < 0.05$ and N.S. denotes not significant.

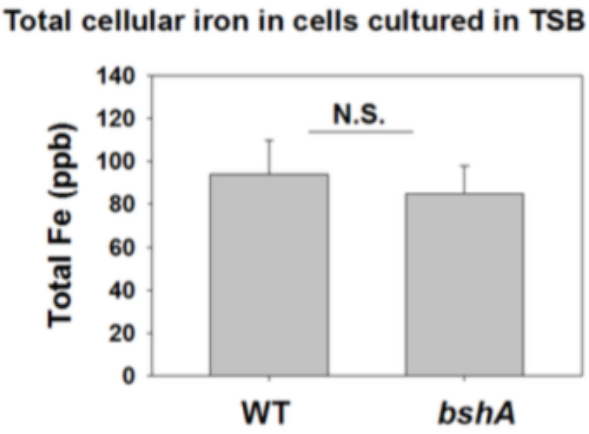

Figure 1.S5. Cells of the WT and *bshA* mutant strains have similar concentrations of cellular Fe when cultured in TSB medium. Total ^{56}Fe was determined in the WT (JMB1100) and *bshA* mutant (JMB1382) grown in TSB medium using ICP-MS. The data represent the mean of three independent experiments conducted in biological triplicate and errors are presented as standard deviations. A paired t-test was performed on the samples and N.S. denotes not significant ($p > 0.1$).

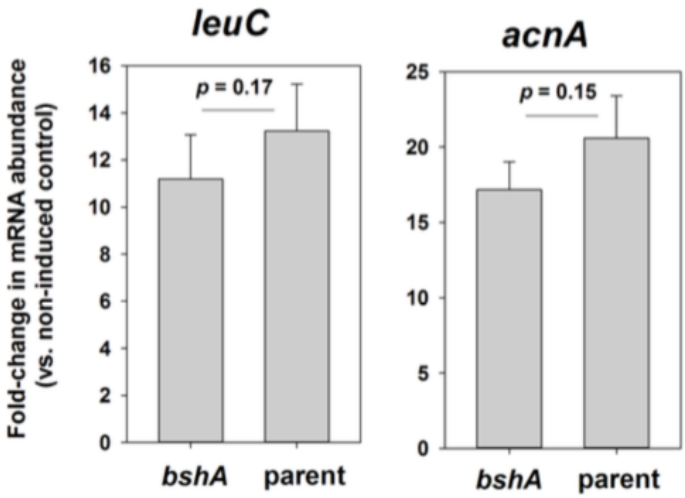

Figure 1.S6. The *leuC* and *acnA* genes are induced to similar levels in the parent and *bshA* mutant strains containing either p*acnA* or p*leuCD*. The mRNA abundances of the *acnA* or *leuC* genes were determined in cells grown in defined media containing 20 amino acids (AA). Panel A; The *acnA* (JMB3702) and *bshA acnA* (JMB5225) mutant strains containing the p*acnA* plasmid were cultured in the presence and absence of 1% xylose to an OD of 1 (A_{600}), RNA was isolated and the *acnA* transcript quantified. Panel B; The *leuD* (JMB3707) mutant and *bshA leuD* (JMB5227) mutant strains containing the p*leuCD* plasmid were cultured in the presence and absence of 1% xylose to an OD of 1 (A_{600}), RNA was isolated and the *leuC* transcript was quantified. Data are plotted as fold-induction relative to non-induced samples. cDNA libraries were prepared from biological triplicates and analyzed two times. All data represent averages with errors presented as standard deviations. Paired t-tests were performed on the samples and *p* values are shown.

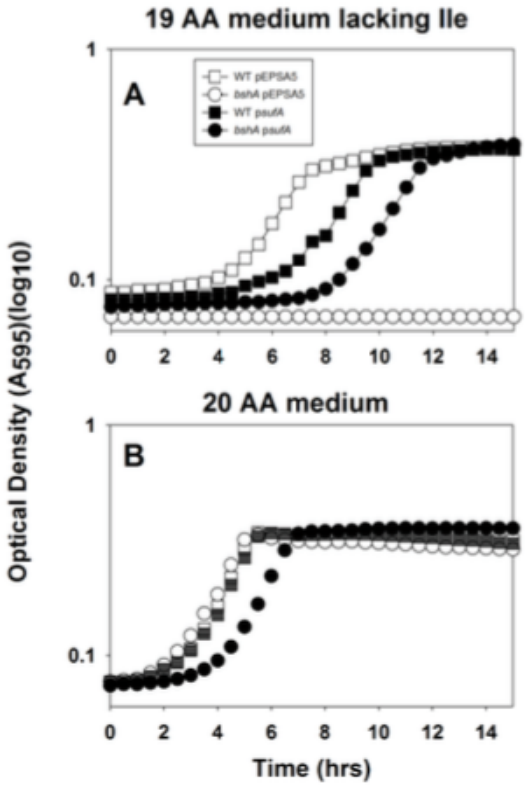

Figure 1.S7. Overexpression of *sufA* corrects the isoleucine-dependent growth defect of a *bshA* mutant in liquid medium. Representative growth analysis of the wild-type (WT) strain (JMB1100) with pEPSA (open squares) or pEPSA_*sufA* (p*sufA*) (filled squares) and the *bshA* mutant (JMB1382) with either pEPSA (open circles) or p*sufA* (filled circles) in chemically defined media containing either 19 amino acids (AA) lacking Ile (Panel A) or 20 AA (Panel B). All media was supplemented with 0.1% xylose.

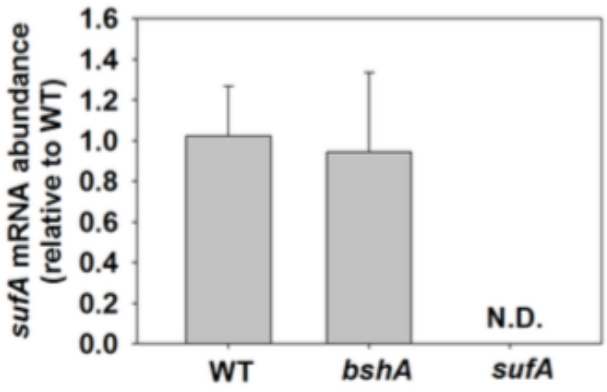

Figure 1.S8. The *sufA* gene is expressed in the *bshA* mutant and the mRNA corresponding to *sufA* accumulates to similar levels in the WT and *bshA* strains. The mRNA abundance corresponding to the *sufA* gene was determined in cells of the WT (JMB1100), *bshA* (JMB1382), and *sufA* (JMB2223) mutant strains previously grown to an optical density of 1 (A_{600}) in chemically defined media containing 20 amino acids. All cDNA libraries were prepared from biological triplicates and analyzed two times. All data represent averages with standard deviations shown. N.D. denotes not detectable.

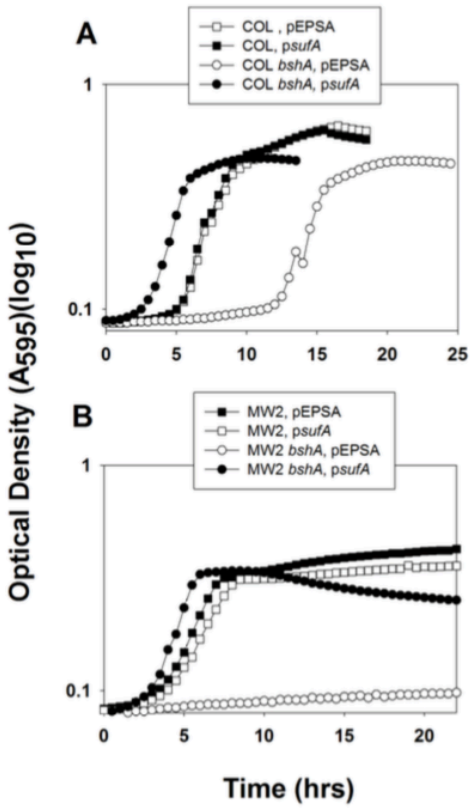

Figure 1.S9. **The growth defects of the *S. aureus* COL and MW2 strains lacking BSH are suppressed by multicopy expression of the *sufA* gene.** Panel A; Multicopy expression of *sufA* corrects the Ile-dependent growth defect of an *S. aureus* COL strain lacking BSH. A representative experiment showing the growth of strain COL (JMB1325) with pEPSA (open squares) or pEPSA_*sufA* (p*sufA*) (filled squares) and the COL *bshA* mutant strain (JMB6167) with pEPSA (open circles) or p*sufA* (filled circles) was monitored in chemically defined media containing 19 amino acids (AA) and 0.1% xylose, but lacking Ile. Panel B; Multicopy expression of *sufA* corrects the Glu and Gln dependent growth defect of the *S. aureus* MW2 strain lacking BSH. A representative experiment showing the growth of the MW2 strain (JMB1324) with pEPSA (closed squares) or p*sufA* (open squares) and the MW2 *bshA* mutant strain (JMB5197) with

pEPSA (open circles) or p*sufA* (filled circles) was monitored in chemically defined media containing 18 AA and 0.1% xylose, but lacking Glu, Gln.

Table 1.S1. Oligonucleotides used in this study.

Oligonucleotide	Sequence (5' → 3')
1349up5BamHIXmaI	GGATCCCCCGGGCAGGATATTTTTCACCATTAGCTAACTTAGCTAG ATTG
1349up3stopMluIKpnINheI	ACGCGTGGTACCGCTAGCTTATCCAGAACCACCCATGGACGGGTA ACATGCATGTTACCCGTCCATGGGTGGTTCTGGATAA
1349down5NheKpnIMluI	GCTAGCGGTACCACGCGTACGCGTGCGAGTGACTATGCTATCCGAT TACTTGAAGATAA
1349down3SalI	CCCGTCGACCGTTCCTCAGCTATACCTACAGTTCTTATTATTCG
1349comp5BamHI	CCCGGATCCGGGCGAACTTGCACGTGAAATAAATCATACC
1349comp3SalI	CCCGTCGACGGCCTTGCCTGTTCAAATAATGATTTATCC
1071up5EcoRI	GGGGAATTCGCGGGTATAGCTACTTGCTGGTTTAATTTTAGAGG
1071upfuse	ACGCGTGGTACCGCTAGCCGCGATTACAAACTATAGTATAAAGTCT ATACCGGTG
1071dwnfuse	GCTAGCGGTACCACGCGTGGGACAGATGTGTTCAAGCCCTCCACCT ATCC
1071dwnSalI	GGGGTCGACGGTTTCGTTTAACATAACGCTGATATGATGAAACACT TCAATTCCTCC
1071vfyup	GGTGAGGATGAAAGACAGCACTCGATTATAGTTGGAGATTCTTTAA CAT
1071vfyDwn	GCAGTTTGGTCTTGATCGATTGCTATTAATCTTCCGTCGTC
nfu5BamRBS	CCCGGATCCTTAGGAGGATGATTATTTATGCCTACTGAAGATACAA CGATGTTTGATCA
nfu3SalI	CCCGTCGACCCCATCAGTCCAATTTGACAGCGAAAAAAGACAGG
nfuveri5	GGCGCATTAACGCAACTTGCACATA
nfuveri3	GGATGAGCAAATTGCGAAACATATGAAAGG
sufAup5EcoRI	GGGGAATTCGCAAGTGTCTTTGATTCATCAATAACCCC
sufAdwn3BamHI	CCCGGATCCGAGCCATTTAATTTCACCTAAGCTTTCATA
ilvDBamHIRBS	GGGGGATCCTTAGGAGGATGATTATTTATGCGAAGCGACATGATC AAAAAAGG
ilvDmulIdwn	GGGACGCGTTTAAATTAAATTCTCAGGGACTTGCATG
pcm28YCCfor	AAAAACCTACAGAAGCTTGCATGCCTGCAAGTTACGCTAGGGATA ACAGGGTAATATAG
sufYCC3	TCTCACGACGTTTTTGGCCGGTACCACGCGTTCCGGACTATATTAC CCTGTTATCCCTA
YccSuf	TCTCACGACGTTTTTGGCCGGTACCACGCGTTCCGGACTATATTAC

	CCTGTTATCCCTA
Sufinternal3	TCTAATATCGGAAAATCCTTGATTACTTCATTAACGTC
Sufinternal5	GACGTTAATGAAGTAATCAAGGATTTTCCGATATTAGA
SufpCM28rev	GATTACGAATTCATGATCGAATGCTAGCGGATCCCGGAAGTCAAG AATGGCTTAACAAC
dpsHindIII	CCCAAGCTTGCCAATCGTATATTATGATGGAAACTG
dpskpnI	GGGGGTACCCACTCCTTAAAATTGTCTACGTCTTGC
sodHindIII	GGGAATCTTCGATTCAATGTGTCATTGCTGCTGTTATGATG
sodKpnI	GGGGGTACCCCTCCTTTTATGAATATACTTTTATAATAATTAATTTC GGG
sufA5ndeI	GGGCATATGCCAACAGTTATATTAACAGAAGCAGC
sufAXhoI	GGGCTCGAGGCAATTTTCAGGATTACCTGCAAC
rpsBfwdRT	GATGCTATCCGTGCGGTTAAA
rpsBrevRT	CCTTGTTGACCTTCTAAGATTGCA
tsffwdRT	CTGGCGCGGGTATGATG
tsfrevRT	ATCGCTTTATCGATGTCACCAT
rpsLfwdRT	GCGTTTATCAAACAACATCGAAAT
rpsLrevRT	ACTGTGTTCTTGTAAGTTATGTCCGATAC
leuCfwdRT	CAGCCTGGCAAGACAATCGT
leuCrevRT	AGCACCAAATGCTCCATGTG
AcnARTFor	GGACAACCTTCTTATTTCCCAATTC
AcnARTRev	TTGCGCCTTGTGGTAATGAA
SufARTFor	TGGGTGGCGGTTTCCA
SufARTrev	CTACCACAGCCACATGAAGCA

Table 1.S2. Generation times for growth analyses conducted in defined media.[a]

Medium	**Figure**	**Relevant genotype of strains assayed**			
		WT, pCM28	*bshA*, pCM28	*bshA*, pCM28_*bshA*	
11AA	Fig 1A	3.4 ± 0.2	9.2 ± 0.2	3.5 ± 0.2	
11AA + 100 μM Fe	Fig 1B	3.5 ± 0.1	6.1 ± 0.1	3.6 ± 0.1	
20AA	Fig 3A	1.3 ± 0.1	2.2 ± 0.2	1.3 ± 0.1	
19AA (- Leu)	Fig 3B	2.1 ± 0.1	NG[b]	2.2 ± 0.1	
19AA (- Ile)	Fig 3C	2.2 ± 0.0	2.6 ± 0.2	2.3 ± 0.0	
		WT 20AA[b]	*bshA* 20AA	WT dropout[c]	*bshA* dropout
20AA or 18AA (- Ile, Leu)	Fig 9A	1.9 ± 0.1	2.5 ± 0.1	1.7 ± 0.1	NG
20AA or 18AA (- Glu, Gln)	Fig 9B	1.5 ± 0.3	1.7 ± 0.2	1.5 ± 0.1	NG
20AA or 19AA (- Ile)	Fig 9C	2.8 ± 0.1	2.9 ± 0.0	1.3 ± 0.1	1.5 ± 0.1
		WT, pCM28	*bshA,* pCM28	*bshA,* pCM28_*bshA*	
11AA	Fig S2A	3.0 ± 0.2	9.0 ± 0.2	3.1 ± 0.2	
11AA + 100 μM Fe	Fig S2B	2.5 ± 0.2	3.1 ± 0.1	2.7 ± 0.0	
20AA	Fig S2C	1.7 ± 0.1	2.5 ± 0.3	2.0 ± 0.1	
19AA (- Leu)	Fig S2D	2.0 ± 0.0	NG	2.0 ± 0.1	
19AA (- Ile)	Fig S2E	1.8 ± 0.1	2.6 ± 0.1	1.7 ± 0.2	

[a] generation times were determined from biological triplicates and are presented in hours.

[b] Abbreviations: NG; no growth. AA; amino acid. Leu: leucine. Ile; isoleucine. Glu; glutamate. Gln; glutamine.

[c] Dropout media is missing one or more amino acids. The growth medium used to generate Figure 7A contains 18 AA without Leu and Ile supplementation. The growth medium used to generate Figure 7B contains 19 AA without Ile supplementation. The growth medium used to generate Figure 7C contains 19 AA without Leu supplementation.

APPENDIX B

Supplementary Material for Chapter 2

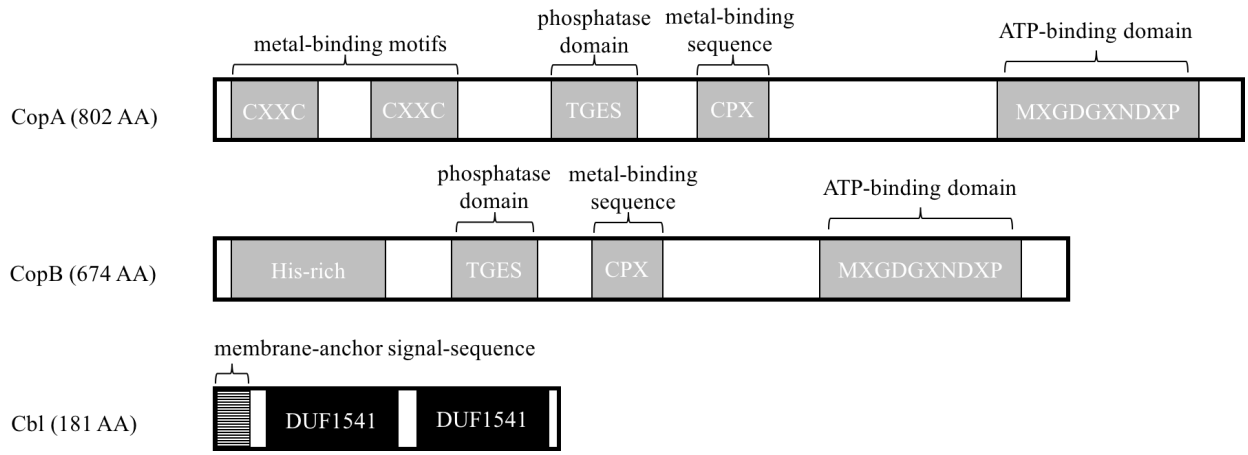

Figure 2.S1. Schematic of the conserved domains in the CopA, CopB, and Cbl proteins. The CopA and CopB proteins are structurally similar in that they both have a phosphatase domain (TGES), a conserved CPX metal-binding sequence, and a ATP-binding domain (MXGDGXNDXP). However, the N-terminus of the CopA protein contains two metal-binding CXXC motifs, while the N-terminus of the CopB protein contains a His-rich region. The Cbl protein contains a membrane-anchor signal-sequence (filled with horizontal lines), as predicted using the TOPCONS web server (Bernsel *et al.*, 2009), and two DUF1541 domains as identified by the National Center for Biotechnology Information's Conserved Domains Database (Marchler-Bauer *et al*., 2015).

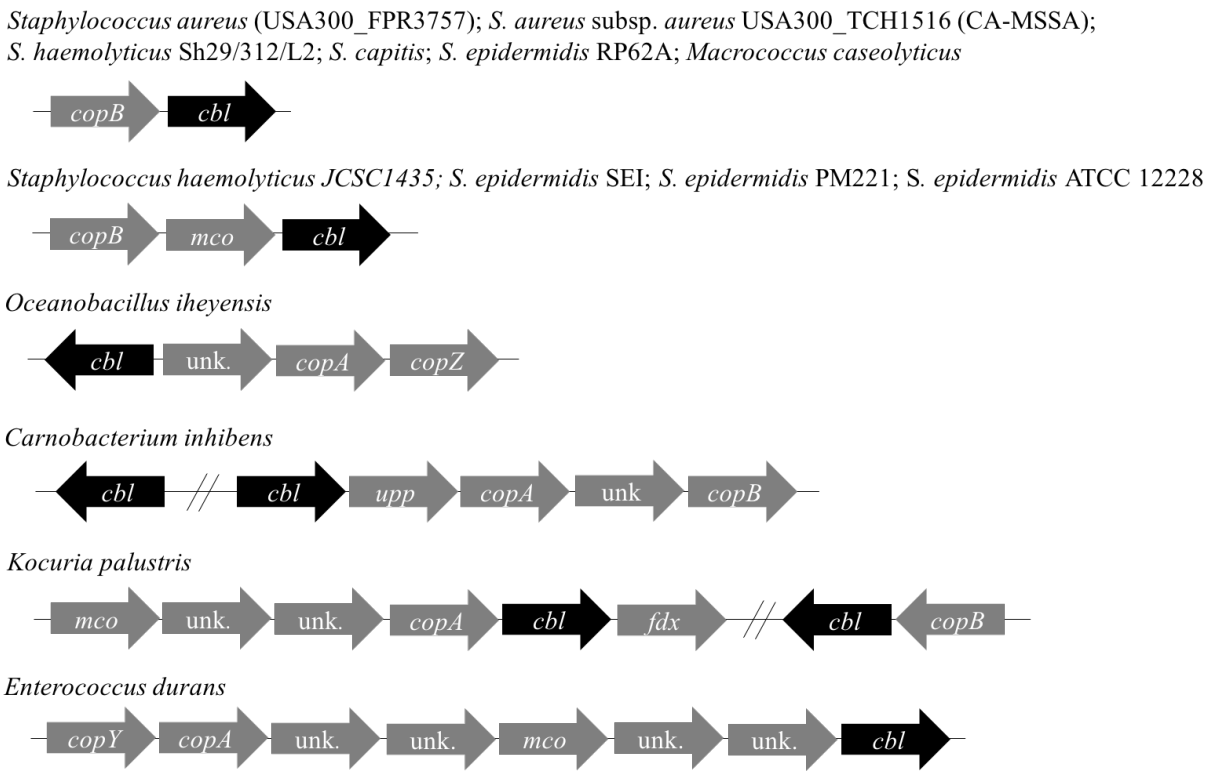

Figure 2.S2. Genomic location of *cbl* from select organisms. In several microorganisms, the Cbl homologue was found to be co-localized with other genes involved in copper homeostasis. A few operonic structures are shown.

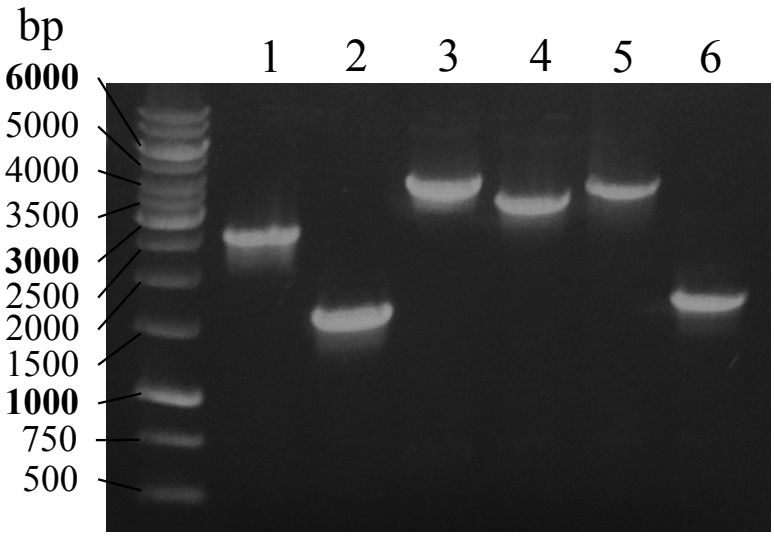

Figure 2.S3. PCR verification of of the *copB*Δ, *cbl*Δ, and *copB-cbl*Δ mutant strains. Amplicons corresponding to the *copB* (SAUSA300_0078) locus amplified from the wild-type (WT) strain (JMB1100; lane 1) and the *copB*Δ strain (JMB7900; lane 2) are shown; amplicons corresponding to *cbl* (SAUSA300_0079) from the WT strain (JMB1100; lane 3) and *cbl*Δ mutant strain (JMB7711; lane 4) are shown; amplicons corresponding to the *copBcbl* (SAUSA300_0078-0079) genes from the WT strain (JMB1100; lane 5) and *copB*Δ *cbl*Δ double mutant strain (JMB7901; lane 6) are shown. The ZRC139 and ZRC201primer pair was used to verify the ~1-kb deletion in the *copB*Δ strain. The ZRC139 and ZRC169 primer pair was used to verify the ~0.5-bp deletion in the *cbl*Δ mutant and ~2.6-kb deletion in the *copB*Δ *cbl*Δ double mutant strain.

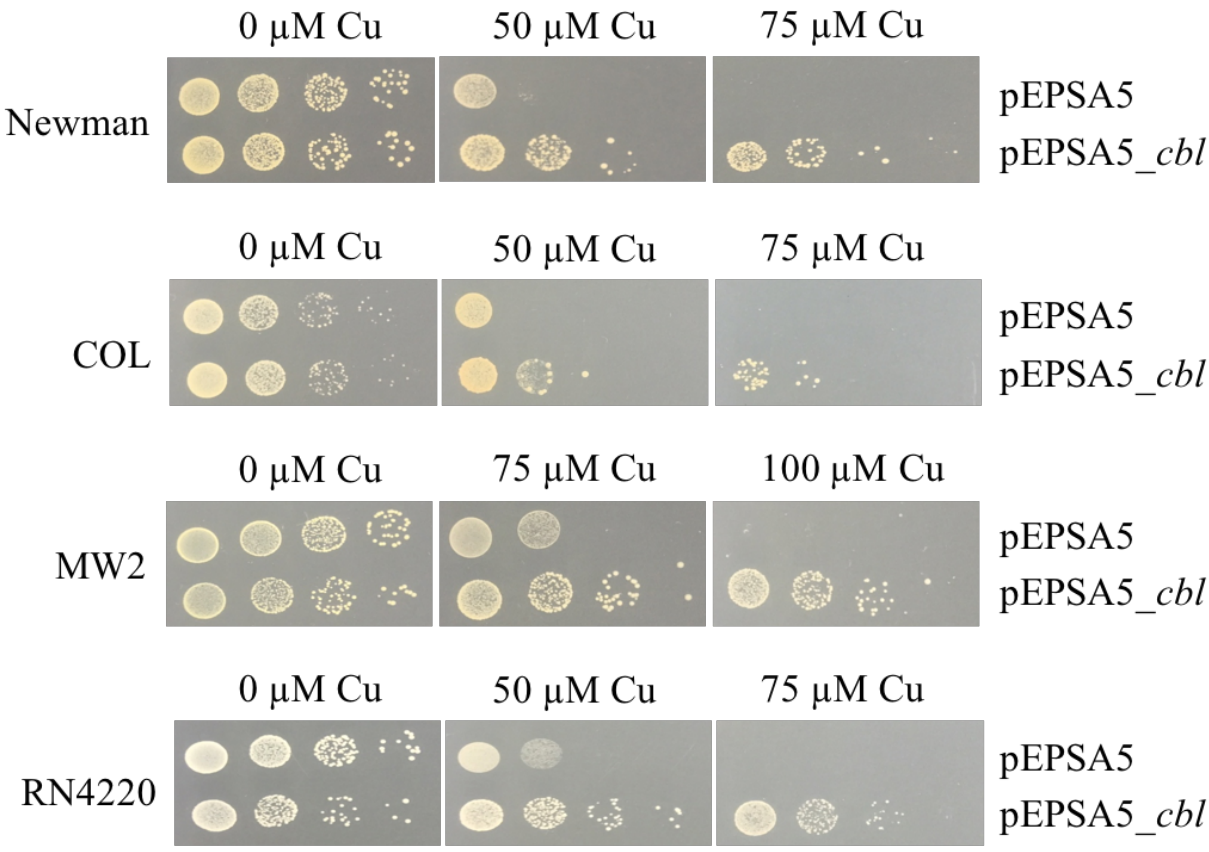

Figure 2.S4. Overexpression of *cbl* confers copper resistance in other *S. aureus* isolates. The Newman (JMB1422), COL (JMB1324), MW2 (JMB1325), and RN4220 (JMB1103) strains expressing either the pEPSA5 and pEPSA5_*cbl* vectors are shown. Strains containing the pEPSA5_*cbl* vector show increased copper resistance compared to the strains containing the pEPSA (empty) vector. Overnight cultures were serial diluted and spot plated on chemically defined media without and with Cu.

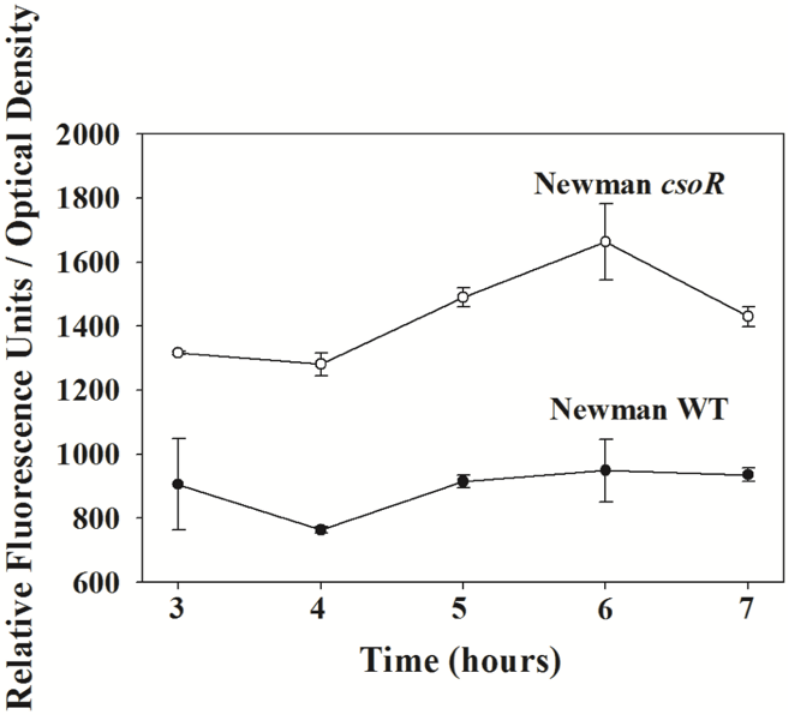

Figure 2.S5. Transcriptional activity of the *copBcbl* operon in the *S. aureus* strain Newman wild-type and *csoR* mutant. The *S. aureus* Newman WT (JMB1422; filled circles) and *csoR* mutant (JMB6338; open circles) strains harboring the *copBcbl* promoter reporter were cultured in chemically defined media. Fluorescence was monitored over time and data was standardized to the optical density (A590) of each culture. Data shown represent the average of biological triplicates with errors presented as standard deviations.

***Staphylococcus aureus* subsp. *aureus* USA300_FPR3757 >saa:SAUSA300_0079**
MIKKLFFMILGSLLILSACSNNDEKDKDTNDQKSESHMKHNDESKVPEDMKSTNEGEFKVGDKVTITAGHMPGMKGAEATVKGAYKTYAYV
VSYKPTNGNEKVNNHKWVVNEEIKDAPKDGFSKGDTVKLEASHMSGMKGATANIDNVKKTTVYVVDYKSKDNGKIIKNHKWMTGNELKAR

***Macrococcus caseolyticus* >mcl:MCCL_0244 (66%)**
MMKKLSLIIVASGLVLSACSTGEEEENSKDQKQEKHMNHKSESKAPDNMKSTDDSKYKKDDKITITADHMPGTKNAKGTVKGAYKTYAYVV
SYTPTNGDEKVNNHKWVVNEEVADAPENGFKKGDTVKLEADHMPGMKGAEAQIDDVEKTTVYMVDYKSTENDEMVKNHKWMTTDELKSR

***Bacillus subtilis* subsp. *subtilis* 168 >bsu:BSU05790 (52%)**
MSAGKSYRKKMKQRRMNMKISKYALGILMLSLVFVLSACGNNNSTKESTHDNHSDSSTHEEMDHSGSADVPEGLQESKNPKYKVGSQVIIN
TSHMKGMKGAEATVTGAYDTTAYVVSYTPTNGGQRVDHHKWVIQEEIKDAGDKTLQPGDQVILEASHMKGMKGATAEIDSAEKTTVYMVDY
TSTTSGEKVKNHKWVTEDELSAK

***Oceanobacillus iheyensis* >oih:OB1140 (45%)**
MTKRFGYFVGVFVLLMGLYACTNENNMDENEERNMLPDNEQVPEGDLEEENKSEHEHSDHDESGEIPEGLIEAEDPTYAAGDEITITASHM
PGMEGASGTIVGAYDTTAYMVSYQPTDGGEMVEDHKWIIQEEIDNANKNPYQSGDEVTINAAHMEGMDGATATIEDGTETTVYMIDYVTES
GEEVKNHKWVTEEELEPNDSE

***Kocuria palustris* >kpl:KPaMU14_01730 (43%)**
MKKSIWTTSMAATAAVSMLALTACGGTAEEEDAQPAPSQTASEAAAAPSTSSESSNMDMGMDHGSGGMAGHNPEGGPPPEGIEAAADPTYP
IDSTAVLTADHMPGMAGSEATITGAFDTTAYSVSYTPTDGGEPVVDHKWVVHEELEDPGEAPLPAGTEVVLEADHMPGMEGAEATIESSTE
ETVYMVDTTIDGMEMANHKWFVESELQPAE

***Corynebacterium marinum* >cmq:B840_13000 (37%)**
MKRTIALAALALTSSLALAACTDDTASDAPETTTTTTSETATQSSEETGMNDQMGAEGHDHPADGGQPPAGIAAEENPTYPVDTEVVLTAD
HMPGMEGAEATIAGAFDTTTYSVSYTPTDGGDPVTDHRWVVHEELVDPGQAPLPEGSEVVLDAEHMSGMKGVEATIDYSTDETVYMVDLTV
DGMTMTNHKWVTESEIAPAE

Figure 2.S6. Analysis of diverse Cbl-like proteins. Strictly conserved residues located within the domain of unknown function (DUF1541) identified using the National Center for Biotechnology Information's Conserved Domains Database (Marchler-Bauer *et al.*, 2015) are shown in red. The lipobox motif typical of lipoproteins and characterized by the presence of a L-[A/S/T]-[G/A]-C sequence (Hutchings *et al.*, 2009) is shown in green.

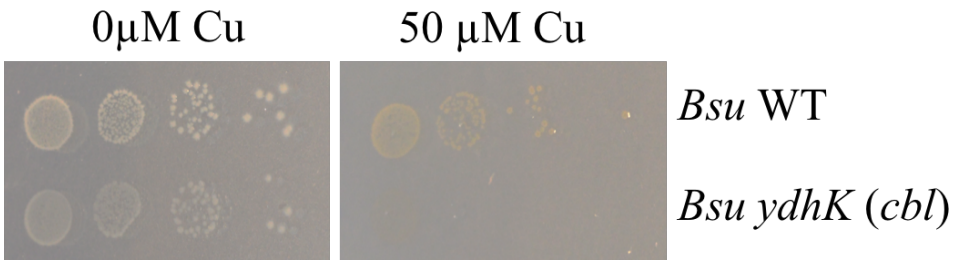

Figure 2.S7. A *Bacillus subtilis ydhK* (*cbl*) mutant is sensitive to Cu intoxication. Overnight cultures were serial diluted and spot plated on chemically defined media without and with Cu.

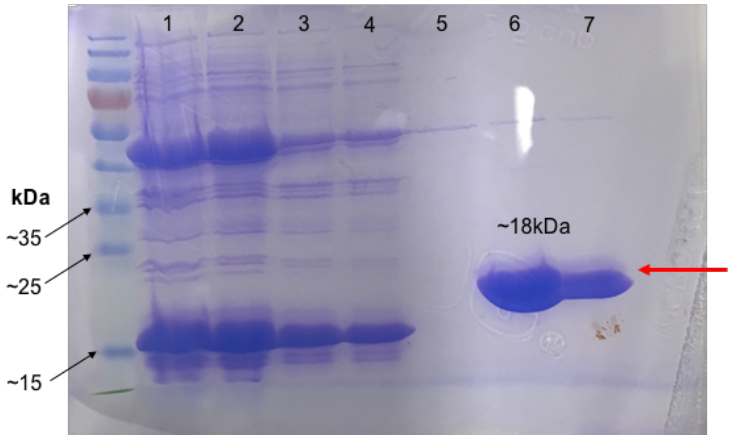

Figure 2.S8. SDS-PAGE analysis of purified *S. aureus* Cbl. Cbl(T) was expressed and purified from *E. coli* BL21 DE3. samples were obtained at various steps to verify for the presence of and purification of the recombinant protein. Lane 1: cell lysate; Lane 2: clarified cell-free lysate; Lane 3: flow-through after applying sample to column; Lane 4: column wash with binding buffer; Lane 5: column wash with high- salt buffer; Lanes 6 and 7: eluent after cleavage with PreScission protease.

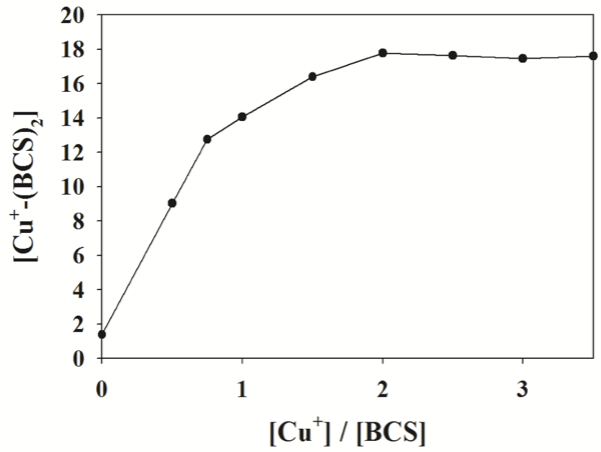

Figure 2.S9. BCS has higher affinity for Cu+ than to apo-Cbl. Titration of Cu+ (0-140 μM) into a solution containing a mixture of apo-Cbl (5 μM) and BCS (40 μM) leads to immediate formation of the Cu+-(BCS)2 complex. The formation of Cu+-(BCS)2 was monitored by plotting the increase in absorbance at 483 nm versus the [Cu+] / [BCS] ratio. Buffer: 10 mM MOPS, 50 mM NaCl, pH 7.4.

Table 2.S1. Oligonucleotides used in this study.

Primer name	Sequence
0078upEcoR1New2 (ZRC199)	GGGGAATTCATGAATCATTCCAATCAAATGCAT
0078upfuseNew2 (ZRC200)	ACGCGTGGTACCGCTAGCGCTAGCCCGACAGCATTCATTTCTATC
0078dwnfuse (ZRC164)	GCTAGCGGTACCACGCGTACGCGTCAGGTGACAATAATGAAGTGGCA
0078dwndelSalINew (ZRC201)	GGGGTCGACGTAAAGGCATTAATTGCAACG
0079delEcoR1 (ZRC166)	GGGGAATTCCAAGACGTTAATAATATTCCAGG
0079upfuse (ZRC167)	ACGCGTGGTACCGCTAGCGCTAGCATCATAATAAAACTCCTATCTTTTATTTTAA
0079dwnfuse (JMB168)	GCTAGCGGTACCACGCGTACGCGTTGAGCTGAAAGCACGATAAAAATCT
0079delSalI (ZRC169)	GGGGTCGACACACCCCTTAATTATATTTTACATC
0078delEcoR1new (ZRC185)	GGGGAATTCTGAGGTTGTATATAACTCACTCTG
0078upfusenew (ZRC186)	ACGCGTGGTACCGCTAGCGCTAGCCAGACAAGAACGGTTTACCACC
pJB38upstream (ZRC196)	CCCGAAAAGTGCCACCTGACGTC
pEPSA5veriup (JMB769)	CGGACCGTCATAAAAAATTTATTTGCT
pEP0078BamH1rbs (ZRC146)	GGGGGATCCAGCATAATCATCAAAATCACATGAATCATTCC
0078dwnSalI (ZRC141)	GGGGTCGACTTATTTTAATTTTAATGTAAAGGCATTAATTGCAACGATAATTGTA
0079BamH1rbs (ZRC149)	GGGGGATCCAAGATAGGAGTTTTATTATGATT
0079BamRBStrunk (ZRC184)	CCCGGATCCAAGATAGGAGTTTTATTATGGATGAAAAAGATAAAGACACTAATGACC
0079dwnSalI (ZRC150)	GGGGTCGACTTATCGTGCTTTCAGCTCATT
0079dwnNheI (ZRC181)	GGGGCTAGCTCGTGCTTTCAGCTCATT
pEP_nuc	TCGGTACCCGGGGATCCTCTAGAGTCGACAAAAAGAGAAGTAG

(ZRC188)	GTGGCAATATGAAGTC
nucFL_0079for	AAACAACAGAAATTAAATATTTGGAGTAAAGATGAAAAAGATA
(ZRC191)	AAGACACTAATGACCA
nucFL_0079rev	TGGTCATTAGTGTCTTTATCTTTTTCATCTTTACTCCAAATATTTA
(ZRC189)	ATTTCTGTTGTTT
nucSS_0079for	GGTGTATTAGCATTTCAATTTATGAATCATGATGAAAAAGATAA
(ZRC192)	AGACACTAATGACCA
nucSS_0079rev	TGGTCATTAGTGTCTTTATCTTTTTCATCATGATTCATAAATTGA
(ZRC190)	AATGCTAATACACC
FLAG_0079rev	TCACCGTCATGGTCTTTGTAGTCGCTAGCTCGTGCTTTCAGCTCA
(ZRC193)	TTTCCTGTCATCCA
0079TBamHIGST5 (ZRC198)	GGGGGATCCATGGATGAAAA
0079XhoIGST3 (ZRC178)	GGGCTCGAGTTATCGTGCTTTCAGCTCATTTCCTGTCATCC
2494CuTransUp5BamH 1 (ZRC133)	CCCGGATCCCGAGTCGTCAGTTGTCAGACAAC
2495CopZDown3SalI (ZRC134)	CCCGTCGACGACAGGGAAGATGTCATATTAACACCAC
2043upBamHI (ZRC153)	CCCGGATCCATGACTGAACAAGATAATGCACATCATTC
2043dwnSalI (ZRC155)	CCCGTCGACTTAGTCTTTAATCAATTTTTGAAAAGTCACTA
0078HindIII5 (ZRC139)	GGGAAGCTTCCGACGTATACAGAATCATTTGAG
0078KpnI3 (ZRC140)	GGGGGTACCGTGATTTTGATGATTATGCTCTTCACC
16sfwdRT	TGAAAGCCCACGGCTCAA
16srevRT	TTCTGCACTCAAGTTTTCCAGTTT
CopARTfwd (ZRT19)	GCTTGTCCATGCGCATTG
CopARTrev (ZRT20)	GCGCGACCAGTACCTACCAT
CopBRTfwd (ZRT21)	CGCTGTCGCAAAAGAATTAGGTA
CopBRTrev (ZRT22)	GCTTTCCTTATCTTCTGGCATGA
CblRTfwd (ZRT23)	AAAAGTGAGAGCCATATGAAGCATAA
CblRTrev (ZRT24)	CTTTAAATTCACCCTCATTAGTCGATT

Table 2.S2. Co-occurrence of *cbl* and other genes involved in copper homeostasis.

Other *Staphylococcus* spp.	**Identity (%)**	**CopA**	**CopZ**	**CopB**	**Cbl or Cbl-like locus tag**
S. xylosus	100				syx:SynWH7803_2395
S. aureus USA300-ISMMS1	100				saui:AZ30_00405
S. aureus USA300_TCH1516	100				sax:USA300HOU_0085
S. aureus ST398 (MRSA)	99				sug:SAPIG0066
S. haemolyticus Sh29/312/L2	99				shh:ShL2_00034
S. haemolyticus JCSC1435	99				sha:SH0107
S. capitis	98				scap:AYP1020_2000
S. epidermidis RP62A	99				ser:SERP2437
S. epidermidis SEI	98				seps:DP17_1330
S. epidermidis PM221	98				sepp:SEB_00082
S. epidermidis ATCC 12228	98				sep:SE0128
Other Bacteria	**Identity (%)**	**CopA**	**CopZ**	**CopB**	**Cbl or Cbl-like locus tag**
Listeria monocytogenes	66				lmn:LM5578_p08
Macrococcus caseolyticus	66				mcl:MCCL_0244
Bacillus subtilis subsp. *spizizenii*	52				bst:GYO_0837
Bacillus subtilis subsp. *subtilis* 168	52				bsu:BSU05790
Bacillus endophyticus	52				beo:BEH_05620

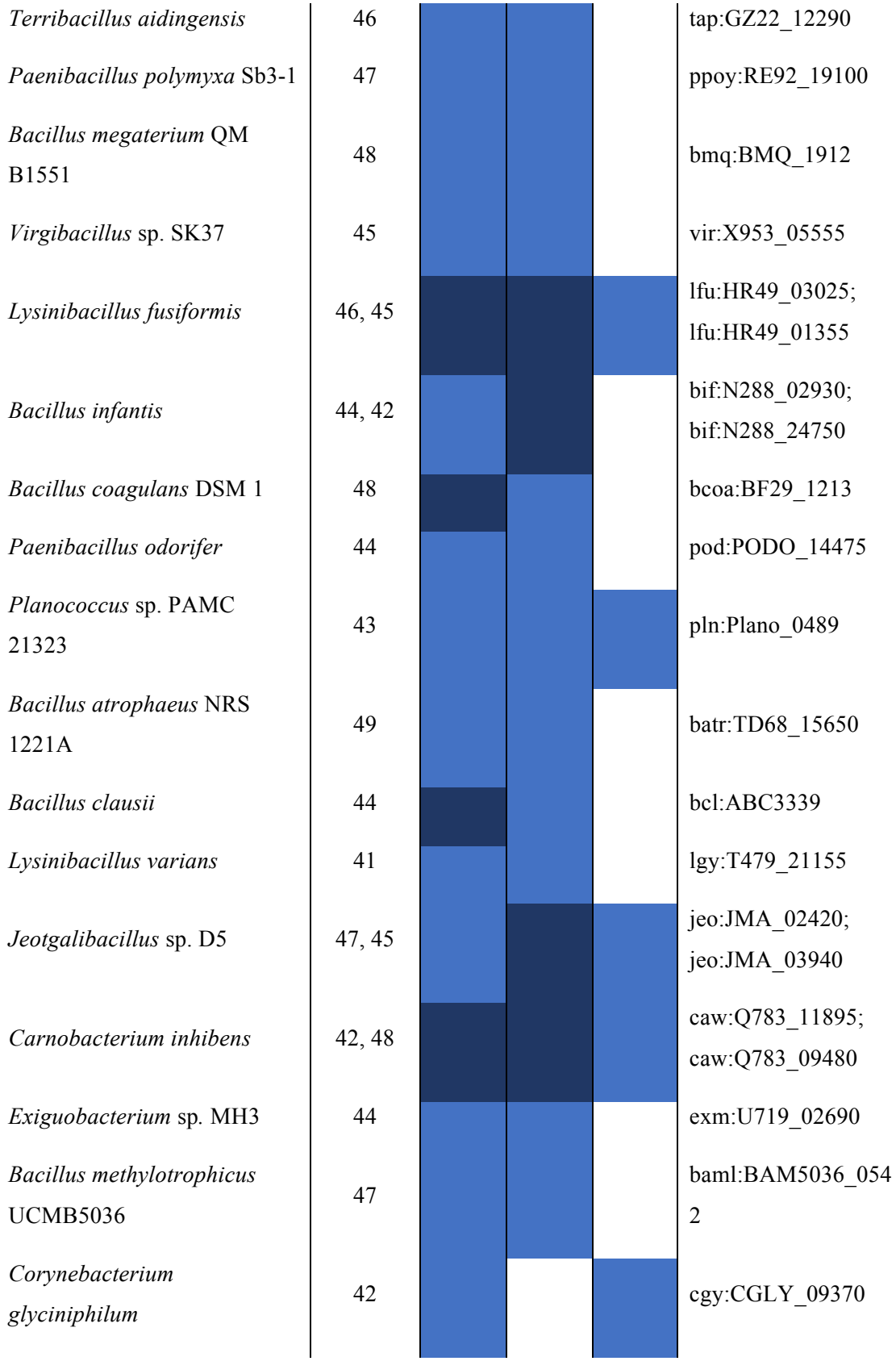
Terribacillus aidingensis 46 tap:GZ22_12290
Paenibacillus polymyxa Sb3-1 47 ppoy:RE92_19100
Bacillus megaterium QM B1551 48 bmq:BMQ_1912
Virgibacillus sp. SK37 45 vir:X953_05555
Lysinibacillus fusiformis 46, 45 lfu:HR49_03025; lfu:HR49_01355
Bacillus infantis 44, 42 bif:N288_02930; bif:N288_24750
Bacillus coagulans DSM 1 48 bcoa:BF29_1213
Paenibacillus odorifer 44 pod:PODO_14475
Planococcus sp. PAMC 21323 43 pln:Plano_0489
Bacillus atrophaeus NRS 1221A 49 batr:TD68_15650
Bacillus clausii 44 bcl:ABC3339
Lysinibacillus varians 41 lgy:T479_21155
Jeotgalibacillus sp. D5 47, 45 jeo:JMA_02420; jeo:JMA_03940
Carnobacterium inhibens 42, 48 caw:Q783_11895; caw:Q783_09480
Exiguobacterium sp. MH3 44 exm:U719_02690
Bacillus methylotrophicus UCMB5036 47 baml:BAM5036_0542
Corynebacterium glyciniphilum 42 cgy:CGLY_09370

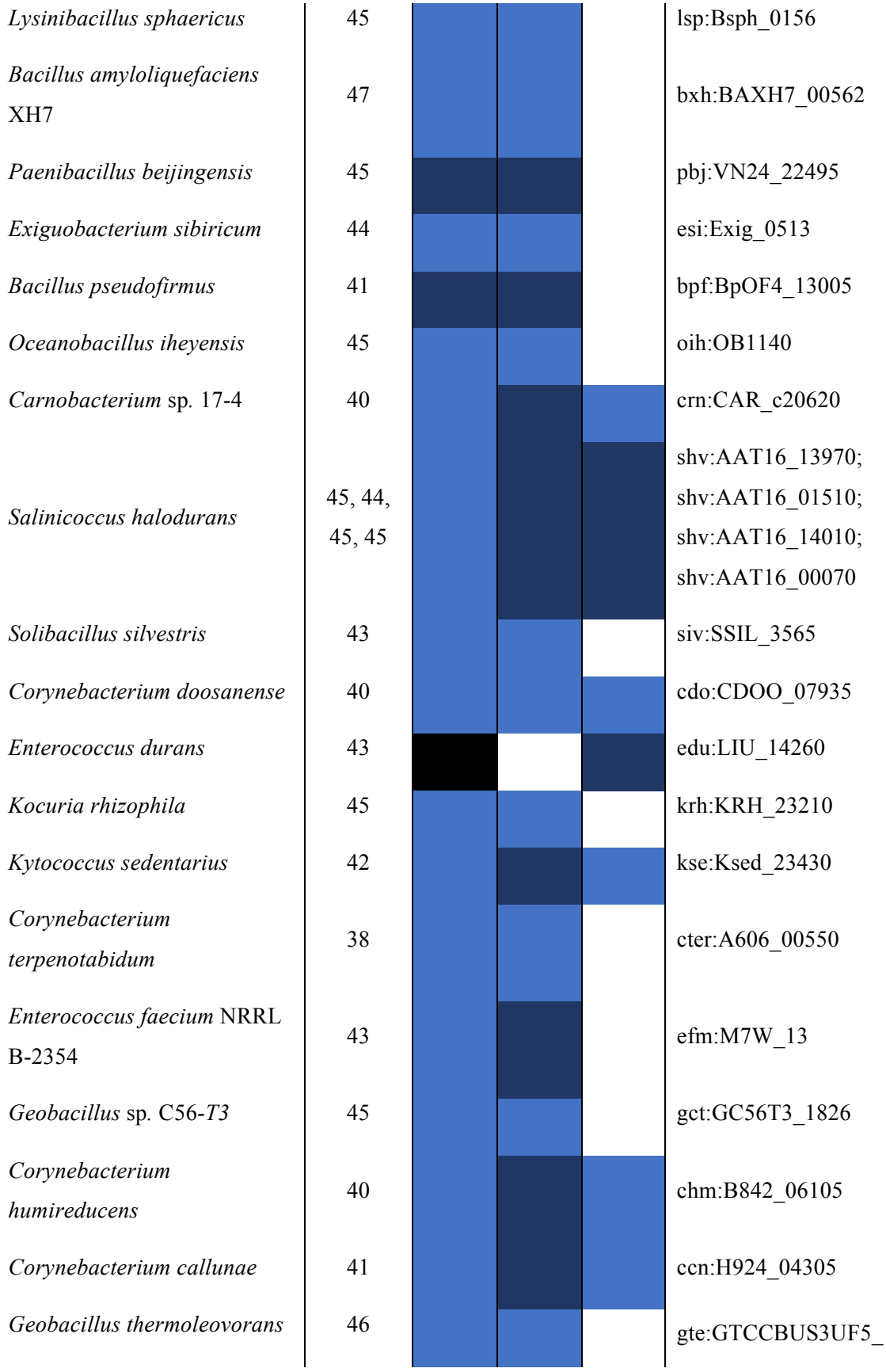

Lysinibacillus sphaericus	45	lsp:Bsph_0156
Bacillus amyloliquefaciens XH7	47	bxh:BAXH7_00562
Paenibacillus beijingensis	45	pbj:VN24_22495
Exiguobacterium sibiricum	44	esi:Exig_0513
Bacillus pseudofirmus	41	bpf:BpOF4_13005
Oceanobacillus iheyensis	45	oih:OB1140
Carnobacterium sp. 17-4	40	crn:CAR_c20620
Salinicoccus halodurans	45, 44, 45, 45	shv:AAT16_13970; shv:AAT16_01510; shv:AAT16_14010; shv:AAT16_00070
Solibacillus silvestris	43	siv:SSIL_3565
Corynebacterium doosanense	40	cdo:CDOO_07935
Enterococcus durans	43	edu:LIU_14260
Kocuria rhizophila	45	krh:KRH_23210
Kytococcus sedentarius	42	kse:Ksed_23430
Corynebacterium terpenotabidum	38	cter:A606_00550
Enterococcus faecium NRRL B-2354	43	efm:M7W_13
Geobacillus sp. C56-*T3*	45	gct:GC56T3_1826
Corynebacterium humireducens	40	chm:B842_06105
Corynebacterium callunae	41	ccn:H924_04305
Geobacillus thermoleovorans	46	gte:GTCCBUS3UF5_

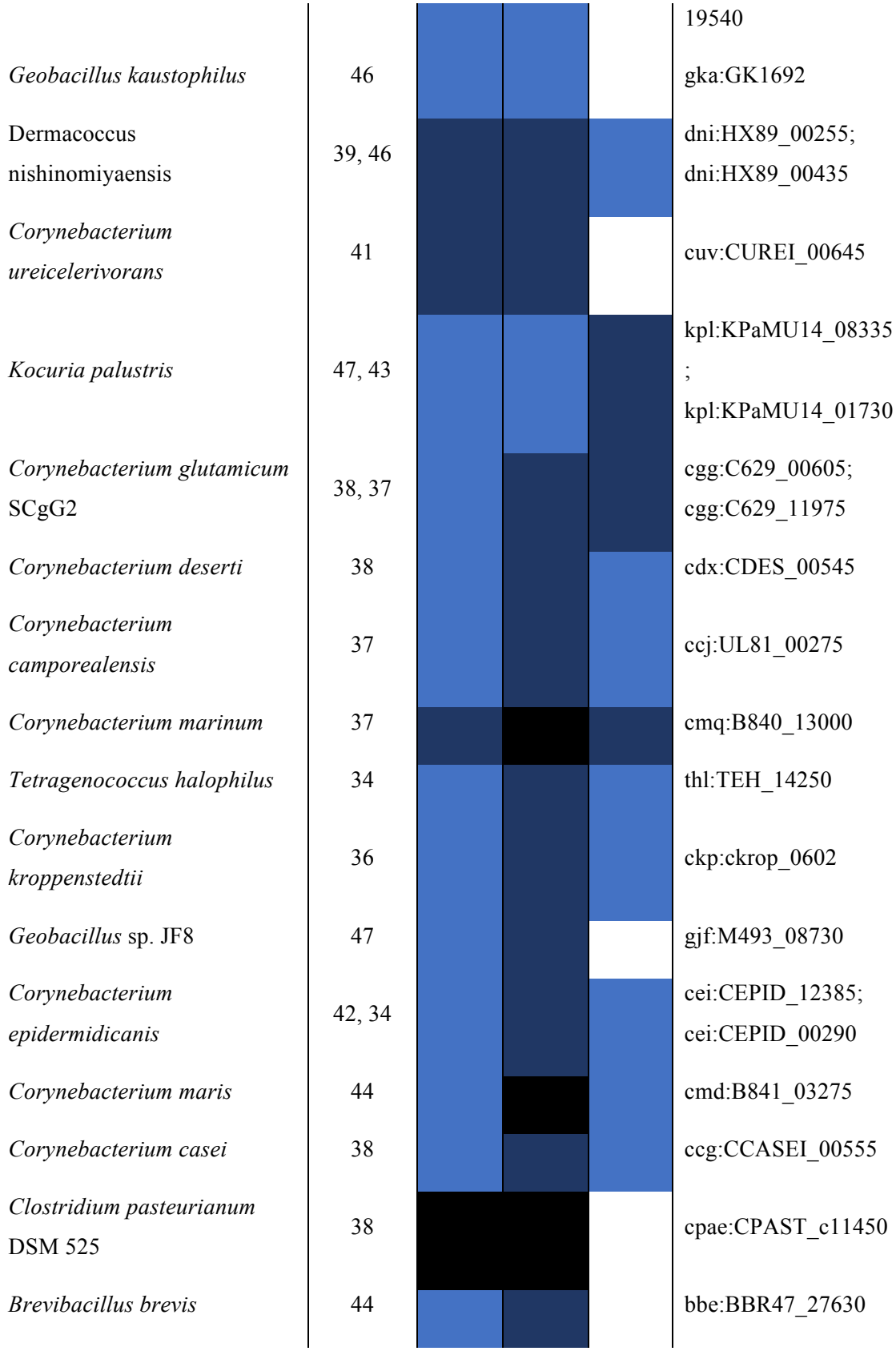

		19540
Geobacillus kaustophilus	46	gka:GK1692
Dermacoccus nishinomiyaensis	39, 46	dni:HX89_00255; dni:HX89_00435
Corynebacterium ureicelerivorans	41	cuv:CUREI_00645
Kocuria palustris	47, 43	kpl:KPaMU14_08335 ; kpl:KPaMU14_01730
Corynebacterium glutamicum SCgG2	38, 37	cgg:C629_00605; cgg:C629_11975
Corynebacterium deserti	38	cdx:CDES_00545
Corynebacterium camporealensis	37	ccj:UL81_00275
Corynebacterium marinum	37	cmq:B840_13000
Tetragenococcus halophilus	34	thl:TEH_14250
Corynebacterium kroppenstedtii	36	ckp:ckrop_0602
Geobacillus sp. JF8	47	gjf:M493_08730
Corynebacterium epidermidicanis	42, 34	cei:CEPID_12385; cei:CEPID_00290
Corynebacterium maris	44	cmd:B841_03275
Corynebacterium casei	38	ccg:CCASEI_00555
Clostridium pasteurianum DSM 525	38	cpae:CPAST_c11450
Brevibacillus brevis	44	bbe:BBR47_27630

Corynebacterium efficiens	43	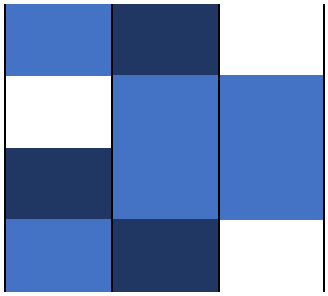	cef:CE0282
Lactobacillus plantarum 16	36		lpz:Lp16_D005
Melissococcus plutonius	39		mpx:MPD5_1685
Bacillus lehensis	33		ble:BleG1_3639

*Light blue indicates the presence of one homologue of the protein of interest. Dark blue indicates 2 homologues of the protein of interest. Black indicates more than 3 homologues of the protein of interest.

APPENDIX C

Suggestions for Future Research

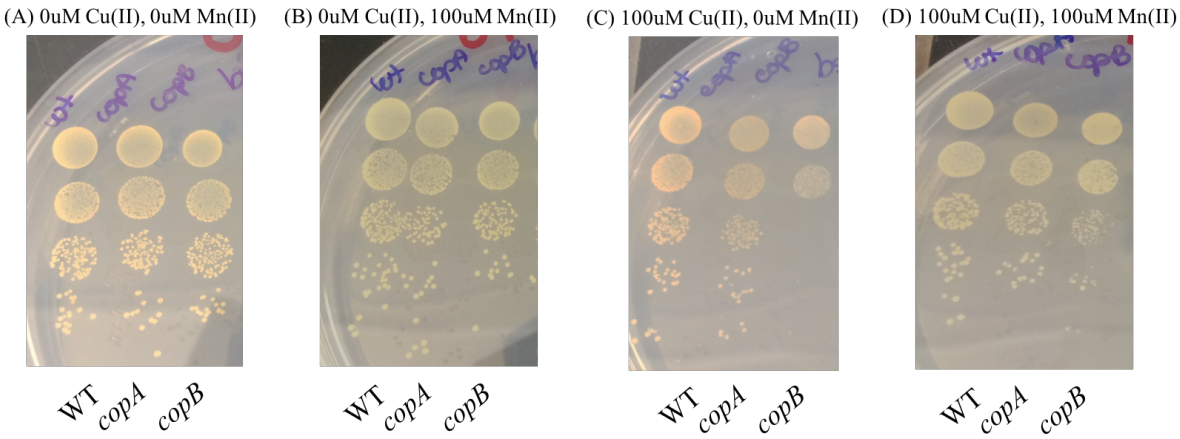

Figure 3.S1. Addition of Mn to the growth medium prevents Cu toxicity. The WT (JMB1100), *copA* (JMB4084), and *copB* (JMB3561) strains were spot plated in chemically defined media (20AA) with (A) 0μM Cu and 0μM Mn, (B) 0μM Cu and 100μM Mn, (C) 100μM Cu and 0μM Mn, or (D) 100μM Cu and 100μM Mn. Addition of Mn alone does not improve or affect the growth of the strains (Panel B). The *copB* strain has increased sensitivity to Cu (Panel C), but addition of Mn corrects the Cu sensitivity phenotype (Panel D).

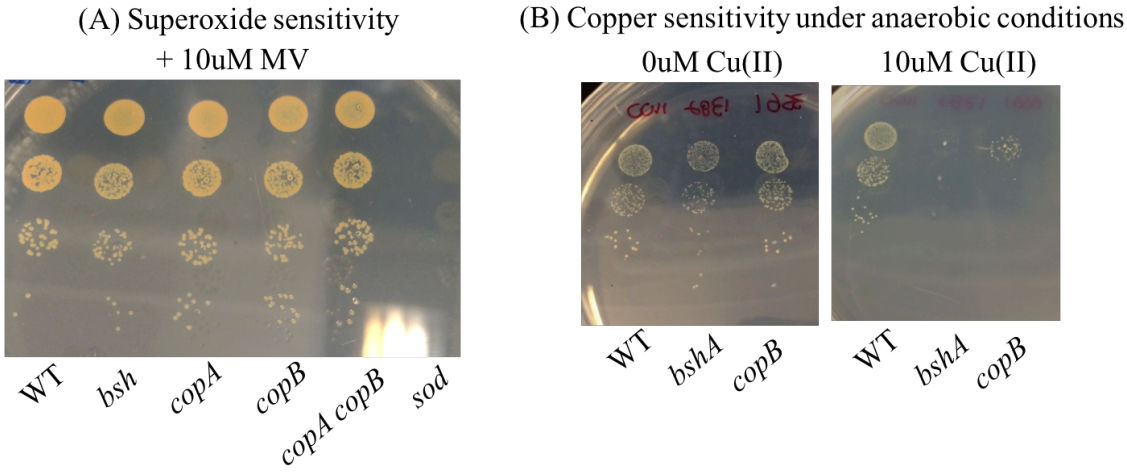

Figure 3.S2. Copper sensitivity in *S. aureus* is independent of oxygen. (A) Strains deficient in copper detoxification (*bshA*, *copA*, *copB*, and *copA copB* mutants) do not have increased sensitivity to the superoxide generator methyl viologen (10 μM; 20AA media). A strain lacking superoxide dismutase (SodA) was used as a positive control. (B) The *bshA* and *copB* strains are sensitive to Cu (10 μM; 20AA media) when incubated under anaerobic conditions. Strains used in panels A and B: WT (JMB1100), *bshA* (JMB1382), *copA* (JMB4084), *copB* (JMB3561), *copA copB* (JMB7281), and *sodA* (JMB6203).

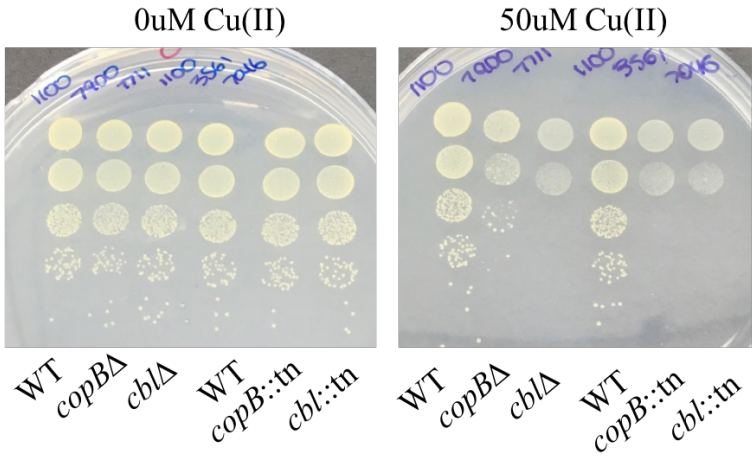

Figure 3.S3. Transposon insertion in *copB* leads to a polar effect in *cbl*. The WT (JMB1100), *copB*::tn (JMB3561), *copB*Δ (JMB7900), *cbl*::tn (JMB7046), and *cbl*Δ (JMB7711) strains were spot platted on chemically defined media (20AA) without (left) and with (right) 50 μM Cu.

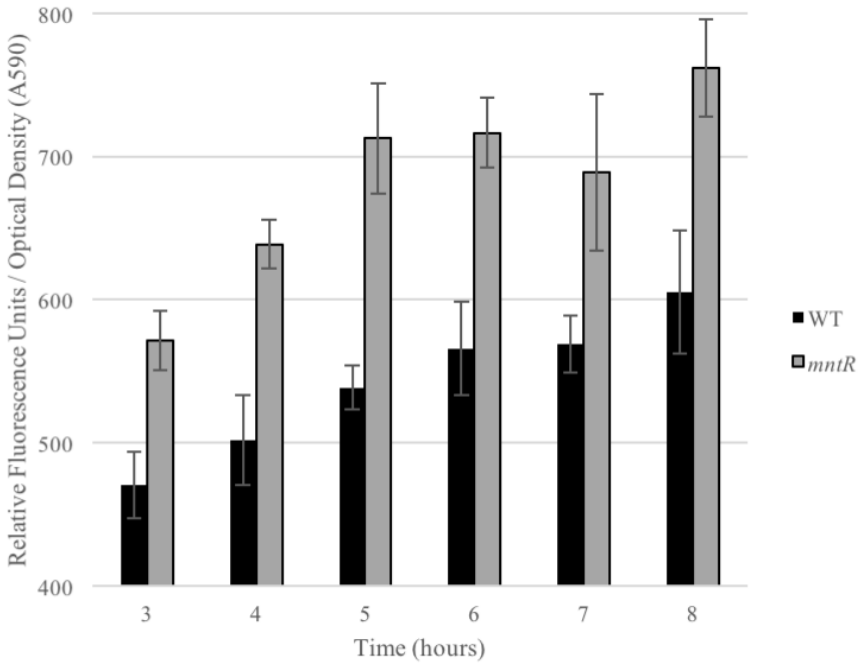

Figure 3.S4. The *copBcbl* operon is upregulated in a strain lacking the MntR regulator. Transcriptional activity of the *copBcbl* reporter was monitored in the WT (JMB1100) and *mntR*Δ (JMB1210) strains cultured in chemically defined media (20AA). Reporter used from strain JMB5372.

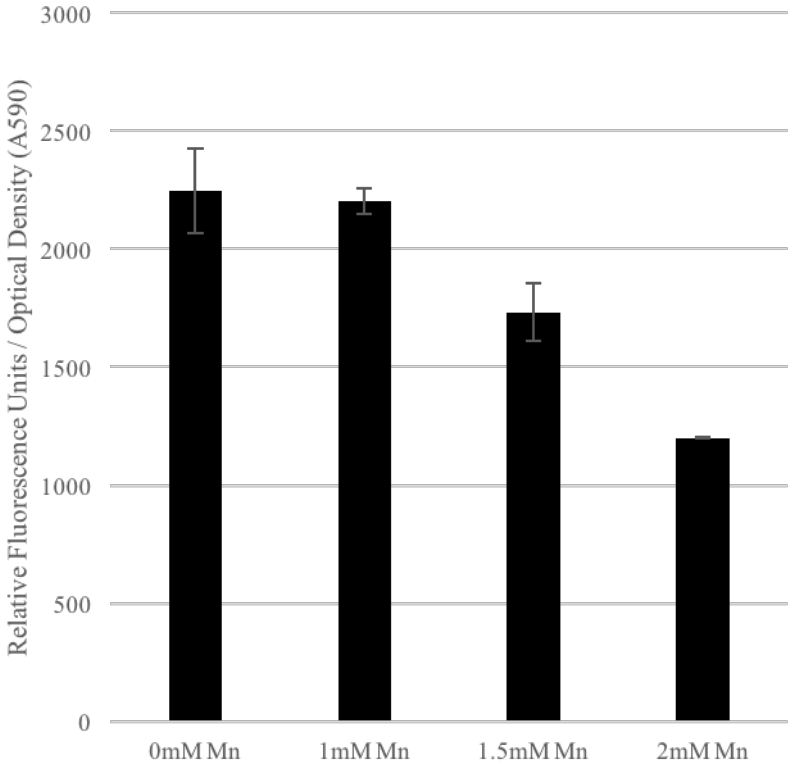

Figure 3.S5. The *copBcbl* operon is repressed under excess Mn conditions. The WT strain (JMB1100) containing the *copBcbl* reporter was grown in rich media (TSB) containing varying concentrations of Mn (0-2mM). Transcriptional activity of *copBcbl* was monitored over time. Data shown represents average of *copBcbl* expression at 8 hrs post sub-culturing using biological triplicates with standard deviation as error bars.

Preliminary results show that the addition of Mn prevents Cu toxicity in strains that are otherwise sensitive to Cu (**Figure 3.S1**). Why and how does Mn prevent Cu toxicity? To start addressing this question, we first need to know what the targets of Cu toxicity in *S. aureus* are. Data shown suggest that Cu toxicity is independent of oxygen; a *copB*::tn strain is not sensitive to oxidative stress and its Cu sensitivity phenotype repeats under anaerobic conditions (**Figure 3.S2**). These phenotypes suggest that, in *S. aureus*, Cu toxicity might not be a result of reactive oxygen species derived via Fenton-type chemistry. Because Cu can compete with other metals like Fe and displace them from metalloproteins, another cellular target of Cu are protein-bound Fe-S clusters. This leads to the following question: Does Mn prevent Cu from targeting Fe-S clusters? A possible mechanism is that Mn outcompetes Cu and prevents it from targeting and damaging Fe-S clusters. Note that these phenotypic assays were conducted using *copB*::tn strains. After constructing a *copB*Δ strain, we noticed that it did not have the same phenotype as the *copB*::tn strain (**Figure 3.S3**). Moreover, the *copB*::tn strain has the same phenotype as the *cbl*Δ strain, suggesting that transposon insertion in *copB* leads to a polar effect in *cbl*.

MntR controls the expression of Mn uptake systems; *mntABC* is derepressed by MntR under low Mn conditions (Horsburgh *et al*., 2002). Preliminary results also show that *copBcbl* transcriptional activity is higher in an *mntR* mutant strain (**Figure 3.S4**), suggesting that the expression of *copBcbl* is negatively regulated by MntR. I also found that addition of Mn to the growth medium represses *copBcbl* expression (**Figure 3.S5**). A possible explanation is that MntR helps prevent copper toxicity by derepressing genes involved in Mn uptake (*mntABC*), leading to increased intracellular levels of Mn, as well as derepression of genes involved in copper detoxification (*copBcbl*). These data also

suggest that MntR controls the CsoR regulon (*copAZ* and *copBcbl*). It would be interesting to know whether strains deficient in copper detoxification (*copA*, *copB*, or *cbl* mutants) have increased expression of genes involved in Mn uptake and/or accumulate higher levels of intracellular Mn. Blocking Mn import would then prevent protection against Cu toxicity.

The host immune system limits Mn availaibility to invading pathogens and studies show that *S. aureus* uses Mn uptake systems as mechanisms to overcome Mn starvation during infection (Kehl-Fie *et al*., 2013). Mn uptake may be an additional mechanism employed by *S. aureus* to prevent Cu toxicity within macrophages. Preliminary studies show that a *cbl* mutant strain has decreased survival in macrophages (data not shown). It would be interesting to look at whether inactivation of the lipoprotein MntC (metal-binding component of MntABC uptake system) in a *cbl* strain further decreases the survival of *S. aureus* in macrophages. Decreased survival of a *cbl mntC* double mutant strain in macrophages would suggest that Mn uptake has a role in preventing Cu toxicity at the host-pathogen interface.

REFERENCES

Achard, M.E.S., Stafford, S.L., Bokil, N.J., Chartres, J., Bernhardt, P.V., Schembri, M.A., *et al.* (2012) Copper redistribution in murine macrophages in response to *Salmonella* infection. *Biochem J* 444: 51–57.

Anderson, A.S., Miller, A.A., Donald, R.G.K., Scully, I.L., Nanra, J.S., Cooper, D., and Jansen, K.U. (2012) Development of a multicomponent *Staphylococcus aureus* vaccine designed to counter multiple bacterial virulence factors. *Hum Vaccin Immunother*. 8: 1585–1594.

Angelini, S., Gerez, C., Ollagnier de Choudens, S., Sanakis, Y., Fontecave, M., Barras, F., and Py, B. (2008) NfuA, a new factor required for maturing Fe/S proteins in *Escherichia coli* under oxidative stress and iron starvation conditions. *J Biol Chem* 283: 14084–14091.

Arenas, F.A., Covarrubias, P.C., Sandoval, J.M., Pérez-Donoso, J.M., Imlay, J.A., and Vásquez, C.C. (2011) The *Escherichia coli* BtuE protein functions as a resistance determinant against reactive oxygen species. *PLoS ONE* 6: e15979.

Argüello, J.M., Eren, E., and González-Guerrero, M. (2007) The structure and function of heavy metal transport P1B-ATPases. *Biometals* 20: 233–248.

Badarau, A., and Dennison, C. (2011) Copper trafficking mechanism of CXXC-containing domains: insight from the pH-dependence of their Cu(I) affinities. *J Am Chem Soc* 133: 2983–2988.

Bae, T., Glass, E.M., Schneewind, O., and Missiakas, D. (2008) Generating a collection of insertion mutations in the *Staphylococcus aureus* genome using *bursa aurealis*. *Methods Mol Biol* 416: 103–116.

Bagchi, P., Morgan, M.T., Bacsa, J., and Fahrni, C.J. (2013) Robust affinity standards for Cu(I) biochemistry. *J Am Chem Soc* 135: 18549–18559.

Baker, J., Sengupta, M., Jayaswal, R.K., and Morrissey, J.A. (2011) The *Staphylococcus aureus* CsoR regulates both chromosomal and plasmid-encoded copper resistance mechanisms. *Environ Microbiology* 13: 2495–2507.

Baker, J., Sitthisak, S., Sengupta, M., Johnson, M., Jayaswal, R.K., and Morrissey, J.A. (2010) Copper stress induces a global stress response in *Staphylococcus aureus* and represses *sae* and *agr* expression and biofilm formation. *Appl Microbiol* 76: 150–160.

Bandyopadhyay, S., Gama, F., Molina-Navarro, M.M., Gualberto, J.M., Claxton, R., Naik, S.G., *et al.* (2008) Chloroplast monothiol glutaredoxins as scaffold proteins for the assembly and delivery of [2Fe–2S] clusters. *EMBO J* 27: 1122–1133.

Bandyopadhyay, S., Naik, S.G., O'Carroll, I.P., Huynh, B.H., Dean, D.R., Johnson, M.K., and Santos, Dos, P.C. (2008) A proposed role for the *Azotobacter vinelandii* NfuA protein as an intermediate iron-sulfur cluster carrier. *J Biol Chem* 283: 14092–14099.

Barber, M. (1961) Methicillin-resistant staphylococci. *J Clin Pathol*. 14: 385–393.

Barber, M., Rozwadowska-Dowzenko, M. (1948) Infection by penicillin-resistant staphylococci. *Lancet*. 1: 641–644.

Barrett, F.F., McGehee, R.F. Jr, Finland, M. (1968) Methicillin-resistant *Staphylococcus aureus* at Boston City Hospital. Bacteriologic and epidemiologic observations. *N Engl J Med*. 279: 441–448.

Beinert, H., Holm, R.H., and Münck, E. (1997) Iron-sulfur clusters: nature's modular, multipurpose structures. *Science* 277: 653–659.

Benjamin, H.J., Nikore, V., Takagishi, J. (2007) Practical management: community-associated methicillin-resistant *Staphylococcus aureus* (CA-MRSA): the latest sports epidemic. *Clin J Sport Med*. 17: 393-397.

Bernsel, A., Viklund, H., Hennerdal, A., and Elofsson, A. (2009) TOPCONS: consensus prediction of membrane protein topology. *Nucleic Acids Res* 37: W465–8.

Bose, J.L., Fey, P.D., and Bayles, K.W. (2013) Genetic tools to enhance the study of gene function and regulation in *Staphylococcus aureus*. *Appl Microbiol* 79: 2218–2224.

Boyd, J.M., Pierik, A.J., Netz, D.J.A., Lill, R., and Downs, D.M. (2008) Bacterial ApbC can bind and effectively transfer iron-sulfur clusters. *Biochemistry* 47: 8195–8202.

Boyd, J.M., Sondelski, J.L., and Downs, D.M. (2009) Bacterial ApbC protein has two biochemical activities that are required for *in vivo* function. *J Biol Chem* 284: 110–118.

Burlak, C., Hammer, C.H., Robinson, M.-A., Whitney, A.R., McGavin, M.J., Kreiswirth, B.N., and DeLeo, F.R. (2007) Global analysis of community-associated methicillin-resistant *Staphylococcus aureus* exoproteins reveals molecules produced *in vitro* and during infection. *Cell Microbiol* 9: 1172–1190.

Carmel-Harel, O., and Storz, G. (2000) Roles of the glutathione- and thioredoxin-dependent reduction systems in the *Escherichia coli* and *Saccharomyces cerevisiae* responses to oxidative stress. *Annu Rev Microbiol* 54: 439–461.

Casey, A.L., Adams, D., Karpanen, T.J., Lambert, P.A., Cookson, B.D., Nightingale, P., *et al.* (2010) Role of copper in reducing hospital environment contamination. *J Hosp Infect* 74: 72–77.

Centers for Disease Control and Prevention. (2002) *Staphylococcus aureus* resistant to vancomycin--United States, 2002. *MMWR Morb Mortal Wkly Rep*. 51: 565-567.

Centers for Disease Control and Prevention. (2003) Outbreaks of community-associated methicillin-resistant *Staphylococcus aureus* skin infections--Los Angeles County, California, 2002-2003. *MMWR Morb Mortal Wkly Rep*. 52: 88.

Centers for Disease Control and Prevention. (2013) Active Bacterial Core Surveillance Report, Emerging Infections Program Network, Methicillin-Resistant *Staphylococcus aureus*, 2013.

Chambers, H.F., DeLeo, F.R. (2009) Waves of resistance: *Staphylococcus aureus* in the antibiotic era. *Nat Rev Microbiol*. 7: 629-641.

Chandrangsu, P., Dusi, R., Hamilton, C.J., and Helmann, J.D. (2014) Methylglyoxal resistance in *Bacillus subtilis:* contributions of bacillithiol-dependent and independent pathways. *Mol Microbiol* 91: 706–715.

Chaudhuri, R.R., Allen, A.G., Owen, P.J., Shalom, G., Stone, K., Harrison, M., *et al.* (2009) Comprehensive identification of essential *Staphylococcus aureus* genes using Transposon-Mediated Differential Hybridisation (TMDH). *BMC Genomics* 10: 291.

Chi, B.K., Gronau, K., Mäder, U., Hessling, B., Becher, D., and Antelmann, H. (2011) S-bacillithiolation protects against hypochlorite stress in *Bacillus subtilis* as revealed by transcriptomics and redox proteomics. *Mol Cell Proteomics* 10: M111.009506.

Chi, B.K., Roberts, A.A., Huyen, T.T.T., Bäsell, K., Becher, D., Albrecht, D., *et al.* (2013) S-bacillithiolation protects conserved and essential proteins against hypochlorite stress in *Firmicutes* bacteria. *Antiox Redox Signal* 18: 1273–1295.

Chillappagari, S., Seubert, A., Trip, H., Kuipers, O.P., Marahiel, M.A., and Miethke, M. (2010) Copper stress affects iron homeostasis by destabilizing iron-sulfur cluster formation in *Bacillus subtilis*. *J Bacteriol* 192: 2512–2524.

Claus, H. (2003) Laccases and their occurrence in prokaryotes. *Arch Microbiol* 179: 145–150.

Clements, M.O., Watson, S.P., and Foster, S.J. (1999) Characterization of the major superoxide dismutase of *Staphylococcus aureus* and its role in starvation survival, stress resistance, and pathogenicity. *J Bacteriol* 181: 3898–3903.

Cosgrove, K., Coutts, G., Jonsson, I.M., Tarkowski, A., Kokai-Kun, J.F., Mond, J.J., Foster, S.J. (2007) Catalase (KatA) and alkyl hydroperoxide reductase (AhpC) have compensatory roles in peroxide stress resistance and are required for survival, persistence, and nasal colonization in *Staphylococcus aureus*. *J Bacteriol*. 189: 1025-1035.

Cosgrove, S.E., Qi, Y., Kaye, K.S., Harbarth, S., Karchmer, A.W., Carmeli, Y. (2005) The impact of methicillin resistance in *Staphylococcus aureus* bacteremia on patient outcomes: mortality, length of stay, and hospital charges. *Infect Control Hosp Epidemiol*. 26(2):166-74.

Crooks, D.R., Ghosh, M.C., Haller, R.G., Tong, W.-H., and Rouault, T.A. (2010) Posttranslational stability of the heme biosynthetic enzyme ferrochelatase is dependent on iron availability and intact iron-sulfur cluster assembly machinery. *Blood* 115: 860–869.

Crosse, A.M., Greenway, D.L., and England, R.R. (2000) Accumulation of ppGpp and ppGp in *Staphylococcus aureus* 8325-4 following nutrient starvation. *Lett Appl Microbiol* 31: 332–337.

Dantes, R., Mu, Y., Belflower, R., Aragon, D., Dumyati, G., Harrison, L.H., *et al*. (2013) Emerging Infections Program-Active Bacterial Core Surveillance MRSA Surveillance Investigators. National burden of invasive methicillin-resistant *Staphylococcus aureus* infections, United States, 2011. *JAMA Intern Med*. 173: 1970-1978.

Delmar, J.A., Su, C.-C., and Yu, E.W. (2013) Structural mechanisms of heavy-metal extrusion by the Cus efflux system. *Biometals* 26: 593–607.

delCardayré, S.B., Stock, K.P., Newton, G.L., Fahey, R.C., and Davies, J.E. (1998) Coenzyme A disulfide reductase, the primary low molecular weight disulfide reductase from *Staphylococcus aureus*. Purification and characterization of the native enzyme. *J Biol Chem* 273: 5744–5751.

Dickinson, D.A., and Forman, H.J. (2002) Cellular glutathione and thiols metabolism. *Biochem Pharmacol* 64: 1019–1026.

Diep, B.A., Gill, S.R., Chang, R.F., Phan, T.H., Chen, J.H., Davidson, M.G., *et al.* (2006) Complete genome sequence of USA300, an epidemic clone of community-acquired meticillin-resistant *Staphylococcus aureus*. *Lancet* 367: 731–739.

Diep, B.A., Phung, Q., Date, S., Arnott, D., Bakalarski, C., Xu, M., *et al.* (2014) Identifying potential therapeutic targets of methicillin-resistant *Staphylococcus aureus* through in vivo proteomic analysis. *J Infect Dis* 209: 1533–1541.

Diep, B.A., Stone, G.G., Basuino, L., Graber, C.J., Miller, A., Etages, des, S.-A., *et al.* (2008) The arginine catabolic mobile element and staphylococcal chromosomal cassette mec linkage: convergence of virulence and resistance in the USA300 clone of methicillin-resistant *Staphylococcus aureus. J Infect Dis* 197: 1523–1530.

Ding, B., Smith, E.S., and Ding, H. (2005) Mobilization of the iron centre in IscA for the iron-sulphur cluster assembly in IscU. *Biochem J* 389: 797–802.

Ding, H., and Clark, R.J. (2004) Characterization of iron binding in IscA, an ancient iron-sulphur cluster assembly protein. *Biochem J* 379: 433–440.

Ding, H., Clark, R.J., and Ding, B. (2004) IscA mediates iron delivery for assembly of iron-sulfur clusters in IscU under the limited accessible free iron conditions. *J Biol Chem* 279: 37499–37504.

Djaman, O., Outten, F.W., and Imlay, J.A. (2004) Repair of oxidized iron-sulfur clusters in *Escherichia coli*. *J Biol Chem* 279: 44590–44599.

Dollwet, H.H.A., and Sorenson, J.R.J. (1985). Historic uses of copper compounds in medicine. *Trace Elem Med*. 2, 80–87.

Dougall, D.K. (1974) Evidence for the presence of glutamate synthase in extracts of carrot cell cultures. *Biochem Biophys Res Commun* 58: 639–646.

Fahey, R.C. (2013) Glutathione analogs in prokaryotes. *Biochim Biophys Acta* 1830: 3182–3198.

Feng, Y., Zhong, N., Rouhier, N., Hase, T., Kusunoki, M., Jacquot, J.-P., *et al.* (2006) Structural insight into poplar glutaredoxin C1 with a bridging iron-sulfur cluster at the active site. *Biochemistry* 45: 7998–8008.

Festa, R.A., Jones, M.B., Butler-Wu, S., Sinsimer, D., Gerads, R., Bishai, W.R., *et al.* (2011) A novel copper-responsive regulon in *Mycobacterium tuberculosis*. *Mol Microbiol* 79: 133–148.

Fey, P.D., Endres, J.L., Yajjala, V.K., Widhelm, T.J., Boissy, R.J., Bose, J.L., and Bayles, K.W. (2013) A genetic resource for rapid and comprehensive phenotype screening of nonessential *Staphylococcus aureus* genes. *mBio* 4: e00537–12.

Fisher, N., and Hanna, P. (2005) Characterization of *Bacillus anthracis* germinant receptors *in vitro*. *J Bacteriol* 187: 8055–8062.

Flint, D.H., and Emptage, M.H. (1988) Dihydroxy acid dehydratase from spinach contains a [2Fe-2S] cluster. *J Biol Chem* 263: 3558–3564.

Flint, D.H., Emptage, M.H., Finnegan, M.G., Fu, W., and Johnson, M.K. (1993) The role and properties of the iron-sulfur cluster in *Escherichia coli* dihydroxy-acid dehydratase. *J Biol Chem* 268: 14732–14742.

Forsyth, R.A., Haselbeck, R.J., Ohlsen, K.L., Yamamoto, R.T., Xu, H., Trawick, J.D., *et al.* (2002) A genome-wide strategy for the identification of essential genes in *Staphylococcus aureus*. *Mol Microbiol* 43: 1387–1400.

Fung, D.K.C., Lau, W.Y., Chan, W.T., and Yan, A. (2013) Copper efflux is induced during anaerobic amino acid limitation in *Escherichia coli* to protect iron-sulfur cluster enzymes and its biogenesis. *J Bacteriol* 195: 4556–4568.

Gaballa, A., Antelmann, H., Hamilton, C.J., and Helmann, J.D. (2013) Regulation of *Bacillus subtilis* bacillithiol biosynthesis operons by Spx. *Microbiology* 159: 2025–2035.

Gaballa, A., Chi, B.K., Roberts, A.A., Becher, D., Hamilton, C.J., Antelmann, H., and Helmann, J.D. (2014) Redox regulation in *Bacillus subtilis*: the bacilliredoxins BrxA (YphP) and BrxB (YqiW) function in de-bacillithiolation of S-bacillithiolated OhrR and MetE. *Antiox Redox Signal* 21:357–367.

Gaballa, A., Newton, G.L., Antelmann, H., Parsonage, D., Upton, H., Rawat, M., *et al.* (2010) Biosynthesis and functions of bacillithiol, a major low-molecular-weight thiol in *Bacilli*. *Proc Natl Acad Sci USA* 107: 6482–6486.

Gao, W., Chua, K., Davies, J.K., Newton, H.J., Seemann, T., Harrison, P.F., *et al.* (2010) Two novel point mutations in clinical *Staphylococcus aureus* reduce linezolid susceptibility and switch on the stringent response to promote persistent infection. *PLoS Pathog* 6: e1000944.

Gardner, P.R., and Fridovich, I. (1993) Effect of glutathione on aconitase in *Escherichia coli*. *Arch Biochem Biophys* 301: 98–102.

Gaupp, R., Ledala, N., and Somerville, G.A. (2012) Staphylococcal response to oxidative stress. *Front Cell Infect Microbiol*. 2:33. doi: 10.3389/fcimb.2012.00033.

Geiger, T., Goerke, C., Fritz, M., Schäfer, T., Ohlsen, K., Liebeke, M., *et al.* (2010) Role of the (p)ppGpp synthase RSH, a RelA/SpoT homolog, in stringent response and virulence of *Staphylococcus aureus*. *Infect Immun* 78: 1873–1883.

Gralnick, J.A., and Downs, D.M. (2003) The YggX protein of *Salmonella enterica* is involved in Fe(II) trafficking and minimizes the DNA damage caused by hydroxyl radicals: residue CYS-7 is essential for YggX function. *J Biol Chem* 278: 20708–20715.

Grandi, G. (2010) Bacterial surface proteins and vaccines. F1000 Biol Rep. 2: 36. doi: 10.3410/B2-36

Grass, G., Rensing, C., and Solioz, M. (2011) Metallic copper as an antimicrobial surface. *Appl Microbiol* 77: 1541–1547.

Gross, S.R., Burns, R.O., and Umbarger, H.E. (1963) The biosynthesis of leucine. 11. The enzymic isomerization of beta-Hydroxy-beta-carboxyisocaproate. *Biochemistry* 2: 1046–1052.

Große, C., Schleuder, G., Schmole, C., and Nies, D.H. (2014) Survival of *Escherichia coli* cells on solid copper surfaces is increased by glutathione. *Appl Environ Microbiol*. 80: 7071–7078.

Grossoehme, N., Kehl-Fie, T.E., Ma, Z., Adams, K.W., Cowart, D.M., Scott, R.A., *et al.* (2011) Control of copper resistance and inorganic sulfur metabolism by paralogous regulators in *Staphylococcus aureus*. *J Biol Chem* 286: 13522–13531.

Gunn, T.R., Macfarlane, S., and Phillips, L.I. (1984) Difficulties in the neonatal diagnosis of Menkes' kinky hair syndrome--trichopoliodystrophy. *Clin Pediatr (Phila)* 23: 514–516.

Gunther, M.R., Hanna, P.M., Mason, R.P., and Cohen, M.S. (1995) Hydroxyl radical formation from cuprous ion and hydrogen peroxide: a spin-trapping study. *Arch Biochem Biophys* 316:515–522.

Gupta, V., Sendra, M., Naik, S.G., Chahal, H.K., Huynh, B.H., Outten, F.W., *et al.* (2009) Native *Escherichia coli* SufA, coexpressed with SufBCDSE, purifies as a [2Fe-2S] protein and acts as an Fe-S transporter to Fe-S target enzymes. *J Am Chem Soc* 131: 6149–6153.

Handtke, S., Schroeter, R., Jürgen, B., Methling, K., Schlüter, R., Albrecht, D., *et al.* (2014) *Bacillus pumilus* reveals a remarkably high resistance to hydrogen peroxide provoked oxidative stress. *PLoS ONE* 9: e85625.

Hao, X., Lüthje, F.L., Qin, Y., McDevitt, S.F., Lutay, N., Hobman, J.L., *et al.* (2015) Survival in amoeba--a major selection pressure on the presence of bacterial copper and zinc resistance determinants? Identification of a "copper pathogenicity island". *Appl Microbiol Biotechnol* 99: 5817–5824.

Helbig, K., Bleuel, C., Krauss, G.J., and Nies, D.H. (2008) Glutathione and transition-metal homeostasis in *Escherichia coli*. *J Bacteriol* 190:5431–5438.

Hider, R.C., and Kong, X.L. (2011) Glutathione: a key component of the cytoplasmic labile iron pool. *Biometals* 24: 1179–1187. Hodgkinson, V., and Petris, M.J. (2012) Copper homeostasis at the host-pathogen interface. *J Biol Chem* 287: 13549–13555.

Hodgkinson, V., and Petris, M.J. (2012) Copper homeostasis at the host-pathogen interface. *J Biol Chem* 287: 13549–13555.

Hood, M.I., and Skaar E.P (2012) Nutritional immunity: transition metals at the pathogen-host interface. *Nat Rev Microbiol* 10:525–537.

Horsburgh, M.J., Clements, M.O., Crossley, H., Ingham, E., and Foster, S.J. (2001) PerR controls oxidative stress resistance and iron storage proteins and is required for virulence in *Staphylococcus aureus*. *Infect Immun* 69: 3744–3754.

Horsburgh, M.J., Ingham, E., and Foster, S.J. (2001) In *Staphylococcus* aureus, Fur is an interactive regulator with PerR, contributes to virulence, and is necessary for oxidative stress resistance through positive regulation of catalase and iron homeostasis. *J Bacteriol* 183: 468–475.

Horsburgh, M.J., Wharton, S.J., Cox, A.G., Ingham, E., Peacock, S., and Foster, S.J. (2002) MntR modulates expression of the PerR regulon and superoxide resistance in *Staphylococcus aureus* through control of manganese uptake. *Mol Microbiol* 44: 1269–1286.

Hurst, J.K., Barrette, W.C., Jr, Michel, B.R., and Rosen, H. (1991) Hypochlorous acid and myeloperoxidase-catalyzed oxidation of iron-sulfur clusters in bacterial respiratory dehydrogenases. *Eur J Biochem* 202: 1275–1282.

Hutchings, M.I., Palmer, T., Harrington, D.J., and Sutcliffe, I.C. (2009) Lipoprotein biogenesis in Gram-positive bacteria: knowing when to hold ‘em, knowing when to fold ‘em. *Trends Microbiol* 17: 13–21.

Imlay, J.A. (2006) Iron-sulphur clusters and the problem with oxygen. *Mol Microbiol* 59: 1073–1082.

Imlay, J.A., and Linn, S. (1988) DNA damage and oxygen radical toxicity. *Science* 240: 1302–1309.

Iwema, T., Picciocchi, A., Traore, D.A.K., Ferrer, J.-L., Chauvat, F., and Jacquamet, L. (2009) Structural basis for delivery of the intact [Fe2-S2] cluster by monothiol glutaredoxin. *Biochemistry* 48: 6041–6043.

Jang, S., and Imlay, J.A. (2007) Micromolar intracellular hydrogen peroxide disrupts metabolism by damaging iron-sulfur enzymes. *J Biol Chem* 282: 929–937.

Johnson, D.C., Dean, D.R., Smith, A.D., and Johnson, M.K. (2005) Structure, function, and formation of biological iron-sulfur clusters. *Annu Rev Biochem* 74: 247–281.

Joshi, G.S., Spontak, J.S., Klapper, D.G., and Richardson, A.R. (2011) Arginine catabolic mobile element encoded *speG* abrogates the unique hypersensitivity of *Staphylococcus aureus* to exogenous polyamines. *Mol Microbiol* 82: 9–20.

Joska, T.M., Mashruwala, A., Boyd, J.M., and Belden, W.J. (2014) A universal cloning method based on yeast homologous recombination that is simple, efficient, and versatile. *J Microbiol Methods* 100: 46–51.

Kaler, S.G. (2011) ATP7A-related copper transport diseases-emerging concepts and future trends. *Nat Rev Neurol* 7: 15–29.

Kamps, A., Achebach, S., Fedtke, I., Unden, G., and Götz, F. (2004) Staphylococcal NreB: an O(2)-sensing histidine protein kinase with an O(2)-labile iron-sulphur cluster of the FNR type. *Mol Microbiol* 52: 713–723.

Karavolos, M.H., Horsburgh, M.J., Ingham, E., and Foster, S.J. (2003) Role and regulation of the superoxide dismutases of *Staphylococcus aureus*. *Microbiology* 149: 2749–2758.

Kehl-Fie, T.E., Zhang, Y., Moore, J.L., Farrand, A.J., Hood, M., Rathi, S., *et al*. (2013) MntABC and MntH contribute to systemic *Staphylococcus aureus* infection by competing with calprotectin for nutrient manganese. *Infect Immun*. 81:3395-405.

Kennedy, M.C., and Beinert, H. (1988) The state of cluster SH and S^{2-} of aconitase during cluster interconversions and removal. A convenient preparation of apoenzyme. *J Biol Chem* 263: 8194–8198.

Kennedy, M.C., Emptage, M.H., Dreyer, J.-L., and Beinert, H. (1983) The role of iron in the activation-inactivation of aconitase. *J Biol Chem* 258: 11098–11105.

Kent, T.A., Dreyer, J.-L., Kennedy, M.C., Huynh, B.H., Emptage, M.H., Beinert, H., and Münck, E. (1982) Mössbauer studies of beef heart aconitase: evidence for facile interconversions of iron-sulfur clusters. *Proc Natl Acad Sci USA* 79: 1096–1100.

Keyer, K., and Imlay, J.A. (1996) Superoxide accelerates DNA damage by elevating free-iron levels. *Proc Natl Acad Sci USA* 93: 13635–13640.

Keyer, K., and Imlay, J.A. (1997) Inactivation of dehydratase [4Fe-4S] clusters and disruption of iron homeostasis upon cell exposure to peroxynitrite. *J Biol Chem* 272: 27652–27659.

Khoroshilova, N., Popescu, C., Münck, E., Beinert, H., and Kiley, P.J. (1997) Iron-sulfur cluster disassembly in the FNR protein of *Escherichia coli* by O2: [4Fe-4S] to [2Fe-2S] conversion with loss of biological activity. *Proc Natl Acad Sci USA* 94: 6087–6092.

Kiedrowski, M.R., Crosby, H.A., Hernandez, F.J., Malone, C.L., McNamara, J.O., and Horswill, A.R. (2014) *Staphylococcus aureus* Nuc2 is a functional, surface-attached extracellular nuclease. *PLoS One* 9: e95574.

Klein, E., Smith, D.L., and Laxminarayan, R. (2007) Hospitalizations and deaths caused by methicillin-resistant *Staphylococcus aureus*, United States, 1999-2005. *Emerg Infect Dis* 13: 1840–1846.

Klevens, R.M., Morrison, M.A., Nadle, J., Petit, S., Gershman, K., Ray, S., *et al.* (2007) Invasive methicillin-resistant *Staphylococcus aureus* infections in the United States. *JAMA* 298: 1763–1771.

Kohlhaw, G.B. (1988) Isopropylmalate dehydratase from yeast. *Methods Enzymol* 166: 423–429.

Kovacs-Simon, A., Titball, R.W., and Michell, S.L. (2011) Lipoproteins of bacterial pathogens. *Infect Immun* 79: 548–561.

Krebs, C., Agar, J.N., Smith, A.D., Frazzon, J., Dean, D.R., Huynh, B.H., and Johnson, M.K. (2001) IscA, an alternate scaffold for Fe−S cluster biosynthesis. *Biochemistry* 40: 14069–14080.

Kreiswirth, B.N., Löfdahl, S., Betley, M.J., O'Reilly, M., Schlievert, P.M., Bergdoll, M.S., and Novick, R.P. (1983) The toxic shock syndrome exotoxin structural gene is not detectably transmitted by a prophage. *Nature* 305: 709–712.

Kreuder, J., Otten, A., Fuder, H., Tümer, Z., Tønnesen, T., Horn, N., and Dralle, D. (1993) Clinical and biochemical consequences of copper-histidine therapy in Menkes disease. *Eur J Pediatr* 152: 828–832.

Landry, A.P., Cheng, Z., and Ding, H. (2013) Iron binding activity is essential for the function of IscA in iron-sulphur cluster biogenesis. *Dalton Trans* 42: 3100–3106.

Lee, J.W., and Helmann, J.D. (2006) The PerR transcription factor senses H_2O_2 by metal-catalysed histidine oxidation. *Nature* 440: 363–367.

Lee, B.Y., Singh, A., David, M.Z., Bartsch, S.M., Slayton, R.B., Huang, S.S., *et al.* (2013) The economic burden of community-associated methicillin-resistant *Staphylococcus aureus* (CA-MRSA). *Clin Microbiol Infect* 19: 528–536.

Li, M., Diep, B.A., Villaruz, A.E., Braughton, K.R., Jiang, X., DeLeo, F.R., *et al.* (2009) Evolution of virulence in epidemic community-associated methicillin-resistant *Staphylococcus aureus*. *Proc Natl Acad Sci U S A* 106: 5883–5888.

Liese, J., Kloos S., Jendrossek, V., Petropoulou, T., Wintergerst, U., Notheis, G., Gahr, M., Belohradsky, B.H. (2000) Long-term follow-up and outcome of 39 patients with chronic granulomatous disease. *J Pediatr*. 137: 687-693.

Lowder, B.V., Guinane, C.M., Ben Zakour, N.L., Weinert, L.A., Conway-Morris, A., Cartwright, R.A., *et al.* (2009) Recent human-to-poultry host jump, adaptation, and pandemic spread of *Staphylococcus aureus*. *Proc Natl Acad Sci U S A* 106: 19545–19550.

Luo, M., Jiang, Y.-L., Ma, X.-X., Tang, Y.-J., He, Y.-X., Yu, J., *et al.* (2010) Structural and biochemical characterization of yeast monothiol glutaredoxin Grx6. *J Mol Biol* 398: 614–622.

Ma, Z., Chandrangsu, P., Helmann, T.C., Romsang, A., Gaballa, A., and Helmann, J.D. (2014) Bacillithiol is a major buffer of the labile zinc pool in *Bacillus subtilis*. *Mol Microbiol* 94: 756–770.

Ma, Z., Cowart, D.M., Scott, R.A., and Giedroc, D.P. (2009) Molecular insights into the metal selectivity of the copper(I)-sensing repressor CsoR from *Bacillus subtilis*. *Biochemistry* 48: 3325–3334.

Ma, Z., Cowart, D.M., Ward, B.P., Arnold, R.J., DiMarchi, R.D., Zhang, L., *et al.* (2009) Unnatural amino acid substitution as a probe of the allosteric coupling pathway in a mycobacterial Cu(I) sensor. *J Am Chem Soc* 131: 18044–18045.

Macomber, L., and Imlay, J.A. (2009) The iron-sulfur clusters of dehydratases are primary intracellular targets of copper toxicity. *Proc Natl Acad Sci U S A* 106:8344–8349.

Macomber, L., Rensing, C., and Imlay, J.A. (2007) Intracellular copper does not catalyze the formation of oxidative DNA damage in *Escherichia coli*. *J Bacteriol* 189:1616–1626.

Mah, R.A., Fung, D.Y.C., and Morse, S.A. (1967) Nutritional requirements of *Staphylococcus aureus* S-6'. *Appl Microbiol* 15: 866–870.

Malone, C.L., Boles, B.R., Lauderdale, K.J., Thoendel, M., Kavanaugh, J.S., and Horswill, A.R. (2009) Fluorescent reporters for *Staphylococcus aureus*. *J Microbiol Methods* 77: 251–260.

Mapolelo, D.T., Zhang, B., Naik, S.G., Huynh, B.H., and Johnson, M.K. (2012) Spectroscopic and functional characterization of iron-sulfur cluster-bound forms of *Azotobacter vinelandii* (Nif)IscA. *Biochemistry* 51: 8071–8084.

Mapolelo, D.T., Zhang, B., Randeniya, S., Albetel, A.-N., Li, H., Couturier, J., *et al.* (2013) Monothiol glutaredoxins and A-type proteins: partners in Fe-S cluster trafficking. *Dalton Trans* 42: 3107–3115.

Marais, F., Mehtar, S., and Chalkley, L. (2010) Antimicrobial efficacy of copper touch surfaces in reducing environmental bioburden in a South African community healthcare facility. *J Hosp Infect* 74: 80–82.

Marchler-Bauer, A., Derbyshire, M.K., Gonzales, N.R., Lu, S., Chitsaz, F., Geer, L.Y., *et al.* (2015) CDD: NCBI's conserved domain database. *Nucleic Acids Res* 43: D222–6.

Martinez-Gomez, N.C., and Downs, D.M. (2008) ThiC is an [Fe-S] cluster protein that requires AdoMet to generate the 4-amino-5-hydroxymethyl-2-methylpyrimidine moiety in thiamin synthesis. *Biochemistry* 47: 9054–9056.

Marty, F.M., Yeh, W.W., Wennersten, C.B., Venkataraman, L., Albano, E., Alyea, E.P., *et al*. (2006) Emergence of a clinical daptomycin-resistant Staphylococcus aureus isolate during treatment of methicillin-resistant *Staphylococcus aureus* bacteremia and osteomyelitis. *J Clin Microbiol*. 44: 595-597.

Mashruwala, A.A., Pang, Y.Y., Rosario-Cruz, Z., Chahal, H.K., Benson, M.A., Mike, L.A., *et al.* (2015) Nfu facilitates the maturation of iron-sulfur proteins and participates in virulence in *Staphylococcus aureus*. *Mol Microbiol* 95: 383–409.

McAdams, R.M., Ellis, M.W., Trevino, S., Rajnik, M. (2008) Spread of methicillin-resistant *Staphylococcus aureus* USA300 in a neonatal intensive care unit. *Pediatr Int.* 50: 810-815.

Menkes, J.H., Alter, M., Steigleder, G.K., Weakley, D.R., and Sung, J.H. (1962) A sex-linked recessive disorder with retardation of growth, peculiar hair, and focal cerebral and cerebellar degeneration. *Pediatrics* 29: 764–779.

Mettert, E.L., and Kiley, P.J. (2005) ClpXP-dependent proteolysis of FNR upon loss of its O2-sensing [4Fe-4S] cluster. *J Mol Biol* 354: 220–232.

Miethke, M., Westers, H., Blom, E.-J., Kuipers, O.P., and Marahiel, M.A. (2006) Iron starvation triggers the stringent response and induces amino acid biosynthesis for bacillibactin production in *Bacillus subtilis*. *J Bacteriol* 188: 8655–8657.

Mikolay, A., Huggett, S., Tikana, L., Grass, G., Braun, J., and Nies, D.H. (2010) Survival of bacteria on metallic copper surfaces in a hospital trial. *Appl Microbiol Biotechnol* 87: 1875–1879.

Mills, G.C. (1957) Hemoglobin catabolism I. Glutathione peroxidase, an erythrocyte enzyme which protects hemoglobin from oxidative breakdown. *J Biol Chem* 229: 189–197.

Miragaia, M., de Lencastre, H., Perdreau-Remington, F., Chambers, H.F., Higashi, J., Sullam, P.M., *et al.* (2009) Genetic diversity of Arginine Catabolic Mobile Element in *Staphylococcus epidermidis*. *PLoS One* 4: e7722–9.

Morrison-Rodriguez, S.M., Pacha, L.A., Patrick, J.E., Jordan, N.N. (2010) Community-associated methicillin-resistant *Staphylococcus aureus* infections at an Army training installation. *Epidemiol Infect*. 138: 721-729.

Mühlenhoff, U., Molik, S., Godoy, J.R., Uzarska, M.A., Richter, N., Seubert, A., *et al.* (2010) Cytosolic monothiol glutaredoxins function in intracellular iron sensing and trafficking via their bound iron-sulfur cluster. *Cell Metab* 12: 376–385.

Myhre, O., Andersen, J.M., Aarnes, H., and Fonnum, F. (2003) Evaluation of the probes 2′,7′-dichlorofluorescin diacetate, luminol, and lucigenin as indicators of reactive species formation. *Biochem Pharmacol* 65: 1575–1582.

Nappi, A.J., and Vass, E. (1997) Comparative studies of enhanced iron-mediated production of hydroxyl radical by glutathione, cysteine, ascorbic acid, and selected catechols. *Biochim Biophys Acta* 1336: 295–301.

Navarre, W.W., Daefler, S., and Schneewind, O. (1996) Cell wall sorting of lipoproteins in *Staphylococcus aureus*. *J Bacteriol* 178: 441–446.

NCIRS, C. (2011) Active Bacterial Core surveillance (ABCs) report emerging infections program network methicillin-resistant *Staphylococcus aureus*, 2011. 1–3 http://www.cdc.gov/abcs/reports-findings/survreports/mrsa11.pdf.

Newton, G.L., Fahey, R.C., and Rawat, M. (2012) Detoxification of toxins by bacillithiol in *Staphylococcus aureus*. *Microbiology* 158: 1117–1126.

Newton, G.L., Rawat, M., La Clair, J.J., Jothivasan, V.K., Budiarto, T., Hamilton, C.J., *et al.* (2009) Bacillithiol is an antioxidant thiol produced in Bacilli. *Nat Chem Biol* 5: 625–627.

Noskin, G.A., Rubin, R.J., Schentag, J.J., Kluytmans, J., Hedblom, E.C., Jacobson, C., *et al.* (2007) National trends in *Staphylococcus aureus* infection rates: impact on economic burden and mortality over a 6-year period (1998-2003). *Clin Infect Dis* 45: 1132–1140.

Noyce, J.O., Michels, H., and Keevil, C.W. (2006) Potential use of copper surfaces to reduce survival of epidemic meticillin-resistant *Staphylococcus aureus* in the healthcare environment. *J Hosp Infect* 63: 289–297.

Novick, R.P. (1991) Genetic systems in Staphylococci. *Methods Enzymol* 204: 587–636.

Olson, B.J., and Markwell, J. (2007) Assays for determination of protein concentration. *Curr Protoc Protein Sci* Chapter 3: Unit3.4.

Orme-Johnson, W.H., Hansen, R.E., Beinert, H., Tsibris, J.C.M., Bartholomaus, R.C., and Gunsalus, I.C. (1968) On the sulfur components of iron-sulfur proteins. I. The

number of acid-labile sulfur groups sharing an unpaired electron with iron. *Proc Natl Acad Sci USA* 60: 368–372.

Osman, D., Patterson, C.J., Bailey, K., Fisher, K., Robinson, N.J., Rigby, S.E.J., and Cavet, J.S. (2013) The copper supply pathway to a *Salmonella* Cu,Zn-superoxide dismutase (SodCII) involves P(1B)-type ATPase copper efflux and periplasmic CueP. *Mol Microbiol* 87: 466–477.

Otto, M. (2010) Basis of virulence in Community-Associated Methicillin-Resistant *Staphylococcus aureus*. *Ann Rev Microbiol* 64: 143–162.

Outten, F.W., Djaman, O., and Storz, G. (2004) A *suf* operon requirement for Fe-S cluster assembly during iron starvation in *Escherichia coli*. *Mol Microbiol* 52: 861–872.

Pan, Q., Shan, Y., and Yan, A. (2012) A region at the C-terminus of the *Escherichia coli* global transcription factor FNR negatively mediates its degradation by the ClpXP protease. *Biochemistry* 51: 5061–5071.

Pang, Y.Y., Schwartz, J., Thoendel, M., Ackermann, L.W., Horswill, A.R., and Nauseef, W.M. (2010) agr-Dependent interactions of *Staphylococcus aureus* USA300 with human polymorphonuclear neutrophils. *J Innate Immun* 2: 546–559.

Parsonage, D., Newton, G.L., Holder, R.C., Wallace, B.D., Paige, C., Hamilton, C.J., *et al.* (2010) Characterization of the N-acetyl-α-D-glucosaminyl l-malate synthase and deacetylase functions for bacillithiol biosynthesis in *Bacillus anthracis*. *Biochemistry* 49: 8398–8414.

Pérez-Pérez, J.M., Candela, H., and Micol, J.L. (2009) Understanding synergy in genetic interactions. *Trends Genet* 25: 368–376.

Planet, P.J., Diaz, L., Kolokotronis, S.-O., Narechania, A., Reyes, J., Xing, G., *et al.* (2015) Parallel epidemics of community-associated methicillin-resistant *Staphylococcus aureus* USA300 infection in North and South America. *J Infect Dis* 212: 1874–1882.

Planet, P.J., LaRussa, S.J., Dana, A., Smith, H., Xu, A., Ryan, C., *et al.* (2013) Emergence of the epidemic methicillin-resistant *Staphylococcus aureus* strain USA300 coincides with horizontal transfer of the arginine catabolic mobile element and speG-mediated adaptations for survival on skin. *mBio* 4: e00889–13.

Pomposiello, P.J., and Demple, B. (2001) Redox-operated genetic switches: the SoxR and OxyR transcription factors. *Trends in Biotechnology* 19: 109–114.

Posada, A.C., Kolar, S.L., Dusi, R.G., Francois, P., Roberts, A.A., Hamilton, C.J., *et al.* (2014) The importance of bacillithiol in the oxidative stress response of *Staphylococcus aureus*. *Infect Immun* 82: 316–332.

Pöther, D.-C., Gierok, P., Harms, M., Mostertz, J., Hochgräfe, F., Antelmann, H., *et al.* (2013) Distribution and infection-related functions of bacillithiol in *Staphylococcus aureus*. *Int J Med Microbiol* 303: 114–123.

Prinz, W.A.W., Aslund, F.F., Holmgren, A.A., and Beckwith, J.J. (1997) The role of the thioredoxin and glutaredoxin pathways in reducing protein disulfide bonds in the *Escherichia coli* cytoplasm. *J Biol Chem* 272: 15661–15667.

Py, B., and Barras, F. (2010) Building Fe–S proteins: bacterial strategies. *Nat Rev Microbiol* 8: 436–446.

Qi, W., Li, J., Chain, C.Y., Pasquevich, G.A., Pasquevich, A.F., and Cowan, J.A. (2012) Glutathione complexed Fe–S centers. *J Am Chem Soc* 134: 10745–10748.

Quinn, M.T., and Gauss, K.A. (2004) Structure and regulation of the neutrophil respiratory burst oxidase: comparison with nonphagocyte oxidases. *J Leukoc Biol* 76: 760–781.

Radford, D.S., Kihlken, M.A., Borrelly, G.P.M., Harwood, C.R., Le Brun, N.E., and Cavet, J.S. (2003) CopZ from *Bacillus subtilis* interacts in vivo with a copper exporting CPx-type ATPase CopA. *FEMS Microbiol Lett.* 220: 105-112.

Rajkarnikar, A., Strankman, A., Duran, S., Vargas, D., Roberts, A.A., Barretto, K., *et al.* (2013) Analysis of mutants disrupted in bacillithiol metabolism in *Staphylococcus aureus*. *Biochem Biophys* 436:128-133.

Ranjit, D.K., Endres, J.L., and Bayles, K.W. (2011) *Staphylococcus aureus* CidA and LrgA proteins exhibit holin-like properties. *J Bacteriol* 193: 2468–2476.

Reiss, S., Pané-Farré, J., Fuchs, S., Francois, P., Liebeke, M., Schrenzel, J., *et al.* (2012) Global analysis of the *Staphylococcus aureus* response to mupirocin. *Antimicrob Agents Chemother* 56: 787–804.

Reniere, M.L., and Skaar, E.P. (2008) *Staphylococcus aureus* haem oxygenases are differentially regulated by iron and haem. *Mol Microbiol* 69: 1304–1315.

Rensing, C., and Grass, G. (2003) *Escherichia coli* mechanisms of copper homeostasis in a changing environment. *FEMS Microbiol Rev* 27: 197–213.

Resch, G., Francois, P., Morisset, D., Stojanov, M., Bonetti, E.J., Schrenzel, J., *et al.* (2013) Human-to-bovine jump of *Staphylococcus aureus* CC8 is associated with the loss of a β-hemolysin converting prophage and the acquisition of a new staphylococcal cassette chromosome. *PLoS One* 8: e58187.

Roberts, A.A., Sharma, S.V., Strankman, A., Duran, S.R., Rawat, M., and Hamilton, C.J. (2013) Mechanistic studies of FosB: a divalent-metal-dependent bacillithiol-S-transferase that mediates fosfomycin resistance in *Staphylococcus aureus*. *Biochem J* 451: 69–79.

Rodríguez-Manzaneque, M.T., Tamarit, J., Bellí, G., Ros, J., and Herrero, E. (2002) Grx5 is a mitochondrial glutaredoxin required for the activity of iron/sulfur enzymes. *Mol Bio Cell* 13: 1109–1121.

Rolfe, M.D., Rice, C.J., Lucchini, S., Pin, C., Thompson, A., Cameron, A.D.S., *et al.* (2012) Lag phase Is a distinct growth phase that prepares bacteria for exponential growth and involves transient metal accumulation. *J Bacteriol* 194: 686–701.

Rosario-Cruz Z., Chahal, H.K., Mike, L.A., Skaar, E.P., and Boyd, J.M. (2015) Bacillithiol has a role in Fe-S cluster biogenesis in *Staphylococcus aureus*. *Mol Microbiol* 98:218-42.

Rudolf, J., Makrantoni, V., Ingledew, W.J., Stark, M.J.R., and White, M.F. (2006) The DNA repair helicases XPD and FancJ have essential iron-sulfur domains. *Molecular Cell* 23: 801–808.

Sakthi, S., and Narayanan, S. (2013) The *lpqS* knockout mutant of *Mycobacterium tuberculosis* is attenuated in macrophages. *Microbiol Res* 168: 407–414.

Salgado, C.D., Sepkowitz, K.A., John, J.F., Cantey, J.R., Attaway, H.H., Freeman, K.D., *et al.* (2013) Copper surfaces reduce the rate of healthcare-acquired infections in the intensive care unit. *Infect Control Hosp Epidemiol* 34: 479–486.

Sánchez García, M., De la Torre, M.A., Morales, G., Peláez, B., Tolón, M.J., Domingo, S, *et al*. (2010) Clinical outbreak of linezolid-resistant *Staphylococcus aureus* in an intensive care unit. *JAMA*. 303: 2260-2264.

Santos, Dos, P.C., Johnson, D.C., Ragle, B.E., Unciuleac, M.C., and Dean, D.R. (2007) Controlled expression of *nif* and *isc* iron-sulfur protein maturation components reveals target specificity and limited functional replacement between the two systems. *J Bacteriol* 189: 2854–2862.

Schafer, F.Q., and Buettner, G.R. (2001) Redox environment of the cell as viewed through the redox state of the glutathione disulfide/glutathione couple. *Free Radic Biol Med* 30: 1191–1212.

Schmidt, M.G., Attaway, H.H., Sharpe, P.A., John, J., Sepkowitz, K.A., Morgan, A., *et al.* (2012) Sustained reduction of microbial burden on common hospital surfaces through introduction of copper. *J Clin Microbiol* 50: 2217–2223.

Selbach, B., Earles, E., and Santos, Dos, P.C. (2010) Kinetic analysis of the bisubstrate cysteine desulfurase SufS from *Bacillus subtilis*. *Biochemistry* 49: 8794–8802.

Sharma, S.V., Arbach, M., Roberts, A.A., Macdonald, C.J., Groom, M., and Hamilton, C.J. (2013) Biophysical Features of Bacillithiol, the Glutathione Surrogate of *Bacillus subtilis* and other Firmicutes. *Chembiochem* 14: 2160–2168.

Singleton, C., Hearnshaw, S., Zhou, L., Le Brun, N.E., and Hemmings, A.M. (2009) Mechanistic insights into Cu(I) cluster transfer between the chaperone CopZ and its cognate Cu(I)-transporting P-type ATPase, CopA. *Biochem J* 424: 347–356.

Singh, V.K., Vaish, M., Johansson, T.R., Baum, K.R., Ring, R.P., Singh, S., *et al*. (2015) Significance of four methionine sulfoxide reductases in *Staphylococcus aureus*. *PLoS One*. 10(2): e0117594.

Sitthisak, S., Howieson, K., Amezola, C., and Jayaswal, R.K. (2005) Characterization of a multicopper oxidase gene from *Staphylococcus aureus*. *Appl Microbiol* 71: 5650–5653.

Sitthisak, S., Knutsson, L., Webb, J.W., and Jayaswal, R.K. (2007) Molecular characterization of the copper transport system in *Staphylococcus aureus*. *Microbiology* 153: 4274–4283.

Skov, R., Christiansen, K., Dancer, S.J., Daum, R.S., Dryden, M., Huang, Y.C., Lowy, F. (2012) Update on the prevention and control of community-acquired meticillin-resistant *Staphylococcus aureus* (CA-MRSA). *Int J Antimicrob Agents*. 39: 193-200.

Skovran, E., and Downs, D.M. (2003) Lack of the ApbC or ApbE protein results in a defect in Fe-S Cluster metabolism in *Salmonella enterica* serovar Typhimurium. *J Bacteriol* 185: 98–106.

Skovran, E., Lauhon, C.T., and Downs, D.M. (2004) Lack of YggX results in chronic oxidative stress and uncovers subtle defects in Fe-S cluster metabolism in *Salmonella enterica*. *J Bacteriol* 186: 7626–7634.

Smaldone, G.T., and Helmann, J.D. (2007) CsoR regulates the copper efflux operon *copZA* in *Bacillus subtilis*. *Microbiology* 153: 4123–4128.

Solioz, M., and Stoyanov, J.V. (2003) Copper homeostasis in *Enterococcus hirae*. *FEMS Microbiol Rev* 27: 183–195.

Song, E., Jaishankar, G.B., Saleh, H., Jithpratuck, W., Sahni, R., and Krishnaswamy, G. (2011) Chronic granulomatous disease: a review of the infectious and inflammatory complications. *Clin Mol Allergy* 9: 10. doi: 10.1186/1476-7961-9-10.

Sousa, F.L., Alves, R.J., Ribeiro, M.A., Pereira-Leal, J.B., Teixeira, M., and Pereira, M.M. (2012) The superfamily of heme–copper oxygen reductases: Types and evolutionary considerations. *Biochem Biophys Acta* 1817: 629–637.

Srinivasan, V., Pierik, A.J., and Lill, R. (2014) Crystal structures of nucleotide-free and glutathione-bound mitochondrial ABC transporter Atm1. *Science* 343: 1137–1140.

Sun, F., Ji, Q., Jones, M.B., Deng, X., Liang, H., Frank, B., *et al.* (2012) AirSR, a [2Fe-2S] cluster-containing two-component system, mediates global oxygen sensing and redox signaling in *Staphylococcus aureus*. *J Am Chem Soc* 134: 305–314.

Takahashi, Y., and Tokumoto, U. (2002) A third bacterial system for the assembly of iron-sulfur clusters with homologs in archaea and plastids. *J Biol Chem* 277: 28380–28383.

Talan, D.A., Krishnadasan, A., Gorwitz, R.J., Fosheim, G.E., Limbago, B., Albrecht, V., *et al.* (2011) Comparison of *Staphylococcus aureus* from skin and soft-tissue infections in US emergency department patients, 2004 and 2008. *Clin Infect Dis* 53: 144–149.

Tavares, P., Pereira, A.S., Moura, J.J.G., and Moura, I. (2006) Metalloenzymes of the denitrification pathway. *J Inorg Biochem* 100: 2087–2100.

Tavares, A.F.N., Teixeira, M., Romão, C.C., Seixas, J.D., Nobre, L.S., and Saraiva, L.M. (2011) Reactive oxygen species mediate bactericidal killing elicited by carbon monoxide-releasing molecules. *J Biol Chem* 286: 26708–26717.

Tenover, F.C., McDougal, L.K., Goering, R.V., Killgore, G., Projan, S.J., Patel, J.B., and Dunman, P.M. (2006) Characterization of a strain of community-associated methicillin-resistant *Staphylococcus aureus* widely disseminated in the United States. *J Clin Microbiol* 44: 108–118.

Thorgersen, M.P., and Downs, D.M. (2008) Analysis of *yggX* and *gshA* mutants provides insights into the labile iron pool in *Salmonella enterica*. *J Bacteriol* 190: 7608–7613.

Thorgersen, M.P., and Downs, D.M. (2009) Oxidative stress and disruption of labile iron generate specific auxotrophic requirements in *Salmonella enterica. Microbiology* 155: 295–304.

Thurlow, L.R., Joshi, G.S., Clark, J.R., Spontak, J.S., Neely, C.J., Maile, R., and Richardson, A.R. (2013) Functional modularity of the arginine catabolic mobile element contributes to the success of USA300 methicillin-resistant *Staphylococcus aureus. Cell Host Microbe* 13: 100–107.

Tokumoto, U., Kitamura, S., Fukuyama, K., and Takahashi, Y. (2004) Interchangeability and distinct properties of bacterial Fe-S cluster assembly systems: functional replacement of the *isc* and *suf* operons in *Escherichia coli* with the *nifSU*-like operon from *Helicobacter pylori*. *J Biochem* 136: 199–209.

Uno, H., and Arya, S. (1987) Neuronal and vascular disorders of the brain and spinal cord in Menkes kinky hair disease. *Am J Med Genet Suppl* 3: 367–377.

Upton, H., Newton, G.L., Gushiken, M., Lo, K., Holden, D., Fahey, R.C., and Rawat, M. (2012) Characterization of BshA, bacillithiol glycosyltransferase from *Staphylococcus aureus* and *Bacillus subtilis*. *FEBS Lett* 586: 1004–1008.

Uziel, O., Borovok I., Schreiber, R., Cohen, G., Aharonowitz, Y. (2004) Transcriptional regulation of the *Staphylococcus aureus* thioredoxin and thioredoxin reductase genes in response to oxygen and disulfide stress. *J Bacteriol*. 186: 326-334.

Valentino, M.D., Foulston, L., Sadaka, A., Kos, V.N., Villet, R.A., Santa Maria, J. Jr., *et al*. (2014). Genes contributing to *Staphylococcus aureus* fitness in abscess- and infection-related ecologies. *mBio* 5:e01729-14.

Vanoni, M.A., and Curti, B. (1999) Glutamate synthase: a complex iron-sulfur flavoprotein. *Cell Mol Life Sci* 55: 617–638.

Vinella, D., Albrecht, C., Cashel, M., and D'Ari, R. (2005) Iron limitation induces SpoT-dependent accumulation of ppGpp in *Escherichia coli*. *Mol Microbiol* 56: 958–970.

Vinella, D., Brochier-Armanet, C., Loiseau, L., Talla, E., and Barras, F. (2009) Iron-sulfur (Fe/S) protein biogenesis: phylogenomic and genetic studies of A-type carriers. *PLoS Genet* 5: e1000497–e1000497.

Voyich, J.M., Braughton, K.R., Sturdevant, D.E., Whitney, A.R., Saïd-Salim, B., Porcella, S.F., *et al.* (2005) Insights into mechanisms used by *Staphylococcus aureus* to avoid destruction by human neutrophils. *J Immunol* 175: 3907–3919.

Wang, J., Fillebeen, C., Chen, G., Biederbick, A., Lill, R., and Pantopoulos, K. (2007) Iron-dependent degradation of apo-IRP1 by the ubiquitin-proteasome pathway. *Mol Cell Biol* 27: 2423–2430.

Wang, H., and Joseph, J.A. (1999) Quantifying cellular oxidative stress by dichlorofluorescein assay using microplate reader. *Free Radic Biol Med* 27: 612–616.

White, C., Lee, J., Kambe, T., Fritsche, K., and Petris, M.J. (2009) A role for the ATP7A copper-transporting ATPase in macrophage bactericidal activity. *J Biol Chem* 284: 33949–33956.

Wollenberg, M., Berndt, C., Bill, E., Schwenn, J.D., and Seidler, A. (2003) A dimer of the FeS cluster biosynthesis protein IscA from cyanobacteria binds a [2Fe2S] cluster between two protomers and transfers it to [2Fe2S] and [4Fe4S] apo proteins. *Eur J Biochem* 270: 1662–1671.

Woodmansee, A.N., and Imlay, J.A. (2002) Reduced flavins promote oxidative DNA damage in non-respiring *Escherichia coli* by delivering electrons to intracellular free iron. *J Biol Chem* 277: 34055–34066.

Wright Valderas, M., and Hart, M.E. (2001) Identification and characterization of a second superoxide dismutase gene (*sodM*) from *Staphylococcus aureus*. *J Bacteriol* 183: 3399–3407.

Xiao, Z., Loughlin, F., George, G.N., Howlett, G.J., and Wedd, A.G. (2004) C-terminal domain of the membrane copper transporter Ctr1 from *Saccharomyces cerevisiae* binds four Cu(I) ions as a cuprous-thiolate polynuclear cluster: sub-femtomolar Cu(I) affinity of three proteins involved in copper trafficking. *J Am Chem Soc* 126: 3081–3090.

Yan, F., LaMarre, J.M., Röhrich, R., Wiesner, J., Jomaa, H., Mankin, A.S., and Fujimori, D.G. (2010) RlmN and Cfr are radical SAM Enzymes involved in methylation of ribosomal RNA. *J Am Chem Soc* 132: 3953–3964.

Yeung, N., Gold, B., Liu, N.L., Prathapam, R., Sterling, H.J., Willams, E.R., and Butland, G. (2011) The *E. coli* monothiol glutaredoxin GrxD forms homodimeric and heterodimeric FeS cluster containing complexes. *Biochemistry* 50: 8957–8969.

Zhang, B., Bandyopadhyay, S., Shakamuri, P., Naik, S.G., Huynh, B.H., Couturier, J., *et al.* (2013) Monothiol glutaredoxins can bind linear $[Fe3S4]^{+}$ and $[Fe4S4]^{2+}$ clusters in addition to $[Fe2S2]^{2+}$ Clusters: Spectroscopic characterization and functional implications. *J Am Chem Soc* 135: 15153–15164.

Zhang, Y.-Q., Ren, S.-X., Li, H.-L., Wang, Y.-X., Fu, G., Yang, J., *et al.* (2003) Genome-based analysis of virulence genes in a non-biofilm-forming *Staphylococcus epidermidis* strain (ATCC 12228). *Mol Microbiol* 49: 1577–1593.

Zheng, L., White, R.H., Cash, V.L., Jack, R.F., and Dean, D.R. (1993) Cysteine desulfurase activity indicates a role for NIFS in metallocluster biosynthesis. *Proc Natl Acad Sci USA* 90: 2754–2758.